AGARD-R-768

AGARD

ADVISORY GROUP FOR AEROSPACE RESEARCH & DEVELOPMENT

7 RUE ANCELLE 92200 NEUILLY SUR SEINE FRANCE

AGARD REPORT No.768

AGARD/SMP Review Damage Tolerance for Engine Structures 1. Non-Destructive Evaluation

NORTH ATLANTIC TREATY ORGANIZATION

DISTRIBUTION AND AVAILABILITY
ON BACK COVER

NORTH ATLANTIC TREATY ORGANIZATION

ADVISORY GROUP FOR AEROSPACE RESEARCH AND DEVELOPMENT

(ORGANISATION DU TRAITE DE L'ATLANTIQUE NORD)

AGARD Report No.768

AGARD/SMP REVIEW

DAMAGE TOLERANCE FOR ENGINE STRUCTURES

1. NON-DESTRUCTIVE EVALUATION

Papers presented at the 66th Meeting of the Structures and Materials Panel of AGARD
in Luxembourg, 1—6 May 1988.

THE MISSION OF AGARD

According to its Charter, the mission of AGARD is to bring together the leading personalities of the NATO nations in the fields of science and technology relating to aerospace for the following purposes:

- Recommending effective ways for the member nations to use their research and development capabilities for the common benefit of the NATO community;
- Providing scientific and technical advice and assistance to the Military Committee in the field of aerospace research and development (with particular regard to its military application);
- Continuously stimulating advances in the aerospace sciences relevant to strengthening the common defence posture;
- Improving the co-operation among member nations in aerospace research and development;
- Exchange of scientific and technical information;
- Providing assistance to member nations for the purpose of increasing their scientific and technical potential;
- Rendering scientific and technical assistance, as requested, to other NATO bodies and to member nations in connection with research and development problems in the aerospace field.

The highest authority within AGARD is the National Delegates Board consisting of officially appointed senior representatives from each member nation. The mission of AGARD is carried out through the Panels which are composed of experts appointed by the National Delegates, the Consultant and Exchange Programme and the Aerospace Applications Studies Programme. The results of AGARD work are reported to the member nations and the NATO Authorities through the AGARD series of publications of which this is one.

Participation in AGARD activities is by invitation only and is normally limited to citizens of the NATO nations.

Published November 1988

ISBN 92-835-0484-4

Printed by Specialised Printing Services Limited
40 Chigwell Lane, Loughton, Essex IG10 3TZ

PREFACE

Most current military and all civil engines are operated under "Safe-life" procedures for their critical components. Experience has shown that this philosophy presents two drawbacks:

(a) The move towards designs allowing higher operational stresses, and the use of advanced high-strength alloys make it likely that a disc burst could happen (following a rapid crack growth) well before the statistically-based "Safe-life" has been achieved.

(b) It is potentially wasteful of expensive components, since it has been estimated that over 80% of engine discs have ten or more low cycle fatigue lives remaining when discarded under "Safe-life" rules.

Damage Tolerance being an alternative lifeing philosophy, the Sub-Committee on "Damage Tolerance Concepts for the Design of Engine Constituents" has therefore decided to conduct a series of four Workshops addressing the areas critical to Damage Tolerant design of engine parts.

The present report includes the papers presented during Workshop 1 which was devoted to Non-Destructive Evaluation of Components. FRANCE (FDS)

It also includes the content of the discussions which followed the presentations. On behalf of the Structures and Materials Panel, I would like to thank the authors, the recorders of the discussions and the session chairmen whose participation has contributed so greatly to the success of the Workshop.

R.LABOURDETTE
Chairman, Sub-Committee on
Damage Tolerance Concepts
for the Design of Engine
Constituents

* * *

La totalité des moteurs civils et la plupart des moteurs militaires sont actuellement mis en oeuvre suivant les concepts de "durée de vie certaine" en ce qui concerne leurs parties vitales. La pratique de cette approche a mis en évidence les deux inconvénients suivants:

(a) La tendance à l'utilisation des moteurs sous contraintes mécaniques plus élevées et l'emploi d'alliages à haute résistance rendent possible l'éclatement d'un disque (à la suite d'une progression rapide de fissure) avant que la "durée de vie certaine", évaluée statistiquement, ait été atteinte.

(b) On observe également un gaspillage de pièces onéreuses, puisqu'on estime que 80% environ des disques retirés du service conformément aux règles de "durée de vie certaine" ont encore un potentiel supérieur à dix durées de vie en fatigue oligocyclique.

La Tolérance aux Dommages constituant une autre approche possible de la définition des potentiels de vie, le Sous-Comité "Concepts de Tolérance aux Dommages pour le dimensionnement des composants de moteurs" a décidé d'organiser une série de quatre Ateliers consacrés aux divers aspects de la Tolérance aux Dommages appliquée aux moteurs.

Le présent rapport contient les diverses présentations effectuées à l'occasion du premier d'entr'eux traitant des techniques de Contrôle Non Destructif. On y trouve également un compte-rendu des discussions qui ont suivi les diverses présentations.

Au nom de la Commission Structures et Matériaux, je remercie les auteurs, les rapporteurs de discussion et les présidents de sessions qui ont grandement contribué au succès de cet Atelier.

R.LABOURDETTE
Président du Sous-Comité
"Tolérance au Dommages pour les
composants de moteurs"

STRUCTURES AND MATERIALS PANEL

Chairman: Professor Paolo Santini
Dipartimento Aerospaziale
Universita degli Studi di Roma
"La Sapienza"
Via Eudossiana, 16
00185 Roma, Italy

Deputy Chairman: Prof. Dr-Ing. Hans Försching
Direktor der DFVLR Institut
für Aeroelastik
Bunsenstrasse 10
D-3400 Göttingen, Germany

SUB-COMMITTEE MEMBERS

Chairman: Mr Roger Labourdette
Directeur Scientifique Adjoint des Structures
ONERA
29 ave de la Division Leclerc
92320 Châtillon, France

SMP MEMBERS

P.Costa	Fr
D.Coutsouradis	Be
A.Deruyttere	Be
M.Doruk	Tu
J.A.Güemes	Sp
J.J.Kacprzynski	Ca
J.S.L.Leach	UK
H.P. van Leeuwen	Nl
J.J. De Luccia	US
P.J.Perry	UK
S.Signoretti	It
M.Theofilou	Gr
W.Wallace	Ca
H.Zocher	Ge

PANEL EXECUTIVE

Mr Murray C.McConnell – UK

AGARD-OTAN
7, rue Ancelle
92200 Neuilly sur Seine
France

Tel:(1) 4738 5790 & 92
Telex: 610176

From USA and Canada
AGARD-NATO
Attn: SMP Executive
APO New York 09777

CONTENTS

THE IMPACT OF ENGINEERING ASSUMPTIONS ON NDE REQUIREMENTS

R H JEAL
Chief of Materials and Mechanical Technology

Rolls-Royce plc
P O Box 31
Derby
DE2 8BJ

1. Introduction

In assessing the performance of a structure or component he has designed the engineer has to make a number of assumptions about its characteristics as it goes into service.

To assess the validity of these assumptions they are best considered in two categories:

a) the geometry

b) the material condition

Geometrical aspects - including surface finish - have the advantage they can be directly measured on the individual parts for comparison with those originally set. The designer can calculate the size of acceptable deviations from the norm and production is accepted or rejected on the basis of these tolerances. Material condition is a more difficult concept to deal with. It covers a wide range of phenomena ranging from cracks, scratches and porosity through to the details of material microstructure which represent a deviation from the designers assumption of a material as a continuous, isotropic, homogeneous media free from defects. These deviations are both difficult to find and their effect on performance is difficult to assess. Designers in the past used to assume safety factors to account for the unseen presence of defects, but which have caused in-service failures. As more efficient use of available materials has been sought these factors have been reduced but at the price of greater "perfection" in the materials. This has led to increasing demands upon the ability of the designer to assess the behaviour of discontinuities and set the defect standards, and for the inspection engineer to establish techniques that will find smaller and smaller defects in more and more difficult situations on ever increasing degree of certainty.

This paper charts the way these changing design requirements have impacted upon the problem presented to the inspection engineer and points the way to the future changes. This workshop will cover the inspection engineers response to these demands and set out the work required for the future.

2. Engineering assumptions

In predicting the behaviour of a structure the design engineer has to assume a material model that relates the stresses he has calculated from the applied loads to strains and then to appropriate failure criteria.

2.1 Traditional Assumptions

At its simplest the model will be one of a homogeneous, continuous, isotropic media with stress directly proportional to strain with failure occurring when the stress reaches a critical value - the tensile strength. (fig 1).

The manufacturer of a structure designed to such a model has to show he has not introduced any deviations from the model ie. it contains no defects which will reduce the load carrying capacity of the structure (cracks, porosity etc). The task he sets his NDT Engineer is to check for such discontinuities and reject all found.

Safety is built into the system by setting an operating stress at a fraction of the failure stress that experience has shown to be safe (either from test or service).

The degree of material perfection this demands is set by the discrimination of the inspection methods used - their sensitivity setting the real meaning of the required 'no defect' standard.

Subsequent in service failures are then dealt with by establishing the cause and then eliminating it by changing the manufacturing method and applying a more sensitive inspection method that would have found the offending discontinuity.

This approach is still the most widely used one even in non-critical aerospace structures.

As the demands on the designer for lighter, higher load bearing, more cost efficient structures has increased however, a number of short falls have been found.

a) Without detailed knowledge of the way a material departs from the ideal assumptions the safety factors required lead to inefficient use of material in the structure.

b) The simple materials model was not applicable to the new high strength alloys being introduced.

c) Under a cyclic stress environment detailed knowledge of the material discontinuities is needed to predict life.

A number of different steps were taken to adapt the behaviour models to meet the demands of these new materials and conditions. These were covered in the AGARD Conference on Damage Tolerance Concepts for Critical Engine Components in 1985 (Ref 1 and 2).

The current behaviour models now being used to predict the behaviour of components under cyclic conditions are based upon an understanding of the total fatigue life as shown in fig 2 (Ref 3). The materials potentially move through each of the life stages shown in the figure in a way that is dependant upon factors relevant to the dominating mode of behaviour in that stage.

The more important factors are listed below:-

(1) Crack Nucleation Phase

The number of cycles in which a crack nucleates will depend upon the applied stress and local stress raisers created by discontinuities in the material. The size of crack that occurs will be related to the critical microstructural elements of the materials.

If a propagating crack is present from the beginning this stage obviously is not applicable.

(2) Small Crack Growth

The rate at which the crack grows will be dependant upon the applied stress and the structural features it is moving through. Provided the nature of the microstructure is known the growth rate is predictable.

(3) Large Crack Growth

The critical failures are crack size and stress levels. Large discontinuities within the material or at the component surface can effect life predictions in this phase.

The total effect can be summed up as a stress/life curve (Fig 3) which shows that relatively long lives can be achieved if life is dominated by stress induced cracks (curve 1), only short lives are predicted in propagating cracks are always assumed to be present (curve 3) - the inspection related lives can be calculated if a probabilistic approach to the presence of propagating cracks or malignant defects is taken (curve 2). (Fig 4).

The design engineer can now make appropriate assumptions about the material from his understanding of defect behaviour and component test/service experience and draw up an appropriate quality standard which the manufacturing engineer has to demonstrate the component meets - by a combination of appropriate process control and non destructive inspections.

The major difference between yesterdays and todays quality standards is the change from "no defects are acceptable" to quantitative limits eg "the surface shall not contain any cracks above 1mm in length".

This demands no longer just applied to the initial condition of the component but also throughout its life.

3. Quality Acceptance Requirements

The original demands by the designer upon the manufacturing engineer were simple. The piece going into the engine must be at least as good as the pieces that were tested to give the design and lifing data. This led to the approach of fixed manufacturing practice and quality standards that rejected parts showing indications found by fixed NDT procedures. The required physical attributes of the component were specified as the product of the defined fixed process (eg microstructure, residual stress) and the inspection process was used to ensure that any gross aberrations could be rejected. Simple release tests, such as tensile and creep of specimens cut from test rings, were used to check the piece had gone through the designated process and responded in the expected way (eg. heat treatment of martenistic steels where the heat treatment was repeated is the designated properties weren't reached).

Todays requirements of the design engineering are far more critical. His assumptions behind the life calculation assume certain physical attributes of the component, relating to material microstructure, surface condition, residual stress and sub-surface discontinuities - all specified on a quantitative basis. Whilst these should be within the process capability (see below) the manufacturing engineer must show by a combination of process control and inspection that the component he produces has the attributes the designer has assumed. The engineering quality demands have, therefore, changes from a simple no "indications" demand to a list of quantitative factors that need individual control statements about the process and inspection from the manufacturing quality

organisation. The role of the NDT specialist is to interpret the engineer's requirement into the quantitative results of an NDT process - both in terms of sensitivity and repeatability, - results that can then be used to monitor the ongoing capability of the manufacturing process.

Whilst this is not too difficult in the controlled environment of the manufacture shop things become far more difficult once the piece goes into service - but the requirement for inspection continues through the component life as it follows its designated life plan.

The factors likely to be called up in fig 5. Whilst some of these can be inspected for non-destructively the list illustrates the line can only be covered by tight on going process control.

4 The Role of NDE Reliability and Component Integrity

This can be best considered by looking at fig 3.

4.1 Lives based upon crack nucleation

If the design engineer is to make safe use of the nucleation life of a component - curve (1) - he must be sure the material does not contain any propagating cracks as new, and that any subsequent in-service incidents such as frettage or fitting damage do not detract from that nucleation life.

If such an assumption were to be based upon inspection alone - a common current assumption - the NDT engineer would have to give 100% guarantees that his methods were completely reliable at all crack sizes. This is clearly not possible - such an approach could only be underwritten by using processes that don't cause the cracks with inspection acting as a check on process capability.

Under these circumstances the inspection does not need to be completely quantitative - the presence of any indication has to be taken as a warning to examine the process because it is going out of the necessary control.

Such an approach does not have any credence in-service as the very need for inspection is created by lack of total understanding of the in-service conditions.

4.2 Lives based upon inspection

If the assumption is made that process control cannot be relied upon at all then the material is assumed to have propagating cracks just outside the sensitivity of the inspection process used (curve 3).

Under these circumstances the sensitivity of the inspection process are paramount in determining the component life. They need full definition as applied to the component under consideration and must be met at all times.

This approach is the only one applicable to in-service inspections when used for component life extension beyond that of the worst of the family.

4.3 Lives on a probabilistic approach

This approach (curve 2) assumes that defects can be present but that the total probability of them effecting life (including being found) lies within acceptable risk. In this case the degree of sensitivity and reliability demand from the NDT engineering is determined by the chance of the process producing the defect - the higher the chance of producing one, the higher the requirement to find it.

This approach is the one most suited to new components, but the NDI sensitivity has to be set higher than the component rejection rate to provide the on-going information to assess the probabilistic behaviour.

The degree to which the NDI process needs understanding is between the above two - exactly where depending upon the quality of the project.

5. Design Intent Process Capability on In-service Life - role of NDE

In an ideal world the design intent and process capability of a component would be matched with a in-service life distribution that let the operator use the majority of useful life of all components under all in service conditions.

Under those circumstances there would be no need of inspection.

The need for inspection in the real world is created, therefore, by a breakdown of the ideal.

a) Lack of match between design intent and process capability.

b) Lack of understanding of in-service conditions.

c) Wide scatter of life capability within any component family.

5.1 Lack of design intent/process capability match

This can occur for two reasons:

a) the designer cannot achieve the engineering objectives within the capability of the total product of the process.

b) the process capability is not consistent and can drift out of the established match.

The role of NDE is different in these two cases.

For a) the NDE process sets the absolute quality standard going on into the engine. Because it acts as such a gate its reliability is critical as failure will let sub-standard parts into service.

The level of dependance on NDE in such circumstances has really been shown by experience to be too high and will inevitably lead to in-service failures. Such circumstances should only have been accepted where such failures are acceptable on both safety and economic grounds.

For b) the NDE is being used to establish trends in the process output and thus the absolute accuracy of the inspection is not critical provided it is reasonably consistent. The adverse trends in findings can then be used to re-examine the process controls and reverse the trend in product quality. This is the ideal use of NDE in a manufacturing environment.

5.2 Lack of full understanding of in-service conditions

This is inevitable because it is not economically feasible to cover all possible conditions in an engine development programme.

As a check on components during the declared life it can be used to confirm that the assumptions made were valid and that no major life reducing factors were missed - by giving early warning of cracking and damage.

As this is a sampling technique the demands on the inspection are not 100% and so, provided the techniques used are well qualified, NDE offers a valid way of checking in-service behaviour.

5.3 NDE can also be used to extend in-service life on a 'life on condition' basis. Such an approach demands a high level of repeatability and reliability in the inspection method - level which are probably achievable in specific circumstances (eg. where the incident of known cracking is being followed) but probably not achievable on a general basis unless a higher risk of failure is acceptable.

6. Conclusion

As the demands of the engine on Components has increased the need for qualitative quality standards for those components has become evident - both as new and in-service. The qualitative demands of the designer cannot be met solely be qualitative NDE - they should be met by relying on enhanced process control supported by trend analysis basis on NDE rather than setting absolute quality levels by NDE.

Fig 6 shows the preferred applications for NDE on this basis.

With such an approach in mind quantitative NDE becomes a feasible proposition as its results can be used on a probablistic basis both by the design and manufacturing engineers.

The papers in this workshop should illustrate the detailed technical needs created by todays quality requirements and show how far we can rely on inspection results in future.

7. References

Reference 1. R H Jeal - Damage Tolerance Concepts for Critical Engine Components - AGARD Conference Proceedings No393, October 1985.

Reference 2. D W Hoeppner - Parameters that input to the Application of Damage Tolerance Concepts to Critical Engine Components - AGARD Conference Proceedings No393, October 1985.

Reference 3. R H Jeal - Defects and their Effects of the Behaviour of Gas Turbine Discs - AGARD Conference Proceedings No317, January 1982.

8. Acknowledgements

The author would like to acknowledge the long-term help and discussion with his friends and colleagues in this field of technology, in particular Dr A C Pickard, Mr G Asquith and Mr R G Taylor.

Thanks is also given to Rolls-Royce plc for permission to publish this paper.

BASIC MATERIAL MODEL

All materials are elastic isotropic homogeneous media free from defects.

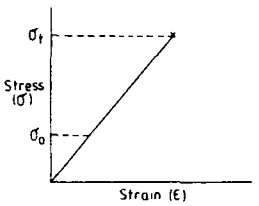

σ = Applied Load / Section Area

$\frac{\sigma}{\varepsilon}$ = E (Modulus)

Fig 1 Basic Material Model

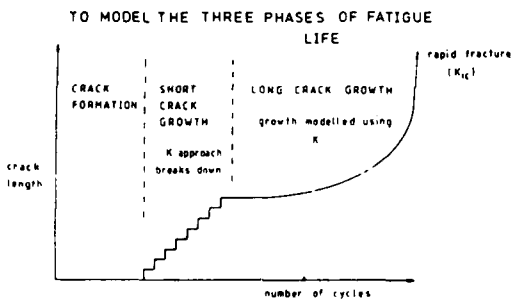

Fig 2 Stages of Fatigue Life

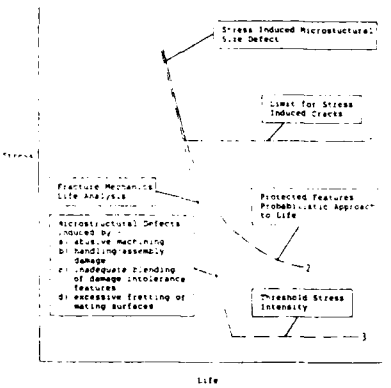

Fig 3 Stress vs Life Defect Curves

P_1 - Probability of a disc containing a defect.

P_2 - Probability of a flaw being missed by inspection.

P_3 - Probability of a defect being in a high stressed region.

P_4 - Probability of a defect behaving as a crack.

P_5 - Probability of variation in crack propagation rates.

P_6 - Probability of variation in fracture toughness.

P_7 - Probability of unknowns.

Fig 4 List of Probabilities for Sub-Surface Life Prediction

FACTORS IN ENGINEERING QUALITY STANDARDS

Surface Requirements

- Permitted Crack Size (mm)
- Grain Size (mm)
- Macrostructural features (mm)
- Microstructural features (mm)
- Inclusions (mm)
- Porosity (mm)
- Machinery abuse/Surface strain
- Scratches (mm)
- Dents/Bruising

Sub-Surface Requirements

- Ultrasonic Response as standard Artificial Defect (SAD).
  - equivalent flat bottom hole size.
- Inclusion Size
- Residual Stress
- Defect distribution (within component and on going)
- Microstructure

Fig 5 Factors in Engineering Quality Standards

APPLICATIONS FOR NDE

Role	Requiring a probabalistic understanding of sensitivity and repeatability	Requiring an absolute understanding of sensitivity and repeatability
Design Intent	Confirming Process Control set quality levels	Lifing based on 'defect free assumptions'.
Process Capability	Monitoring product quality trends	Setting quality levels where design intent exceeds process capability.
In-service Monitoring	Confirming calculated design lives	Life extension beyond family minimum (Life-on-condition).

Fig 6 Applications for NDE

REVIEW OF EXISTING NDT TECHNOLOGIES AND THEIR CAPABILITIES

Leonard J. Bond
Non-Destructive Evaluation Centre
Department of Mechanical Engineering
University College London
Torrington Place London WC1E 7JE U.K.

ABSTRACT

This paper presents a review of the current and expected future defect detection and characterisation capability for selected NDT technologies: four technologies were considered; dye penetrants, eddy currents, various ultrasonic techniques and radiography. It will be shown that no single figure should be used as the detection limit to characterise the capability of a particular NDT technology. A specific NDT technology or system is best characterised using a probability of detection (POD) curve and/or reliability of characterisation (ROC) curve. Any evaluation of an NDT technology must include consideration of the human factors associated with its operation. No single POD or ROC curve is adequate to characterise a particular technology as both part geometry and material have a signigicant impact on performance.
With the exception of eddy current technology it would appear that the measured defect detection limits established in the laboratory in the mid 1970's have not been changed significantly since then. However in recent years there have been significant changes in the NDT performed in production and inservice, not least through the collection of some POD and ROC data. Further work is required on the statistics used to estimate the performance capability for NDT. Major advances have been made in automation, instrumentation and systems which are used to implement NDT.
It is to be expected that through the increased use of automation and computer based technologies the best defect detection limits for the various NDT technologies, that are now only available in the laboratory; performance close to this level, could become reliably available in production and in due course result in improvements in the capability of in-service inspections for use as part of life-extension or retirement for cause programmes.

1. Introduction

This paper presents a review of selected NDT technologies with regard to their capability and reliability to detect and characterise defects in critical aero-engine components such as discs and blisks (integrally bladed discs), both in production and after service.

The performance of non-destructive testing is considered both at the time of manufacture and after service for parts fabricated from powder metals including API and with particular consideration given to the needs of the new European Fighter Aircraft (EFA).

Various NDT technologies have been considered with the aim of establishing the current capability of each technology; in terms of defect detection capability and probability of detection rates. The cause of the limits on performance are reviewed and areas where development can be expected in these and other NDT technologies within the next 5 to 10 years have been identified.

The NDT technologies selected for consideration were;

i. dye penetrants, including automated systems.

ii. eddy-current and other electromagnetic NDT technologies.

iii. ultrasonic NDT in various forms.

iv. radiography.

This review considers the application of NDT to aero-engines measured in terms of the reliability with which any NDT technology can be expected to perform in production or in-service and as part of any fracture mechanics based life extension or retirement for cause programme.

A major review of NDT methods for propulsion systems is given in a previous AGARD document (1). A variety of new lifing philosophies are being considered for critical aero-engine components and these include Damage Tolerance (DT), Fracture Mechanics based Life Extension and Retirement-for-Cause (RFC). At a more recent AGARD meeting the complete range of damage tolerance concepts for critical engine components have been considered (2) and the proceedings include some consideration of NDT. There has also been a growing realisation of the impact of human reliability on inspection (3,4).

The current capabilities of the various selected NDT technologies are reviewed and compared in general terms in Section 2. Section 3 then presents a summary of the various factors limiting the performance of these specific NDT technologies. The current and expected developments in NDT capability are considered in Section 4. Some conclusions are provided as Section 5.

2. NDT Technologies; current capability

The literature has been reviewed and material collected so as to establish what are; i. defect detection limits, and ii. the probability of defect detection, for particular types and sizes of defects, for each NDT technology considered.

The general problem of how to establish a methodology to determine the reliability of flaw detection by NDT, its relation to design, statistics, demonstration programs and an assessment of inspection reliability has been considered by Packman et al (5).

The details of the requirements and methods used to validate the capability of a specific technique or technology applied to a specific problem are outside the scope of this review and they have not been considered in detail. The general area of reliability strategies has been considered by Buck and Wolf (6) and more recently specific models for predicting NDT capability have been developed. (e.g. 7,8,9 and 10).

In a paper by Comassar (11), in an AGARD monograph on 'NDI methods for propulsion systems', data was provided which compares the probability of detection (POD) capability for various technologies which detect surface defects. However no specific crack lengths are given and the specific geometry involved is not specified. It may be interesting to note that in this paper it was said that the NDT requirement for aero-engines is to be able to detect 0.01" (254 μm) surface defects. In the same report various additional general data is also to be found.

The most recent paper to be found which gives comparative figures for the defect detection capability for various NDT technologies was by Branco (12). He, in turn, quotes data collected by Pettie & Krupp (13) and the paper by Branco states that 'NDT is not able to detect flaws with sizes below those quoted in Table 1'.

Table 1 gives performance data for NDT on steel and when reviewing the various published studies it is this data which is used as a base line. Of particular interest are the three headings under which the NDT techniques are given; (i) Test specimens, laboratory inspection, (ii) Production parts, production inspection and (iii) Cleaned structures, service inspection.

In some sense the data in Table 1 is presented in a simplistic fashion; the data is that for 25 mm ferritic steel samples with a surface 63 RMS, there are no details for the various forms of the technology that were employed, and the geometry involved is not specified. Also there is no consideration given to the ability to detect a range of possible types of inclusions which is of considerable importance for the inspection of components fabricated from powder metal.

In my review I had expected to find that there had been significant improvements in the NDT limits for defect detection capability since the data in Table 1 was prepared in 1974. However, for the laboratory inspection this has not proved to be the case. If a single number is required to characterise the capability of a particular NDT technology, in terms of its detection limit these figures can still be considered to be valid. The significance of this data is considered further in section 3.

Data from an ENSIP NDT evaluation of NDT capability is given as Table 2. (14) The data is in the form of the preliminary conclusions of the USAF 'ENSIP NDT' study and it is quoted as the detection capability achieved by the average, of the majority, and by the best 10%, of technicians. Human factors are clearly an important consideration and need further attention. When the data shown in Tables 1 and 2 is compared the stated capability for the best in-service MPI and ultrasonic NDT are in close agreement. The ENSIP study found penetrant to perform significantly worse than would be expected from the Table 1 data; however the ENSIP eddy current performance was much improved and it was closer to the laboratory inspection limit given in the Table 1.

There have been various more recently reported studies in the USA which try and provide NDT-POD data. (15,16) A great deal of data is presented in these documents and it is not truly valid to try and extract just single numbers; there are simply too many variables involved and these include part geometry. The best detection levels achieved are close to those given in the ENSIP data, however in certain tests and with certain groups of inspectors results appear to fail to get even near the ENSIP levels of performance.

Less comparative data would appear to be available for radiography in all its forms using either X or gamma rays. Several groups simply reject radiography as being unsuitable for the detection of tight cracks. The fundamental resolution for radiographic systems is set by the spot size which for research, has been reduced a little below the stated detection limit given in Table 1. There have been three recent major development areas in X-radiography and these are micro-focus, real time and computerised tomography (CT). (17). Much work has been performed in the medical fields which has significance to the NDT community, however the capital costs for even research instrumentation can be high. Microfocus and projection radiography are now being used on critical parts in production and in such work the best systems give good dimensional measurement capability. These topics are considered further in section 4.

Among recently reported work Norriss (18) considered the performance of the same eddy current and ultrasonics systems evaluated against both real and artificial cracks. It is clear from this work that the performance of NDT systems, as measured against real and artificial cracks has significance differences; at a given POD it is consistantly possible to detect smaller artificial cracks than real features. In one eddy current test in plate a 50% POD was achieved for artifical cracks at about 2.0 mm length and at about 4.5 mm length for real cracks and this was by no means the largest variation in sensitivity. Similar comments can be made about any size given in terms of the Flat Bottom Hole (FBH) size as an ultrasonic sizing standard; a natural defect which gives an echo in an A-scan which is the same height as that from a particular size of FBH can be due to a defect with a true geometric size which may well be significantly larger. The use of the echo amplitude data for sizing in ultrasonics increases the uncertainty attached to any size estimate given.

In reports which consider the NDE needs for RFC applied to military engines such as the F100, F101 and F110 King et al (19) state that a detection capability down to 0.030 inch (0.76 mm) surface length is required. They claim that eddy current NDT can reliably detect surface flaws down to 0.005 inch. (0.12 mm or 120 μm). They also comment that the requirement for fluorescent penetrant inspection is to detect down to 0.030 inch surface length, but that this capability has not yet been adequately demonstrated The probability of detection for eddy current NDT in a range of geometries is shown as Fig 1 and the POD for fluorescent penetrant inspection is shown as Fig 2.

There have also been various other studies which have given single numbers for 'NDT detection limit'. In a Canadian study into damage tolerance based life extension, (Koul et al (29)), the figure 1.75 mm was given for '100% detection', In a paper which reports the AGARD co-operative test program on titanium alloy engine disc material. Mon and Raizenne (21) claimed that under proper conditions well motivated people with very special equipment can detect 0.375 x 0.125 mm (0.015 x 0.005 in) surface cracks with a 90% probability, 95% confidence level. However it is reported that it is more realistic to assume crack size for the detection limit is at a level of 0.75 x 0.375 mm (0.030 x 0.015 in). In a paper on aspects of small crack growth James and Knott (22) state that the normal NDT detection limit is at about 0.5 to 1.0 mm, although under certain situations perhaps 0.2 mm defects can be foun . In another place in the same paper the figure of 400μm is given for the NDT detection limit. This figure is also defined as being near the boundary for short and long crack growth behaviour in high strength aerospace alloys. However in this work no specific NDT methods are identified.

In a study by Fiorentin and Walther (23) which specifically considered the detection of small defects in powder metals, the conclusion was that conventional ultrasonics in powder metal has a detection limit for volume defects set between 500 and 300μm. Using other NDT techniques, neither x-ray or eddy current techniques were reported to be capable of detecting these defects over the required depth range. Their work using ultrasonic frequencies between 10 and 20 MHz claimed to provide an improved capability for the detection of ceramic inclusions down to 50μm, in 10μm grain size material, with 70% POD. For Astroloy type material if inspections are to be performed to a depth of 10 mm a pulse centre frequency of 20 MHz is considered optimal. A figure showing POB for various inclusions is shown as Fig 3. This detection limit cannot however be assumed to be valid for any powder metal sample as the base material grain size has a significant effect in the determination of the detection limits. The effect of microstructure on ultrasonic noise generation in powder metals has been investigated by Tittmann et al (24) and equations which can be used to predict the acoustic noise levels are derived and confirmed with experimental data.

In most studies performance is specified in terms of a 'detection capability'. The problem of the false call, i.e. giving an indication when there is no real defect present needs further consideration. Also further work is required to consider the effects of the probability of NON-detection as it is this which gives the probability for the presence for the largest defect with particular characteristics which may be missed. This parameter is central to any fracture mechanics based component life evaluation; the NDT data for defect type, shape and size needs to be in a form in which it can be used in fracture mechanics calculations.

The causes of the limitations for selected technologies are now considered.

3. Causes of the limitations on NDT performance

When the various studies which consider the detection and sizing capability of the various NDT technologies are reviewed it is seen that the laboratory, production and in-service inspection capabilities are significantly different.

Four fundamental areas can be identified as the causes for the limitations on NDT capability:

i. The physics of the fundamental interactions.

ii. The instrumentation which is used.

iii. The inspection techniques, including human factors.

iv. The defect population; its range of types and sizes, base material properties and the component geometry.

From an engineering viewpoint (14) the problems associated with the current NDT technologies have been summarised as;

1. Lack of NDT considerations at the design stage.
2. Inadequate 'engineering' of the NDT techniques.
3. Defect detection requirements which are often too close to the detection threshold.
4. Human factors in the inspection cycle.

The two lists of problems/limiting factors are complementary and are expressing the same problems from different viewpoints. It is also clear that effective NDT can only be provided if its requirements are an integral part of the design process. The ideal is that there should be design-for-testability; in practice the capability of NDT and its limitations resulting from design decisions and their implications for the reliability of inspection need to be quantified.

It would appear that the major factors which limit the detection capability for laboratory NDT to the levels given in Table 1 are those of the interaction of fundamental physics with particular defect populations and material properties. In laboratory measurements the geometry tends to be simple, the surface finish is good and the quality of staff is high.

In the case of practical work performed in production or in-service conditions it would appear to be the instrumentation and the inspection techniques, including the human factors which are much more significant. Also in such situtations the part geometry is more complex and small changes in geometry or material can have very significant inspection implications. The importance of human factors in field NDT is clearly indicated by the data given in Table 2.

In the mid-1970's it was recognised that there was a lack of an adequate science base for NDT to become a quantitative science, in particular it was necessary to improve the reliability of inspections. Major progress has since been made to correct this through several research programmes including one sponsored through the USAF-DARPA which has looked at quantitative NDE required to meet aero-space needs. This work initially concentrated on ultrasonics but it then expanded to consider eddy-currents and more recently it has been widened further to consider most of the other NDT technologies and also a range of new materials. More than 60% of QNDE Research over the last 10 years has concentrated on ultrasonics and it is in this field that the best science base has now been developed. Major progress is now also being made with other technologies.

When any particular technology or system is reviewed it is important to understand what it is that is limiting the capability of that particular system, technique or technology.

The important area from the point of view of inspection in production and in-service is the NDT capability in these non-ideal environments, which is seen to be significantly poorer than in the laboratory. (See Table 1) Three aspects of NDT performance are important and can be used to measure system performance and these are the probability of detection, minimum detectable defect and the sizing capability. The automation of conventional inspection has, in general, been found to improve repeatability of data collection and hence the POD through the reduction of the uncertainty inroduced by inspectors. However automation to date has appeared, in general, to reduce the sensitivity of the detection capability measured in terms of the smallest detectable defect.

If the data shown in Table 1 is considered further three sets of NDT detection limit are shown. When these limits are considered in detail those for laboratory inspection are found, in most cases, to be clearly linked to the fundamental physics.

3.1 Ultrasonic NDT

For example if the case of the detection limit for ultrasonic NDT of 0.12 mm is considered it is found that in steel this corresponds to a defect with dimensions of one wavelength at 50 MHz or about $\lambda/4$ at about 12 MHz. For powder metals significant penetration cannot be achieved much above 20 MHz, and this size feature would then correspond to a feature with a dimension of 1/5th of a wavelength.

A range of computer based forward scattering models have now been developed which can predict ultrasonic performance. The best models appear to be those produced at Ames Laboratory, Iowa State University. (Thompson and Gray (10)).

For current NDT practice on turbine discs with conventional equipment and techniques, ultrasonic limitations diagrams can be produced which can highlight regions where poor inspection capability is found in a particular geometry. Such schemes also enable scanning procedures to be specified. This data then requires to be evaluated in terms of the complete design and the corresponding service parameters to give a life for a part, given a particular defect at a specified location. In many cases when conventional ultrasonic shear or compression wave techniques are employed, for finished components, it is the part geometry which limits the NDT capability.

3.2 Eddy current and other EM NDT

This is a technology which has seen considerable improvements in detection capability in recent years. However many simple problems involving cylindrical coils and simple defects remain analytically intractable.

It is however found that it is the eddy current skin depth and the probe characteristics, in particular those of the ferite core material and the ratios of these parameters with defect dimensions that in general determines detection capability.

To extract more data from eddy current inspection multifrequency systems are now being used. Also some work is in progress to use data collected as a part is scanned. However much work remains to be done if an adequate science base for eddy current defect interactions is to be developed and more quantitative analysis provided.

For the electromagnetic inspection technique known as ACFM two famalies of approximate theory solutions are available for field-defect interaction and these correspond to thick and thin skin approximations both defined in terms of the D/δ ratio, where D is the defect depth and δ is the skin depth. For ACFM the theory is simpler than for eddy currents as the problems in general reduce to calculation of the potentials in a surface skin and hence only involved two space dimensions. (Dover et al (25)).

3.3 Radiography

The fundamental aspects of X and gamma - radiography are well established. A full review of the basic concepts for high resolution radiography can be found in various papers including Parish (26).

The most important parameter which can be used to characterise a radiography system is its spot size. This is determined by the wavelength for tne radiation given at a particular energy and the geometry of the x-ray tube and detector employed. Spot size down to 0.5 mm and now much less are being achieved. It is then the detector geometry and the sensitivity of the film/detector employed, given the number of photons received which determines detection and resolution limits and the sensitivity. To reduce exposure time and improve imaging capability for thick metal sections gamma radiography is used.

For the material under examination it is the variation in the various absorption and scattering processes which combine to give the variations in exposure seen at the radiographic detection system.

If the focal spot for the system is used to define an image pixel then the use of projection radiography can further improve performance in terms of resolution and also increase the radiographic contrast. However some types of defects such as tight fatigue cracks, at least in some orientations, may not be detected using conventional radiography.

When production inspection is considered inspection time, limits on radiation levels and part geometry will all limit performance. The most interesting areas for development are micro-focus radiography and CT scanning.

Forward models for simulated radiographs have been developed in some fields and CT-computed tomography system modelling is now being developed. The capability of advanced radiographic systems is considered further in section 4.

3.4 Penetrant NDT

This family of inspection techniques can be considered in two groups; i. dye penetrants and ii. fluorescent penetrants.

For both these groups of substances and their related cleaners, removers, developers and contrast agents the fundamental properties as well as their analysis is based in the field of physical chemistry. There would appear to be no simple parameter which corresponds to the ultrasonic D/λ ratio or the eddy current skin depth δ which can be used as a measure of expected detection capability.

The key properties of the penetrants are their low viscosities and their ability to penetrate into open fine cracks. The second aspect of the technology is that sufficient penetrant will remain in a fine small crack after cleaning and developing to give either a dye or a fluorescent indication which can be easily (?) detected by either an inspector or an automated inspection system. It is interesting to note that the data given in Table 1 gives penetrant as the technology which provides the lowest detection limit, at 1.25 mm, when used for in-service inspection. The data given in Fig 2 clearly indicates the current variability found with this technology.

3.5 Imaging systems

The range of acoustic imaging techniques employed in NDE has been reviewed by Tittmann (27). For all technologies which produce an image such as a B or a C-scan in ultrasonics, or similar display for other technologies, in particular those which employ digital systems, it is the 'pixel' or picture element size which sets detection limits and this is combined with the number of sensitivity levels which can be resolved within each pixel. A defect smaller than a pixel in size will in most cases not be seen. False colour is now used to enhance defect identifiction in an image and this can improve performance. A range of time sequence analysis and inversion tools can be used to give data on defect characterisitics. However all systems have limits to performance set by the fundamental physics.

4. Current trends and future developments

With the improved understanding of the NDT requirements and the complete systems that have been developed, new inspection techniques are being introduced to improve the probability of detection and also give quantitative defect characterisation.

A series of major research studies continue to be followed in the investigation of fundamental phenomena upon which the various NDT technologies are based. Work has now diversified into all the common NDT technologies.

The focus of the more fundamental NDE research is changing and projects are now considering the monitoring of material properties in the fabrication process as an extension of process monitoring or NDT in new materials, metal-metal composites, fibre reinforced ceramics etc, rather than basic NDT applied to traditional metals. Also work is considering the consolidation of the last decades research achievements into industrial applications and the introduction of artificial intelligence and knowledge based systems for data analysis are being investigated.

The current changes in NDT are to be seen most vividly in the changes in the instrumentation used in NDT. Analog electronics and systems which require skilled human manipulation are being replaced with automated inspection, as in the Rolls Royce 'No Eyes NDT' programme (14). Computers, digital systems, automation and now robotics of all types are increasingly being drawn into use in industrial NDT. Computer based signal processing, data display and inversion schemes are now being developed together with artificial intelligence and knowledge based systems.

Probably the most significant change has been the increasing attention and the level of the funds being devoted to the development of inspection systems. In particular early NDT reliability studies had tended to show poor probability of detection capability in manual inspection systems. The move to automated NDT wherever it is practical in the aerospace industry is to be clearly seen. With regard to NDT equipment requirements the needs highlighted in the ENSIP report are shown as Table 3.

When these moves towards systems are reviewed it is found that although progress has clearly been made much of the technology that has been developed still requires evaluation under field conditions and for the results of such trials to be fully reported.

What is probably the largest group of new NDT inspection technology has been developed by the USAF at Kelly Air Force base. These facilities have been reported to have cost $15M US and were due to come into operation in mid-1986. This system has been reported in several publications (28,29). Although significant evaluation work has been performed on the system it will be interesting to learn what its capability is under real inspection conditions when the evaluation is performed on parts that have been in-service. It should also be noted that much of the potential capability which is clearly available in USAF Kelly systems has yet to be fully employed with the field application of the new advanced quantitative NDE defect characterisation schemes.

All the major aero-engine manufactures have quantitative NDE or NDT improvement projects in progress. In the UK Rolls Royce have said that they have made improvements to their NDT in the areas of; real x-ray, penetrant blade inspection, ultrasonic disc inspection, MFI applied to shafts and various eddy current applications. These developments have been combined under the general heading of'No Eyes NDT' (14).

In a paper such as this it is probably best to seek to highlight the key elements in the various technological advances which could form the basis for systems to inspect EFA components both at fabrication and which would be needed to give data for use in any fracture mechanics base lifeing programme.

4.1 Ultrasonic NDT

This has been the area that has received most research interest for more than a decade. A wide range of theoretical developments have been made and models of a range of types can now be used in the design and validation of new NDE techniques. Current interest is in the extension of theory to cover more complex and rough scatterers and solve inverse scattering problems.

Central to almost all advanced ultrasonic NDT is the move to computer based systems which are either mixed analog/digital or completely digital. This new technology has opened the door to a wide range of improved imaging, image processing, signal processing and inversion schemes (30). A key area in this change has been the increased capability of high speed analogue to digital conversion. For transient 20 MHz signal capture, a 100 or 125 MHz sampling capability is now available in several instruments. The availability of standard ultrasonic transducers which can operate at frequencies above 50 MHz has significantly improved the potential detection capability in high frequency C-scan or acoustic microscopes. Standard analogue ultrasonic instruments are now available which work up to 150 MHz.

Ultrasonic NDT considers data in two ways (27); i) an image such as in the form of a C-scan or ii) analyses of scattered signals. In scattered wave analysis data is extracted from the wave type, magnitude, time of flight or spectra or through the use of some form of inversion scheme such as Born inversion which gives a defect size as a number, rather than data in the form of a normal image.

The ranges of sizes of defects of interst for powder metal inspection defects are in most cases small and in the range of 50 to 1000 μm which gives scatterers in the mid-frequency scattering regime for a range of ultrasonic frequencies. Simple imaging with a C-scan will not adequately characterise a defect unless measurements are made at a very high frequency, where attenuationis higher and inspection depth is then limited.

When the detection capability of an ultrasonic system is evaluated using the responses for flat bottom holes signals from '2/64" holes can be detected quite easily. However any amplitude based size calibration has its limitations as real defects are found to have acoustic responses which are much weaker than a FBH of the same physical size. In any particular alloy it is the grain boundary scattering which can be expected to set the sensitivity limit for the system.

Conventional ultrasonic disc scanning would provide a C-scan which records signals measured on the A-scan that cross various gates that correspond to a spcific volume of interest. The number of bits or digitisation levels then becomes a key factor in the derimination of system sensitivity and dynamic range. Several C-scan systems on the market are only working to 4 bit resolution.

Given computer based systems and digitised data, improvements can be made to the system signal-to-noise performance. Most techniques which improve the S:N have implications with regard to either scan times or computer power needed or both. Increasing the power to the transducer has been shown to be able to increase signal levels by up to 12 dB. The use of focused transducers can also provide improvements in power levels by up to 6dB.

Averaging is found to improve S:N performance by several dB, for example, in theory if only random noise is present given some 10 cycles an improvement of 40 dB could be achieved. In practice between 3 and 6 dB reductions in noise are achieved by 64 averages; however this does depend on material properties and grain size. More

complex techniques such as cross correlation and autocorrelation could be employed. Given a real system an improvement of the order of 30dB in S:N can be achieved for a given signal. Various forms of deconvolution can also be employed to remove constant background signals and reduce signals to their impulse response given the optimum filter. Dynamic averaging can be used on course grained materials where the transducer step is small compared with significant defect sizes and the signals are averaged in groups of three or more nearest neighbours. Signal processing, such as deconvolution, is also an integral part of ultrasonic spectroscopy.

Many papers have been written on signal processing for NDT; however most systems in use for engine component inspection at present appear to use simple pulse-echo measurements and A-scans with sensitive analog ultrasonic equipment where the record is a C-scan that shows where signals have crossed gates set at particular levels. Over the next few years there can be expected to be increased use of digital ultrasonic instrumentation. New transducer configurations and direct computer based inversion such as Born inversion or SPOT employed. Both immersion and water jet couplant systems are being employed.

It must be stressed that although the use of a digital system to scan parts can provide improved detection and characterisation capability, this can only be achieved, through an increase in the time required to inspect a part. The scanning speed available with on-line A/D conversion is relatively slow, when compared with the data rates for peak height gate detection achieved in conventional analog instruments.

When the ultrasonic aspects of inspection are considered there are three basic types of ultrasonic NDT that appear to show the greatest potential for aero-space critical components such as discs and all these remain under investigation.

a. For bulk inspection with improved transducers;

Using broad band or focused high frequency ultrasonics. (10 to 50 MHz). Such bulk inspections can be used to produce an image (C-scan) or individual reflected pulses can be studies and inversion schemes such as SPOT or Born inversion can be employed. The digital systems now being developed with colour graphics systems can give improved detection capability. The capability of the various inversion schemes which are being used to characterise small scatterers remains the subject of debate and further evaluation work is clearly required.

b. For surface inspection two specific technologies are under consideration.

These involve; i. the use of leaky Rayleigh waves and ii. the acoustic microscopic at about 50 MHz. (31); a major part of the contrast in the acoustic microscope is due to the presence of leaky Rayleigh waves, so these technologies are related.

In the case of leaky Rayleigh waves generated with a compression wave transducer set at the leaky Rayleigh wave angle, a study which uses about 20 discs with both real and simulated defects is understood to have been performed in Canada to evaluate the detection and characterisation of the technique, and also to make a comparison with eddy current methods. This study would appear to indicate that there is considerable potential for this type of inspection, although the findings of the work have yet to be fully reported (32).

The acoustic microscope has been developed significantly as an industrial tool by GE in the USA (31) to give an instrument working mostly at 50MHz, but it can be used at almost any frequency between 10 and 100 MHz, and this has the scanning capability to look at complete discs. This work at GE has taken this technology from the laboratory onto the shop floor.

One difference between an acoustic microscope and a normal C-scan system used near a surface has been said to be that the C-scan looks at the compression wave signals reflected from a particular plane, whereas an acoustic microscope looks at a combination of compression and leaky Rayleigh waves generated at a surface. The compression/leaky Rayleigh wave interaction is characterised by the V(Z) cuve.

Various other aspects of ultrasonics remain of interest and are areas for development. In the field of transducers the PVDF and related plastic transducer materials have considerable attraction in terms of their bandwidth capability, however todate their sensitivity has not been as good as that achieved with conventional ceramics. Work in the SONAR field may well bring further developments which will help NDT and improved piezoelectric polymers can be expected within 5 years.

Other areas for possible development are the EMATS, laser generated ultrasound to give non-contact inspection and the use of phased arays for improved scanning.

EMAT's (Electromagnetic Acoustic Transducers) have now been developed which can operate up to a frequency of about 5 MHz. The major problem is the generation of a very high magnetic field in a small volume and the heating due to the high currents

required to flow in fine wires. They are also attractive as they can generate shear waves, both SH, SV and Compression waves depending on the design used. They are one of the few practical ways to provide SH waves which have considerable attraction for use as an inspection wave field, not least because the mathematics used to analyse the scattering problems is much easier than for SV-C wave problems.

However it is doubtful that EMAT's using conventional technology will be available to operate above 10 MHz within 5 years. The use of superconductivity may provide the necessary technology, but such ideas have not yet started to be developed.

Laser generation of ultrasound is an area of current work (33). It has considerable potential for non-contact inspection. Given optical fibre technology using this form of ultrasound generation and detection it may be possible to provide inspection inside a complete engine in much the same way that an optical inspection can be performed now. Work is in progress to understand, and use, both the surface waves and the bulk waves given using laser generation of ultrasound. This is at present a laboratory technology, although at least one equipment company has demonstrated a commercial instrument.

There has been significant interest in the development of phased array ultrasonic systems. Most of this work has been limited to the inspection of thick steel sections in the nuclear industry. Todate many systems have operated at low frequencies and the numbers of elements in the arrays have been limited, not least because of the complexity of the electronics involved. Complex arrays are used extensively in medical ultrasonics and in the fields of Sonar and Radar. If the costs can be reduced there is potential for the application of this type of technology in NDT. Linear arrays and simple cylindrical arrays are being employed in medical systems, but as with nuclear inspection this tends to be at a lower frequency (5MHz) than that used in aero-space NDT.

In addition to a vast programme of NDT research for aero-space disc inspections, a wide range of projects and systems have been developed for power generation turbine inspection. This has included work on blade, disc and shaft inspection. Digital NDT sets have been developed in the USA for EPRI (34). One type of system of possible interest for use on EFA are the rotor shaft bore inspection tools. These include heads with a range of transducers connected to a multiplexer and a computer based data recording system. Similar technology is under development in the UK.

In the 1974 data given in Table 1 it was stated that a laboratory detection limit for surface cracks in steel using ultrasonics is 0.12 mm (120 μm) and a production limit of 3mm could be achieved. Using leaky Rayleigh waves at 10 MHz, cracks of 0.05 mm (50 μm) are easily detected on a good surface. When focused ultrasound has been used on powder metal with a grain size of 10 μm ceramic inclusion down to 50 μm can be detected with a 70% POD.

Various defect characterisation schemes such as Born and SPOT (which give type, size and orientation data) are now available for evaluation on real components. Given improvements in transducers and automated digital instrumentation production ultrasonic NDT should be capable of development within 5 years to get close to the 50 μm limit for reliable inspection of powder metals where the grain size is 10 μm or less. When the system now available at the USAF Kelly Air Force base is evaluated and the results reported it may be found that this level of performance has already been achieved in an automated system for use outside the laboratory.

For complex parts the use of robotic systems using non-contact ultrasonic techniques, leaky Rayleigh waves, EMAT's and laser generated ultrasound all have attractions and can be expected to be evaluated.

4.2 Eddy Current NDT

Eddy currents have been demonstrated to have a good capability for defect detection using automated linear probe scanners for disc and blade fir tree regions and rotating probes for use in bore holes. Eddy current NDT can in many geometries be expected to detect defects with a high reliability down to crack depths smaller than 0.010 inch (≈ 0.24 mm) and in some cases to half this figure.

The science base for the quantitative understanding of eddy current defect interaction is weak. Theory based on analytical solutions is limited to symmetric geometries and non-magnetic (linear) isotropic media with coils made from a single loop. A summary of much of the available theory has been provided by Tegopoulos and Kriezis (35). The current state of mathematical modelling for NDT, including for eddy currents has been reviewed by Georgiou and Blakemore (36). Most recently there has been progress with an exact analytical solution for short air cored coils near a halfspace provided by Burke (36,37).

Todate little has been done to extract more quantitative sizing data from the conventional eddy current impedance plane displays. Multifrequency instruments have been introduced and eddy current arrays are being investigated. However most systems still use a relative rather than quantitative sizing technique.

Further significant improvements in the fundamental science base for eddy current defect interaction can be expected within 5 to 10 years. Progress is being made by several groups. The complete analytical solutions for many 3-D probe-field-defect interactions cannot be expected, at least in the short term, but numerical models and approximate theories are being developed, although progress does remain slow.

Major progress has been made in terms of detection capability using small ferrite cored probes such as those produced by Rolls Royce (14). In the USA the YIG sphere has been developed as a sensor at Stanford University and this is under evaluation by GE, with USAF support.

As with ultrasonics, advanced analog and digital eddy current NDT systems are under development. Also automated scanning has already significanly improved the detection capability that has been achieved on real components. Multifrequency instruments can be expected to be developed further. New forms of data treatment, eddy current inversion and data display are all under consideration. At present the major problem is the lack of adequate forward models for the field-defect interactions.

Eddy current systems which employ the Nortec 33 are part of the Kelly USAF base inspection system. (28) Also as part of this program a range of small probes are being developed and evaluated. (38) For eddy current inspection the probe design is a crucial element.

In addition to conventional eddy current NDT there are various potential drop techniques; DC-PD and AC-PD. Significant progress has been made in the application of ACPD or ACPM to offshore structures. (25) The theory involved in field-defect interaction is simpler than for conventional eddy currents. It is a technique which has been extensively developed to monitor crack growth in fatigue studies. Point contacts are required to measure the potential on the part. As yet little data is available to indicate what its detection limit is for the smallest detectable defect and no POD data is available for disc inspection.

Two new electromagnetic NDT systems have recently become available. The first system is made by FN Industries and it is designed for turbine disc inspection. The system uses Nortec eddy current equipment, and Intelledex Robot and DEC computers. Few details have been released but its specification states that it inspects discs with a maximum diameter of 1200 mm and with a thickness of 500 mm. The claimed inspection capability is detection down to 0.8 mm (800 μm) surface length.

The second system uses Electric Current Perturbation methods and it has been developed by Southwest Research Institute for use on non-magnetic super alloys and evaluated on the F-100 engine discs. The ECP system can be used to scan a wide range of disc regions. Traces have been shown with indications from notches down to 0.22 x 0.05 mm. Good signal to noise is being given for defects of 0.47 x 0.17 mm.

In the data given in Table 1 the eddy current laboratory limit was given as 0.15 mm (250 μm) and the production limit was given at 2.5 mm. It has been reported that using Rolls Royce probes with conventional equipment defects down to 30 thou long and 10 thou deep (≏ 0.65 x 0.25 mm) are being detected. A crucial element in determination of the detection limit is combination of surface state, probe design and its frequency, and both the material properties and the geometry.

4.3 Radiography

There have been very considerable advances in radiography in recent years. Much work has been performed in the medical field and there is technology which could be applied to NDT problems.

Two areas where there have been particular developments are in microfocus X-ray and computed Tomography (CT). This is now being developed for limited sector scanning which has considerable potential for both turbine blade and olisk inspection.

The use of microfocus techniques has reduced the spot size and projection radiography combined with new thin solid state detectors has improved system resolution when compared with the data given in Table 1.

The major developments have been in the sytems which have been produced. A system XIM; x-ray automated turbine blade inspection system (39) has been developed by GE. This claims that the goals of 90% probability of detecting flawed blades at 95% confidence were exceeded when running automatically with automatic image processing. This sytem uses both digital fluoroscopy and computerised tomography. As yet no complete statistics are available and a full evaluation in a factory away from the production team has yet to be completed. It is however clear that this system is a significant development.

Some of the best quality images of blades available appear to be those obtained using a Bio-Imaging Research Inc system known at RADAPT(4); which has 16 bit digital data capture and a range of image processing. This company is also working on limited angle CT systems. In addition to a range of hardware a computer based image simulation system is available to enable predictions of performance to be made. Using the limited angle CT there would appear to be potential for scanning blisks, but it is going to depend on specific geometries.

It is to be expected that within 10 years CT systems will be used for the routine inspection of turbine blades. Real time radiography, and digital radiography based on solid state detectors can be expected to be develped further. A major factor which may limit their use in NDT is the initial capital cost of a system.

When a CT system is used there can be solid state detector widths down to 4 thou which can give 25 micron spatial resolution. The detection capability for density change is 0.02%. This figure was obtained for CT on a hemisphere of polymer of about 6" in diameter. This data can be compared with defect detection limits in steel of 0.5 mm given in Table 1.

4.4 Penetrant NDT

Dye and fluorescent penetrant inspection are commonly used inspection techniques applied to blades and small discs. However as already stated the capability of this technology can be unreliable. The major problems have been associated with the human factors involved in viewing each individual blade in a dark room. There is a large uncertainty in the POD due to this human factor. It has been shown that the best improvements in POD are achieved through the use of several independent inspections.

As in other fields of aero-space NDT automated blade viewing systems are being developed. Work has been performed by Rolls Royce to give a system which uses laser scanning to detect remaining penetrant. Similar work is in progress in the USA. Only limited data has been found which quantifies the performance of the current automated and semiautomated penetrant inspection. This technology can be expected to remain in common use for large area inspection; the current best practice must become the norm. In the course of the next few years the various completely automated penetrant systems can be expected to be in operation and evaluated.

It has been predicted that the detection of surface cracks, inclusions and large grains in forged and cast materials will within the next 5 to 10 years be performed by automatic systems that will replace humans used for surface inspection in dye penetrant inspection.

4.5 Characterisation of defect populations

As new materials are introduced, in particular powder metals data is needed to establish expected defect types and their characteristics. Data is needed to establish possible inclusion materials. Also it is clear that as soon as a particular class of defects are identified steps will be taken to change the production process to remove them. Defects in powder metal material can therefore be expected to be random in their nature and characteristics.

5. Conclusions

The best detection capability for the various NDT technologies available in the laboratory would in all cases appear not to have significantly improved since the mid 1970's. However the ability to apply the technologies in industrial environments has been significantly improved over the past decade.

The largest single factor which has caused the probability of detection improvement in industrial NDT has been instrumentation development.

Computer based digital systems, automated inspection and increasingly robotics will increasingly be employed in engine NDT.

The improved science base has also been of importance in the general move from qualitative to quantitative NDE.

When the various NDT technologies are considered;

5.1. Ultrasonics (in all its various forms)

An adequate science base for forward modelling is now available for many problems which involve simplest defects. For specific systems the ability to make good predictions of performance is now available. Major developments are expected to be in the field of automated systems, digital instrumentation, automated inversion schemes and possibly through the introduction of artificial intelligence (AI) techniques. Ultrasonics can be used for both surface and body defects. On powder metals various forms of ultrasonic NDT can be expected to perform well down to defect sizes of 100 μm and probably down to 50 μm (0.05mm) for defects including voids, inclusions and open fatigue cracks. Complex geometry does introduce limitations on where it can be employed on finished parts. In new materials more information on defect populations is required.

5.2 Eddy current/other electromagnetic techniques

The science base for eddy-current defect interaction is still weak. This is an area of considerable current work. Conventional eddy current instruments display the impedance plane; such displays and data extraction are not adequate for quantitative NDE. The use of multifrequency instruments can be expected to be extended. Improved probes can be expected to be introduced into many systems. New displays and data extraction techniques which include scanning data are being researched. Defects down to 30 thou. surface breaking length and about 10 thou. deep (0.75 x 0.25 mm) and in some cases down to 0.005 inch (0.12 mm or 120 μm) deep cracks can now be detected in many components including where the geometry is complex such as in bolt holes or on blade fir trees.

5.3 Radiography

There is a well established science base. The major developments here are in the fields of microfocus systems and the development, and move to use, real time imaging systems, including those which employ digital image processing. Automated image analysis is under consideration; however manufacturing tollerances and image analysis tollerances are causing very high defect identification rates. Defect detection capability depends on contrast between defect and host; definable detection levels. Computerised tomography can be expected to become routine for blade inspection.

5.4 Penetrants

Completely automated systems which include defect analysis can be expected to be available within 10 years. The current performance is variable; defects with depths of 0.010 inch (0.24 mm) or less can be detected but the reliability is poor. The best current practice must become the norm. This technology is in common use and it can be expected to remain a major inspection tool for large areas, but it is only sensitive to surface breaking indications. There is a lack of a quantitative science base.

6. References

1. AGARD, (1979) NDI Methods for Propulsion Systems and Components. AGARD Lecture Series No 103. Report No AGARD-LS-103.

2. AGARD, (1985) Damage Tolerance Concepts for Critical Engine Components. AGARD Report No AGARD-CP-393.

3. Thompson D.O. and Chamenti D. Ed. (1987) Review of Progress in QNDE, Vol 7. Session on Human Factors. Plenum, (New York)

4. Spanner J.C. (1986) Human reliability impact on in-service inspection. Proceedings, 8th International Conference on NDE in the Nuclear Industry, November 17-20, Orlando, Florida.

5. Packman P.F. (and 7 others) (1978) Reliab''ity of flaw detection by NDI. In "Metals Handbook, Vol 11, NDI and Quality Control" 8th Edition, Am. Soc. for Metals.

6. Buck O. and Wolf S.M. (1980), Nondestructive Evaluation: microstructural characterisation and reliability strategies. Conference Proceedings; The Metallurgical Society of AIME.

7. Beissner R.E. (1985) Predictive models and reliability improvement in electromagnetic NDE. Review of Progess in QNDE, Vol 5, Ed. D.O. Thompson and D. Chamenti, Plenum. pp 919-927.

8. Gray T.A. and Thompson R.B. (1985) Use of Models to predict ultrasonic NDE reliability. Review of Progess in QNDE, Vol 5, Ed. D.O. Thompson and D. Chamenti, Plenum. pp 911-918.

9. Sturges D.J. Gilmore R.S. and Hovey P.W. (1985) Estimating the POD for subsurface ultrasonic inspection. Review of Progess in QNDE, Vol 5, Ed. D.O. Thompson and D. Chamenti, Plenum. pp 929-936.

10. Thompson R.B. and Gray T.A. (1986) Use of ultrasonic models as tools in the design and validation of new NDE techniques. Novel Techniques of NDE, Ed. E.A. Ash and C.B. Scruby, The Royal Society. pp 169-180.

11. Comassar D.M. (1979) State-of-the-art of NDI of aircraft engines. AGARD Lecture Series No. 103. NDI Methods for propulsion Systems and components, Paper 2.

12. Branco C.M. (1985) Damage tolerance acceptance methods in structural components of a medium carbon steel and a medium strength Al-Mg Alloy. AGARD Conference Proceedings CP-393. Paper 7 (16 pages).

13. Pettit D.E. and Krupp W.E. (1974) the role of NDI in fracture mechanics application. In; ASM 3. Fracture Prevention and Control. American Society of Metals.

14. Taylor R.G. (1985) Limitations of manual NDT systems and the 'No Eyes' concept. AGARD Conference Proceedings, CP-393, Paper 5.

15. Rummel W.D.,Christner B.K., Mullen S.J. and Long D.L. (1986) Characterisation of structural assessment testing. NDI Reliability - SAT Assessment; Kelly AFB. Final Report SA-ALC/MMEI-1/86.

16. Rummel W.D.,Christner B.K., Mullen S.J. and Long D.L. (1986) Assessment of eddy current II Inspection capabilities. Kelly AFB. Final Report SA-ALC/MMEI-/2/86.

17. Pfeifer W.H. (1960) Computed tomography of advanced composite materials. Proceedings Advanced Composites Conference, Michigan 2-4 December 1985. (Preprint) American Society for Metals.

18. Norriss T.H. (1985) The role of NDT in relation to damage tolerant aircraft design. British Journal of NDT, Vol 27, pp 345-350.

19. King T.T., Cowie W.D. and Reimann (1985) DTC for military engines. AGARD Conference Proceedings, CP-393, Paper 3.

20. Koul A.K., Thamburaj R., Raizenne M.D., Wallace W. and DeMalherbe M.C. (1985) Practical experience with damage tolerance based life extension of turbine engine components. AGARD Conference Proceedings, CP-393, Paper 23.

21. Mom A.J.A. and Raizenne M.D. (1985) AGARD co-operative test programme on titanium alloy engine disc material. AGARD Conference Proceedings, CP-393, Paper 9.

22. James M.N. and Knott J.F. (1985) Aspects of small crack growth. AGARD Conference Proceedings CP-393, Paper 10.

23. Fiorentine S. Re and Walther H. (1985) Small defect characterisation in powder metallurgy materials. AGARD Conference Proceedings CP-393. Paper 13

24. Tittmann B.R., Ahlberg L.A. and Fertig K.W. (1984) Ultrasonic microstructural noise parameters in a powder metal alloy. Review of Progress in QNDE, Vol 3A, Edited by D.O. Thompson and D. Chamenti, Plenum. pp 57-63.

25. Dover W.D., Collins R. and Michael D.H. (1986) The use of AC-field measurements for crack detection and sizing in air and under water. Novel Techniques of NDE, Edited by E.A. Ash and C.B. Scruby, The Royal Society. pp 111-123.

26. Parish R.W. (1979) High resolution radiography in the aero-engine industry. AGARD Lecture Series NO. 103. NDI Methods for propulsion System and components.

27. Tittmann B.R. (1980) Imaging in NDE. In "Acoustical IMagine, Vol 9" Edited by K.Y. Wang, Plenum Publishing Corp. pp 315-340.

28. Birx D.L. and Doolin D.G. (1985) Manufacturing technology for NDE systems to implement RFC procedures for gas turbine engine components. Review of Progress in QNDE, Vol 5. Edited by D.O. Thompson and D. Chamenti, Plenum. pp 877-884.

29. Birx D.L. and Taylor F.M. (1985) Manufacturing technology for NDE systems to implement RFC procedures for gas turbine engine components. AGARD Conference Proceedings CP-393, Paper 8.

30. Wade et al (1984) Special Issue on Digital Acoustical Imaging, IEEE Trans. Sonics & Ultrasonics Vol. SU-31, (4).

31. Gilmore R.S., Tam K.C., Young J.D. and Howard D.R. (1986) Acoustic microscopy from 10 to 100 MHz for industrial applications. Novel Techniques of NDE, Edited by E.A. Ash and C.B. Scruby, The Royal Society. pp 55-75.

32. Sturrock W. (1987) Summary of NAE Research on NDI reliability.

33. Cooper J.A., Dewhurst R.J. and Palmer S.B. (1986) Characterisation of surface breaking defects in metals with laser generated ultrasound. Phil Trans. R. Soc. Lond. A320, 319-328.

34. EPRI, NDE Program Progess Reports 1979 (annual).

35. Tegopoulos J.A. and Kriezis E.E. (1985) Eddy Currents in linear Conducting media. Studies in Electrical and Electronic Engineering, Vol 16. Elsevier.

36. S.K. Burke (1985)
'A perturbation method for calculating coil impedance in eddy current testing'.
J. Phys. D. Appl. Phys. 18 p 1745-1760.

37. S.K. Burke (1986)
'Impedance of a horizontal coil above a conducting half space'
J.Phys. D. Appl. Phys. 19 p 1159-1173

38. Hoppe W.C. and Stubbs D.A. (1985) RFC eddy current probe tests. Review of Progress in QNDE, Vol 5, Edited by D.O. Thompson and D. Chamenti, Plenum. pp 893-900.

39. Olier D.W. (and 23 others) (1985) XIM: X-ray inspection module for automated high speed inspection of turbine blades and automated flaw detection and classification. Review of Progress in QNDE, Vol 5, Edited by D.O. Thompson and D. Chamenti, Plenum. pp 817-814.

40. RADAPT (1986) RADAPT X-ray Inspection Systems.
Bio-imaging Research Inc. USA.

ACKNOWLEDGEMENT

This work has been carried out with the support of the Procurement Executive, Ministry of Defence.

This paper is a summary of material first presented in a report to the RAF (U.K.), Air Engineering Branch; L.J. Bond, January 1987,
"Review the capability of non-destructive testing to inspect critical aero-engine components". Report; University College London, RAE (Pyestock) Acceptance; LSC/-/12316026 and UCL Reference; 33/170

TABLE 1-Estimated variations in flaw detection limits by type of inspection (in mm) (in Pettit & Krupp,1974).

NDT Technique	Surface cracks		Internal flaws	
	Processing	Fatigue	Voids	Cracks
Test specimens, laboratory inspection				
Visual†	1.25	0.75	+	+
Ultrasonic	0.12	0.12	0.35	2.0
Magnetic particle	0.75	0.75	7.5	7.5
Penetrant	0.25	0.5	+	+
Radiography	0.5	0.5	0.25	0.75
Eddy current	0.25	0.25	+	+
Production parts, production inspection				
Visual	2.5	6.0	+	+
Ultrasonic	3.0	3.0	5.0	3.0
Magnetic particle	2.5	4.0	+	+
Penetrant	1.5	1.5	+	+
Radiography	5.0	*	1.25	*
Eddy current	2.5	5.0	+	+
Cleaned structures, service inspection				
Visual	6.0	12.0	+	+
Ultrasonic	5.0	5.0	4.0	5.0
Magnetic particle	6.0	10.0	+	+
Penetrant	1.25	1.25	+	+
Radiography	12.0	*	4.0	*
Eddy current	5.0	6.0	+	+

+ Not applicable. † Use with magnifer. * Not possible for tight cracks. (Based on 25-mm ferritic steel, surface 63 RMS.)

TABLE 2

ENSIP NDT Preliminary conculsions - Aero engine parts

	Average	Best	mm
Magnetic inspection POD	60% - .300" crack	65% - .250"	6.35
Penetran inspection	90% - .220"	90% - .175"	4.45
Eddy current	90% - .090"	90% - .030"	0.76
Ultrasonic	80% - .375"	90% - .180"	4.57

Average results obtained from majority of technicians

Best results obtained from top 10% technicians

TABLE 3

ENSIP Requirements for Equipment improvement

Equipment	Improved signal-noise ratio
	Channel attention of inspector to flaws
	Provide positive assurances equipment is performing intended function
	Automate control and programme functions susceptible to human error

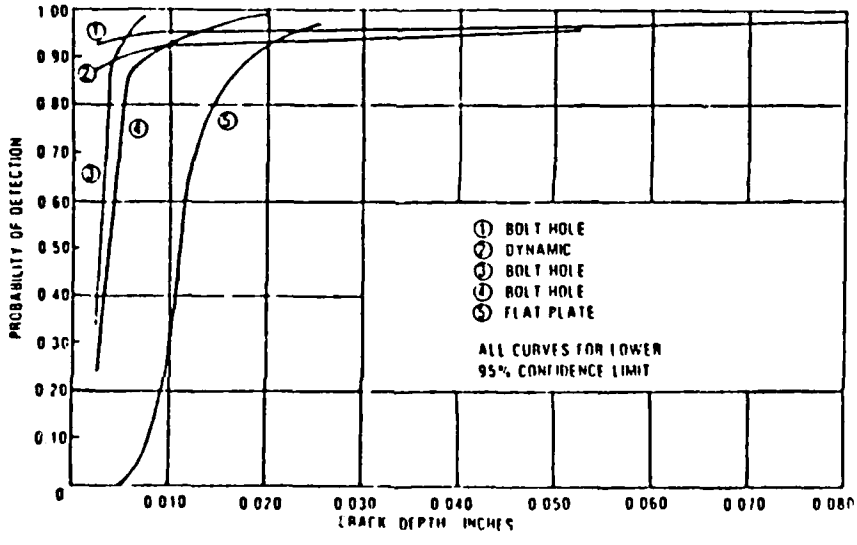

Figure 1 - Probability of Detection using Eddy Currents

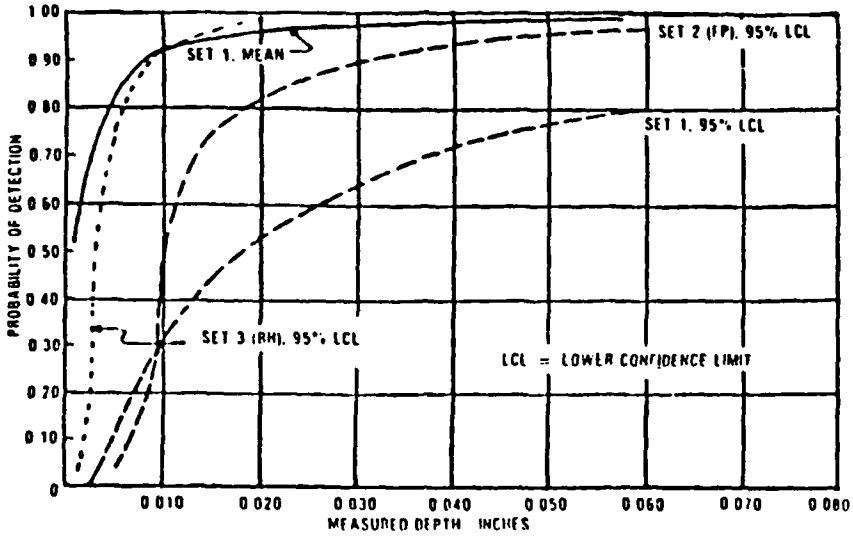

Figure 2 - Probability of Detection using Fluorescent Penetrant Inspection (FPI)

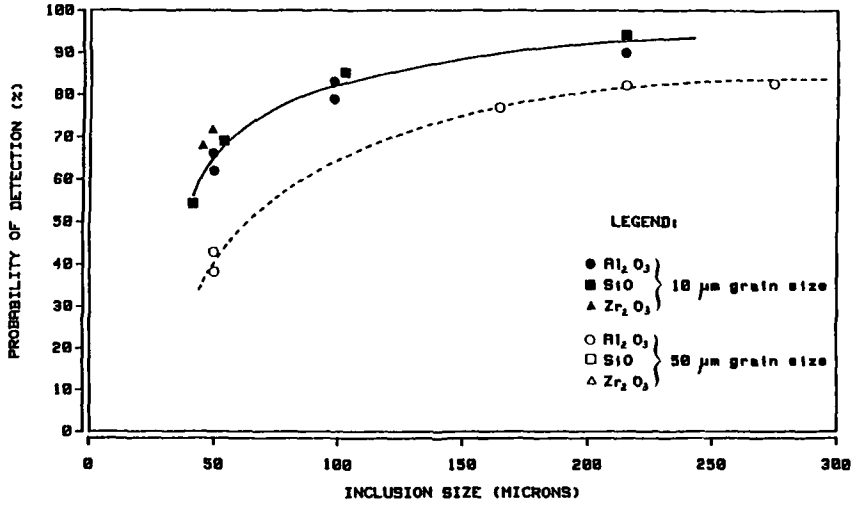

Figure 3 -Probability of detection for inclusions in ceramics.

RELATIONSHIPS OF NONDESCTRUCTIVE EVALUATION NEEDS AND COMPONENT DESIGN

by
John A. Harris Jr.
M.C. VanWanderham

Pratt & Whitney
Materials Engineering
P.O. Box 109600
West Palm Beach,
Florida 33410-9600 U.S.A.

Synopsis

Several well publicized engine and airframe failures which occurred in the late 1960 to mid 1970's time frame resulted in emphasis on development, application and quantification of nondestructive evaluation (NDE) as opposed to reliance on a "Zero Defecus" design philosophy. As the use of fracture mechanics as a basis for damage tolerance and retirement analysis of components became established, additional emphasis was placed on screened flaw sizes, NDE and quantification of reliability. In the late 1970's a structural assessment was conducted on the design of the F100 engine which resulted in a series of relatively sophisticated "safety inspections" for selected critical components. The Retirement for Cause philosophy also coupled NDE and component lifing analyses to enable return to service decisions for engine components. These activities were (and are) performed usually after the component designs have been finalized. The establishment of "Engine Structural Integrity Programs (ENSIP)" for new U.S. military engine systems has now made NDE considerations an integral part of the design process. Classification of components, fracture mechanics analyses, critical flaw sizes, material quality, NDE and quantification of inspection reliability are now incorporated in the initial design process and directly influence the resultant component deigns Statistically based probabilistic approaches are supplementing the deterministic methods previously used. This paper discusses the relationships of NDE needs and component design in light of the evolution of the ENSIP approach for gas turbine engine component designs.

Background

Nondestructive evaluation (NDE) requirements for aircraft gas turbine engine components had traditionally been defined after the designs of those components have been established and the engines were in production and operation. The usual scenario had stringent inspection requirements imposed upon an engine component, or class of components, as a result of an unexpected operational occurrence. To maintain safety or reduce maintenance costs, an inspection requirement was defined, and all suspect components inspected, allowing the components to be cleared for continued use or mandating their replacement. Often the resulting inspection requirements pressed the state-of-the-art of nondestructive evaluation technology. The common complaint of the NDE specialist was that with no advance notice the required NDE techniques were not available, requiring frantic development and implementation activity. In response, the engine designer would apologetically state that the particular occurrence was unforeseen; therefore no advance notice could be given, (but please hurry).

The root cause of this dichotomy was the design philosophy in use in the 1960's. This philosophy emphasized reduction in engine weight to maximize thrust-to-weight ratio. Low cycle fatigue was the criteria for lifing purposes, with life expressed as operating time or cycles to initiate some detectable crack size, usually 0.8mm. Materials development goals were to increase the strength of materials enabling higher operating stresses resulting in weight reduction. Generally, increasing the strength of metal alloys also increased the low cycle fatigue crack initiation life of the alloys. Components were designed to be retired and replaced at that life. Experience has shown however, that increasing the strength of a material often results in a reduction in its resistance to crack growth or its damage tolerance capability. This trend is shown schematically in Figure 1, with example engines plotted for reference. At the time however, this was not the primary concern. Inspection was used in the manufacturing process to support the "Zero Defects" philosophy. That is, if something was found the component was rejected; if nothing was found the component had no flaws. Inspection techniques were generally not quantified. What was known was only what was found, not what may have existed but was not found. The consensus was that nondestructive evaluation practitioners could find anything that might be present - But then, designers and manufacturers didn't produce components with flaws anyway.

Several well publicized engine and airframe failures in the ensuring time period resulted in a change in this philosophy. Failure of a high energy (rotating) component in an aircraft engine usually results in catastrophic consequences for that engine. Although most engines are designed to

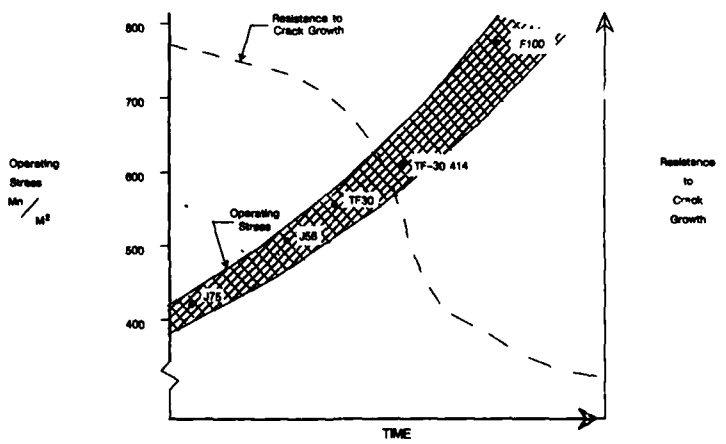

Figure 1. Early Design Philosophy Emphasized Increased Material Strength At The Expense of Damage Tolerance Capability

contain blade failures, failure of a fan, compressor or turbine disk or spacer results in loss of power, destruction of the engine and often significant damage to adjacent structures. Even a contained blade failure can cause loss of power or engine shutdown which can also have catastrophic consequences for a single engined aircraft. Structural integrity of the high energy components in a gas turbine engine is therefore a critical factor in aircraft safety.

Cooper and Forney (reference 1) reviewed United States Air Force (USAF) engine structural failure incidents over the time period 1962 through 1977. In that fifteen year period 235 accidents were reported to have occurred as a result of engine component failures. These failures may be segregated (Table 1) by component type and engine section: 73 in fan/compressor sections; 67 in the turbine section; 41 in the combustor section; 39 in bearings and 15 in the augmentor (afterburner or reheat) section. Similar data exist for commercial engine failure incidents. The principal cause of most of these failures was reported to be either an inherent material or manufacturing flaw that escaped detection during the manufacturing process, or service induced flaws resulting from inadequate design, foreign object or handling damage, or a change in the usage of the engine.

TABLE I

REPORTED USAF STRUCTURAL FAILURE INCIDENTS
IN TIME PERIOD 1962 - 1977*

Engine Section	Component Type	Number	Total
Fan/Compressor	Fan Blades	5	
	Fan Disks	1	
	Compressor Blades	34	
	Compressor Disks	9	
	Vanes	12	
	Other	12	73
Turbine	Blades	35	
	Disks	20	
	Vanes	3	
	Other	9	67
Combustor			41
Bearings			39
Augmentor			15
		Total	235

* From Cooper and Forney, Reference 1.

The immediate impact of a failure is usually well publicized in terms of human tragedy and loss of hardware. The significant economic impact ----the expense necessary to remedy the cause of failure---- is not often immediately visible. This includes the cost of one time, or continuing, inspections of the components, the replacing/retrofitting of components and/or the unplanned maintenance burden necessary to prevent similar failures in the future. When one considers the large number of gas turbine engines in service world wide, the economic incentive to minimize the number of component failures is immense. The realization of the safety and economic impact of these failures promoted the evolution of the damage tolerance philosophy in the design and operation of gas turbine engines. The "Zero Defects" concept, while admirable, could not solely stop component failures, as the Cooper and Forney information indicates. To prevent failures from occurring, the relationship between NDE needs and design had to change from a failure driven, after the fact imposition of requirements on the inspection community, to an interaction of NDE needs while the components were in the initial design phase. The current expression of this philosophy for new USAF engine designs is the Engine Structural Integrity Program (ENSIP) embodied in a United States military standard (reference 2). Adherence to this standard assures that interaction of NDE needs and engine design occurs in the initial design and manufacturing stages with the goal of failure prevention. It is hoped that the unexpected failure - reaction mode of the past will be minimized, thus both lowering system life cycle costs and improving the state of system readiness.

F100 Structural Assessment and Retirement For Cause

Two activities which started in the late 1970's will be reviewed here as much of the philosophy and many of the concepts used in damage tolerance design, and incorporated into ENSIP, were developed or demonstrated by these activities.

The F100 engine is an augmented turbofan in the 110 kN thrust class with a thrust to weight ratio of 8 to 1. The engine became operational in the early 1970's in the F-15 fighter aircraft, and is currently in operational service around the world in both the twin engine F-15, and the single engine F-16 fighter aircraft. This engine is an axial flow, low-bypass, high compression ratio, twin-spool gas turbine with an annular combustor and common flow augmentor. It has a three-stage fan driven by a two-stage, low-pressure turbine and a ten-stage compressor driven by a two-stage high-pressure turbine. A composite sketch of some rotor components of this engine is shown in Figure 2. This sketch illustrates some typical rotor component configurations and delineates nomenclature that is used in this paper.

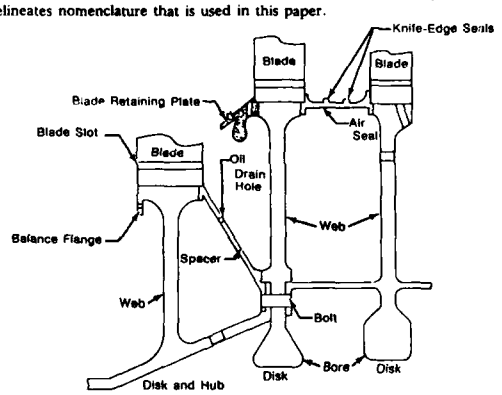

Figure 2. Composite Sketch Of Typical Rotor Components Of A Gas Turbine Engine

In light of the past experiences with component failures of other engines and because of the critical nature of the F100 engine to the USAF's (and other Air Force's) F-15 and F-16 weapon systems, it was important to obtain the best possible visibility of that engine's future structural maintenance needs and component life expectations.

Accordingly, an in depth structural assessment was performed on this engine by a multi-disciplinary team. The general objectives and process for that assessment are shown schematically in Figure 3 (Reference 3).

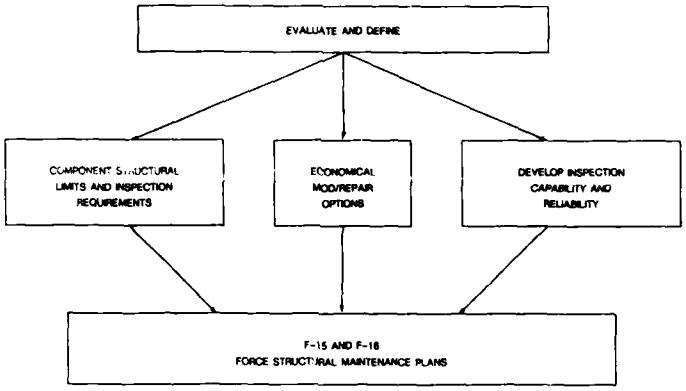

Figure 3. Objectives And Major Elements Of Structural Assessment And Retirement For Cause Activities For The F100 Engine

One of the primary objectives was to define inspection requirements necessary to protect the structural safety throughout the anticipated service life, thus preventing failures. This included identification of components and features to be inspected, when the inspections should be conducted, what inspection procedures should be used and the attendant logistics impacts. This information was then used to guide the development of the required inspection capability. A second objective was to establish economical modification and/or repair options where it was anticipated they could be utilized. All of these activities were integrated to form an overall force structural maintenance plan for the engine.

Retirement for Cause is a methodology that allows each component to be used to the full extent of its safe total fatigue life. This methodology allows use of selected components beyond their classically calculated crack initiation low cycle fatigue life. It also emphasizes the use of NDE and fracture mechanics for failure prevention, and has provided a means for the ultimate coupling of NDE needs and engine design via probabilistic techniques. The procedure has been implemented for selected rotating components of the F100 engine. This activity was discussed in detail at the 1981 AGARD Specialists Meeting "Maintenance in Service of High Temperature Parts" (reference 4), and in subsequent USAF reports (reference 5).

These F100 engine activities were important in that they formalized the approach and methods now in use to define the relationship of NDE needs and component design for United States military gas turbine engines. The balance of this paper will discuss this relationship from that perspective and from within the ENSIP context. Rotating components such as disks, hubs, and airseals/spacers will be emphasized.

The Design Approach

The overall sequence by which an engine progresses from concept to reality is shown in Figure 4. At every step, lessons learned feedback to the detailed mechanical design stage, which is the heart of the process. This feedback can result in an alteration of the design which then proceeds anew through the process. In addition to the classical form, fit and function considerations, damage tolerance is addressed at this stage, and permeates all aspects of the design activity. It is herein that NDE concerns are initially addressed.

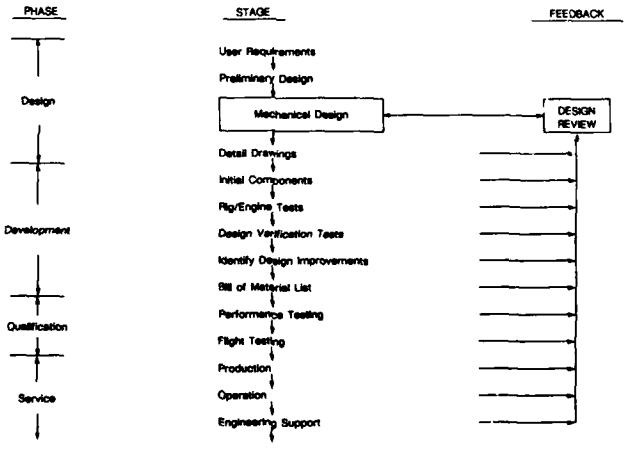

Figure 4. Detailed Mechanical Design Is The Heart Of The Engine Maturation Process

The current component design approach now recognizes that: (1) Damage, such as cracks or crack-like defects can occur despite stringent preventative actions taken to protect against it; (2) NDE capability exists that will permit detection of damage prior to complete component failure; and (3) High energy components must be designed with adequate residual strength and crack growth capacity to preclude failures from damage incurred between scheduled maintenance and/or inspection actions. That damage may result from either manufacturing or in-service related occurrences. Manufacturing damage typically occurs from material or process related anomalies, while in-service damage may occur as a result of mishandling, foreign object damage (FOD) or low cycle fatigue initiated cracks.

Damage from manufacturing defects and fatigue initiated cracks can be minimized by use of damage tolerance criterion. These criteria are usually based on fracture mechanics analyses tied to an acceptable initial flaw size which is supported by demonstrated manufacturing and/or in-service NDE capability. The acceptable assumed flaw size is generally considered to be the smallest size which can be reliably detected (found) with available NDE techniques for a given component configuration.

The term NDE reliability as traditionally used encompasses both a probably of detection (POD) and a confidence level for a specific flaw size: NDE capability implies both an inspection technique and its reliability. The flaw size established is then used as a starting point for fracture mechanics analyses to predict remaining life during crack growth and residual strength capacity of a component's features and hence the component.

Component Classification

Early in the design stage (or as a first step in a damage tolerance assessment of an existing design) all components are reviewed for failure consequences to identify critical components. Critical components are those that experience significant combinations of centrifugal, maneuver, pressure or gas bending loads, steady state or transient temperatures, and vibration. Functional type items such as seals, springs, fasteners and mechanical mechanisms are also included in the review. The preliminary segregation of components into classes is based on collective "corporate experience"; - historical records, experience gained during engine development testing, the lessons learned and engineering judgement. The major focus is usually on life limited components, particularly those in the high energy (rotating) sections of the engine. From this review components can be classified as either fracture critical or durability critical depending on their failure impact. The classification must also consider the airframe applications for the engine.

A fracture critical component is one whose failure would likely result in loss of engine power preventing sustained flight as a direct result of the failure or as a result of progressive events subsequent to the failure. High energy rotating components such as disks and spacers are usually classified as fracture critical as the component failure would probably be uncontained or likely cause failure of other systems that could prevent sustained flight even in a multi-engined application. Damage tolerance requirements are normally only imposed on components which fall into this classification.

A durability critical component is one whose failure could result in a significant maintenance burden but would not likely result in total power loss or failure of other systems, or might result in engine power loss but not necessarily loss of flight (in a mulu-engined application).

It should be noted that identical components could have different classifications depending upon a single or multi-engined application. An example might be a compressor blade whose contained failure could result in loss of power and sustained flight (thus be fracture critical) in a single engined aircraft, but would be durability critical in a multi-engined aircraft, as flight could be sustained on the remaining engine(s). Because of potential confusion in component classification due to engine application, the term "Mission Critical" is beginning to be used in place of fracture critical. A mission critical component is one whose failure could cause the aircraft to abort its mission, regardless of the number of engines involved. To aid in the classification of components, Failure Modes Effects Analyses are often performed.

Conceptually, a third classification might apply to those items which history and experience indicate do not clearly fit the definitions of fracture or durability-critical. For these items, reliance is placed on the manufacturing operation using such techniques as statistical process control to ensure integrity. This class of components could include certain types of seals, fasteners or fittings which are replaced in the normal course of engine refurbishment, or whose demonstrated life greatly exceeds system requirements.

At this point in the design sequence, specific NDE needs for the components have not been identified, as the classification is based on failure consequences. After establishing the classifications, low cycle fatigue and fracture mechanics screening of the components takes place.

It is at this time that preliminary NDE needs are established. Should these preliminary NDE needs exceed current or anticipated state-of-the-art NDE capabilities, some redesign of the component or component feature may be required.

Design Quality Assumptions

Assessment of components for damage tolerance is predicated on the assumption that initial defects can exist at all life limiting component features. Therefore, working stress levels are established that will enable their fracture mechanics residual life to meet the required life goals. Defects of concern are of two types: (1) Surface flaws which are linear imperfections in the form of a break, fissure or other discontinuity on the surface of the component. A surface flaw is characterized as having a depth and a length. (2) Subsurface flaws which are internal (sometimes called embedded or volumetric) material defects in the shape of an irregular void that is open or partially healed. The void may contain or conform to matter that is inhomogeneous with the surrounding material (such as an inclusion). Subsurface flaws are characterized as having an equivalent planar diameter based upon inspection technique and comparison to a known standard.

Often the term "near surface" is used to describe a flaw that is located close to the surface of a component, but is not contiguous with that surface. This type of flaw is a subsurface flaw: The terminology has evolved because the inspection techniques which detect near-surface flaws are usually those used for surface inspections, and because of the inability of most subsurface inspections to reliably detect anomalies within 1 mm of the surface.

Assumed initial flaw sizes are based on defined intrinsic material defect data, known manufacturing microstructural process limitations and/or demonstrated reliability of nondestructive inspection methods employed during manufacturing. Nondestructive inspection methods typically employed during manufacturing include visual, florescent penetrant, eddy current and magnetic particle techniques for surface flaws and ultrasonic and x-ray for subsurface flaws. For some components, proof loading may also be a viable technique for manufacturing (and in-service) inspections. Variations of these techniques can be used for both surface and subsurface inspections; examples include ultrasonic surface wave inspection for surface defects on airfoils, magnetic particle inspection for surface and near surface flaws in ferromagnetic materials, and proof loading for very small surface or subsurface flaws.

Knowledge of the capabilities of the NDE methods is required because the assumed initial flaw sizes must be based on the type of inspection to be used during manufacturing or subsequent maintenance of the engine components. In addition to the inspection method, the means of performing

the inspection should be known. Three types of inspection means are usually acknowledged: manual, where the inspection device is maneuvered by hand and the interpretation of results is by the individual inspector; semiautomatic, where inspection device maneuvering may be automated but interpretation of results is operator dependent (or the converse); or automated, where maneuvering of the inspection device and inspection accept-reject criteria are preprogrammed. Typical minimum initial flaw size assumptions for flaw types and inspection means are listed in Table 2 for generic component features.

TABLE II

MINIMUM INITIAL FLAW SIZE ASSUMPTIONS

Flaw Type	Flaw Configuration	Inspection Means	Flaw Size	Primary NDE Technique
Surface Flaw (Smooth Features)	Surface Crack	Manual	0.38mm Depth X0.76mm Length	Penetrant/ Eddy Current
	Corner Crack	Manual	0.38mm Depth X0.38mm Length	Penetrant/ Eddy Current
Surface Flaw (Notched Features)	Surface Crack	Manual	0.38mm Depth X0.76mm Length	Penetrant/ Eddy Current
	Surface Crack	Automated	0.13mm Depth X0.25mm Length	Eddy Current
	Corner Crack	Manual	0.38mm Depth X0.38mm Length	Penetrant/ Eddy Current
	Corner Crack	Automated	0.13mm Depth X0.13mm Length	Eddy Current
Subsurface Flaw	Embedded Crack/Void	Automated	0.42mm Diameter* to 1.19mm Dia.	Ultrasonic

* Dependent on material and configuration.

Deterministic Lifing

Flaw location and orientation assumptions are a function of the particular system used to calculate life. Two methods are currently used. Deterministic lifing systems utilize single valued inputs or assumptions, and result in a single valued output of predicted life. Deterministically, given an initial flaw size, a crack geometry, a specified stress and temperature and the appropriate material crack growth rate model, a single value of life will result. Usually, mean input values are used and the resulting prediction represents a typical life. Factors can be applied to establish desired life other than typical. Obviously, assuming all worst case input values will produce a conservative life. In deterministic life calculations, the flaw is assumed to be of a size, located and oriented in the component or feature, so as to produce its most rapid growth. No credit is taken for incubation life; the flaw is assumed to grow immediately upon the components operation in service. NDE reliability is not an input in the life calculation, and does not directly influence the life prediction, other than to determine the assumed starting crack size. NDE reliability may be used subsequently in performing an assessment of risk in reaching the calculated life.

Probabilistic Lifing

Probabilistic lifing systems utilize a combination of data based statistical distributions of the life-controlling variables and computing techniques to predict a distribution of lives for a specified population of components. Simulation techniques are most often utilized because closed-form analytical solutions accounting for all the influencing parameters become intractable. Simulation involves construction of a mathematical model of the entire system (component life cycle) in terms of individual statistical events representing the various elements of the system. The variables which affect component life are quantified in terms of probability distributions. These distributions might include inherent material quality, crack initiation behavior, crack propagation behavior, stress and temperature variability, usage variability and NDE variability. More sophistication can be added in the form of sequencing of failure sites or fleet aging. By randomly sampling from each of the input distributions, calculating a life from each sample, and then repeating this process a sufficient number of times, an output distribution of the desired resolution can be obtained. For example, if an output resolution of 1 in 1000 is desired, 10,000 sample calculations might be conducted. Monte Carlo techniques are computationally efficient for these types of analyses.

Probabilistic techniques enable the designer to account for occurrence of material microstructural anomalies as well as the actual inspection probability of detection associated with the initial flaw size assumption. In the probabilistic approach, the entire probability of detection curve for a given inspection is used, as opposed to a single point such as the 90% POD at 95% confidence used in the deterministic flaw size assumption.

Figure 5 illustrates reliability curves for two inspection processes which have the same probability of detection at a given size surface flaw. While one could state that for an initial flaw assumption based upon demonstrated reliability either process is adequate for deterministic calculations, the predicted in-service component life could vary considerably. This is due to the shape of the curves. Using probabilistic techniques, this difference in shape can be accounted for, and may impact the assumptions used in the component design. In fact, the design of the component could be changed to enable less costly inspections to be performed, or to increase service intervals. Because of the options available to the designer, probabilistic approaches are preferred in that a more realistic evaluation of potential flaws, their occurrence, and their affect on component life capability will result.

Component Inspectibility

As the entire premise for damage tolerance is based upon preventing failure from prior or service induced flaws, and nondestructive inspection is used to detect these flaws, it follows that component inspectibility is a prime design concern. Therefore, fracture critical components or features thereof, are subclassified as in-service inspectible, or in-service noninspectible. This classification impacts the initial flaw assumptions used to evaluate damage tolerance, and the criteria used in designing and lifing components. In-service noninspectible components generally must have a flaw growth life which exceeds the desired propulsion system life by some factor. In-service inspectible components generally must have a flaw growth life which exceeds the desired propulsion system maintenance interval by some factor. As system maintenance intervals are usually a portion of the expected system service life, the assumed initial flaw size for an in-service inspectible component or feature may be larger than for an in-service noninspectible component or feature. In-service noninspectible component features have initial flaw size assumptions which reflect manufacturing NDE capability, while in-service inspectible features utilized a combination of manufacturing and maintenance NDE capabilities.

An example of an in-service noninspectible component feature might be a disk bore or rim area. In the manufacturing process, subsurface flaw

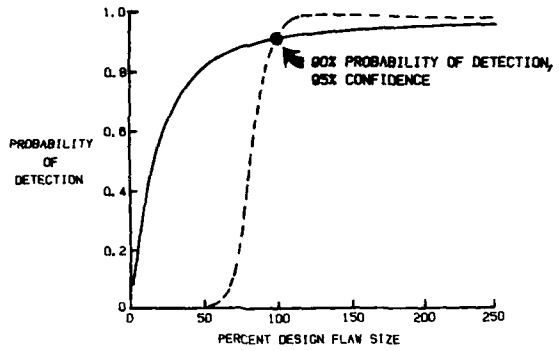

Figure 5. The Shape Of The NDE Reliability Curve Is Accounted For In Probabilistic Life Analyses

inspection is normally conducted using ultrasonic techniques with the disk in a semifinished shape. This semifinished shape is optimized for inspectibility. After clearing this inspection, the disk is finished machined. In the finished machined configuration, the bore or rim areas are not ultrasonically inspectible to the required sensitivity, therefore, subsequent maintenance inspections for subsurface flaws would be impossible. (Author's Note: Progress is being made in ultrasonic inspection technology which will ultimately allow this type of inspection on finished components, both in manufacturing and maintenance). The bore and rim areas of the disk would therefore be classified as in-service noninspectible for subsurface flaws and perhaps require more stringent initial flaw size assumptions and thus more sensitive NDE capability to meet the damage tolerance lifing criteria. Certain types of bonded joints could also fall in this category.

Surface flaw inspection is generally possible for all features of a disk using penetrant or eddy current techniques. In-service inspection for surface flaws may require sophisticated inspection equipment, but unless the configuration precludes inspection access, very few surface features would be classified as in-service noninspectible.

Maintenance/Inspection Intervals

To minimize life cycle costs, it is desirable to have no in-service inspection requirements during the engine design lifetime. However, to design all fracture critical components to enable an in-service noninspectible classification could impose significant engine weight penalties. In-service noninspectible component features are usually designed such that flaw growth life is at least twice the engine design life. Therefore, the in-service noninspectible classification should be reserved for components or features which cannot be reliably reinspected at the engine maintenance facility. For most components, the design approach would be expected to result in an "in-service inspectible" classification.

Inspection intervals for fracture critical components are predicated on a safety limit established by fracture mechanics analyses. The safety limit is the service time (or cycles) beyond which the risk of component failure is considered to be unacceptably high if corrective action, such as an in-service inspection, is not taken. This limit therefore does not represent component usable life or retirement limits; but does represent a limit on a service interval where an inspection should be imposed to prevent potential component failure. These inspection intervals are then interacted with other maintenance concerns to establish overall engine force structural maintenance intervals. Iterations may be required to optimize the component design and NDE capabilities to obtain maintenance interval goals.

It is desirable to have component residual crack growth lives (safety limits) be at least twice these inspection intervals for in-service inspectible features. This requires that the largest assumed flaw not grow to failure in two times (2X) the planned inspection interval. The relationship of safety limit and inspection interval is illustrated in Figure 6. Use of factors less than two is possible, but should be done on an individual component or feature basis predicated on mutually acceptable risk and review of available redesign options.

The frequency of inspections is therefore determined by component classification, and for a fracture critical component by it's inspectibility

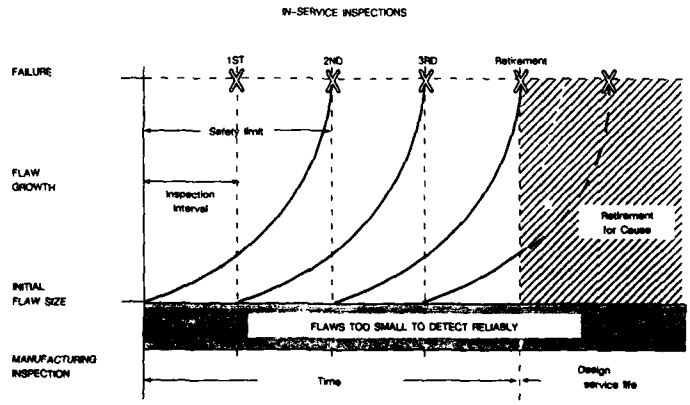

Figure 6. Relationship OF Safety Limit And Inspection Internal

in-service. For components classified as in-service noninspectible , inspection is required during manufacture and at the completion of one design lifetime if the component or system life is to be extended (Retirement for Cause). For components classified as in-service inspectible, inspection is required during manufacture and at completion of each maintenance or inspection interval. The factor relating residual crack growth life and inspection intervals is called the propagation margin and is, in effect, a safety factor. It serves as protection against unknowns in the life analysis, and also protects against failures from material property variations where crack growth rate may be faster than the mean.

Geometry Considerations

Design engineers are admonished to consider inspectibility when working with specific component features. Particular attention is called to radii and hole diameters. Selection of the largest practical hole diameter often results in improved inspectibility as does selection of a larger fillet radius for a difficult to access location. A 12 mm diameter hole is easier to inspect than a 6 mm diameter hole. These guidelines not only result in improved inspectibility, but often reduce concentrated stresses, with subsequent lifing benefits. In some locations on a component, these instructions are easily adhered to. Most often, other functional criteria require compromise of pure inspectibility considerations. This makes it imperative that the designer be knowledgeable of NDE capabilities or have NDE consultants readily available. Damage tolerance concerns emphasize the importance of this interaction. Design reviews, where each feature of each component is examined are an essential part of this process.

Examples of typical sites and the flaws that can occur in engine rotating components (disks, hubs, shafts and seals) are shown in Figure 7. For most of these flaw types, penetrant or eddy current inspection methods are usually used. In the case of subsurface flaws, ultrasonic inspections are used. Recent developments in ultrasonic inspection techniques now allow in-service inspections for some smooth geometry features such as portions of disk bores and webs. Flaw reject limits are based upon the detectable flaw size, the residual crack growth life and the maintenance (or inspection) interval.

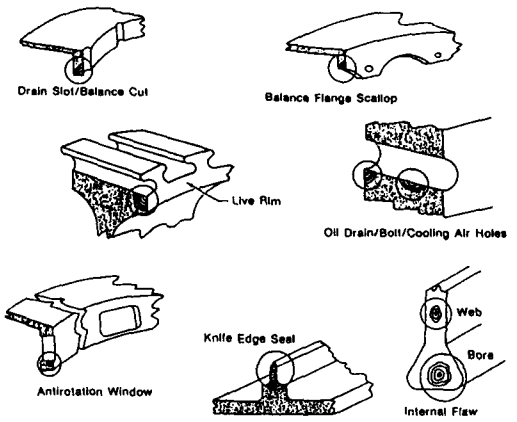

Figure 7. Examples Of Typical Flaws And The Geometric Locations Where They Occur In Rotating Components

This paper has emphasized NDE and component design relationships for high energy rotating components such as disks, hubs and airseals. Airfoil sections can also be treated in a similar manner, however, the presence of vibratory stresses must be accounted for. The usual approach is to limit the assumed initial flaw size such that the flaw, if present, would not grow under the anticipated vibratory stress field. For those cases where the flaw size is smaller than demonstrated NDE capability, redesign may be required.

Joints or bonded structures are also treated in the same manner. Again, appropriate material properties and NDE capability must be used.

A final consideration in the relationship of NDE needs and component design is the use of surface treatments. Shot peening, coldworking, and coatings affect inspectibility. In the manufacturing process, inspection can be conducted prior to the surface treatment. However, in-service inspections could be difficult if the surface treatment is not removed. Where surface treatments are to be used in manufacturing, the designer must consider the impact on in-service inspection preparations and techniques for the effected component.

Summary

The use of damage tolerance concepts in design has integrated NDE needs into the design process. These needs are now addressed as an integral part of establishing component designs, and directly influence those designs. In addition to utilizing damage tolerant materials in satisfying low cycle fatigue and fracture mechanics life requirements, configurations must reflect realistic NDE limitations and capabilities, provide for (good) inspectibility, and address manufacturing and material processing limitations. Despite initial misgivings, experience has shown damage tolerance can be achieved with little weight penalty. There is every indication that unexpected failure occurrences wi" be reduced as a result. The evolution and application of damage tolerance concepts for US military aircraft engines was accelerated by the implementation of the Engine Structural Integrity Program (ENSIP) by the USAF. This program has also been effective in defining the relationship of NDE needs and component design.

In developing a common approach for application of damage tolerance concepts within the AGARD Community, the USAF ENSIP standard could be used as a reference. It does address the basic requirements and assumptions necessary in developing a "safe" design. The approach should address what is required, not necessarily how it is to be obtained. By doing this, flexibility in meeting requirements will be maintained and options in the methods used will be allowed. It is the author's contention that probabilistic methods are the optimum means for addressing NDE concerns in the design process.

References

1. Cooper, T.D. and Forney, D.M., Materials Laboratory, Air Force Wright Aeronautical Laboratories "Increased Inspection Requirements for Critical Air Force Engine Components." Paper presented at 1981 Air Transport Association Nondestructive Testing Forum, Phoenix, Arizona, USA, September 1981.

2. MIL-STD 1783 (USAF), "Military Standard - Engine Structural Integrity Program (ENSIP)." United States Air Force, 30 November 1984.

3. Nethaway, D.H., Cargill, J.S. and VanWanderham, M.C., Pratt & Whitney "NDE and Engine Design - Then and Now." Presented at Spring 1987 meeting, American Society for Nondestructive Testing, Phoenix, Arizona, USA, April 1987

4. Harris, J.A., Jr., Annis, C.G. Jr., VanWanderham, M.C. and Sims, D.L. Pratt & Whitney, "Engine Component Retirement for Cause", AGARD Conference Proceedings No. 317 - Maintenance In-Service of High Temperature Parts, Neuilly Sur Seine, France, AGARD, January 1982.

5. Harris, J.A., Jr., Pratt & Whitney, "Engine Component Retirement for Cause" 1988. United States Air Force, Air Force Wright Aeronautical Laboratories (AFWAL) Report TR-87-4069-1.

Acknowledgements

The concepts and information presented in this paper are based upon the work of many individuals within the industrial, academic and government communities. Special acknowledgement is accorded to the structural and material specialists of the USAF Aeronautical Systems Division, and the Air Force Wright Aeronautical Laboratories, Wright- Patterson Air Force Base, Ohio, USA and to H.E. Johnson of Pratt & Whitney.

IMPORTANCE OF SENSITIVITY AND RELIABILITY OF NDI TECHNIQUES ON DAMAGE TOLERANCE BASED LIFE PREDICTION OF TURBINE DISCS

by
A.K. Koul*, A. Fahr*, G. Gould** and N. Bellinger**

*Structures and Materials Laboratory
National Aeronautical Establishment
National Research Council of Canada
Ottawa, Ontario, Canada

**Dept. of Mechanical and Aeronautical Eng.
Carleton University, Ottawa,
Ontario, Canada

SUMMARY

This paper reports the results of a demonstration programme carried out to determine the influence of the sensitivity and reliability of nondestructive inspection (NDI) techniques on the damage tolerance based life assessment of aero engine turbine discs. The programme was carried out on the 5th stage compressor discs of the J85-CAN40 engine, made from the AM-355 stainless steel. The sensitivity and reliability of several NDI techniques, in detecting service induced low cycle fatigue (LCF) cracks in the disc bolt hole regions, are assessed on the basis of detectable crack sizes at 90% probability of detection (POD) and 90% POD with 95% confidence level. The NDI techniques examined are the liquid penetrant inspection (LPI) technique, a manual eddy current inspection (ECI) technique using two gain settings and an ultrasonic leaky wave (ULW) technique using an automated C-scan system. The safe inspection intervals (SIIs) for the 5th stage compressor disc are calculated using deterministic fracture mechanics (DFM) and probabilistic fracture mechanics (PFM) principles. These calculations involve the use of the NDI data, finite element analysis and the experimental fatigue crack growth rate (FCGR) data generated on compact tension specimens machined from discs.

The results indicate that the manual ECI technique with a high gain setting and the automated ULW technique are the most sensitive and reliable in detecting LCF cracks. The percentages of false calls for the sensitive ECI and the ULW techniques were measured to be 2.4% and 0.6% respectively. The demonstration programme suggests that the guidelines for the assumed initial crack length (a_i) values provided for LPI, ECI and ultrasonic techniques in the United States Air Force Military Standard MIL-STD-1783 are too optimistic for widely used manual NDI procedures.

The results demonstrate that the sensitive ECI and the ULW techniques yield the largest SII values when the longest crack missed and the detectable crack sizes at 90% POD and 90/95 POD are substituted for a_i values in DFM calculations. In all cases, however, the SII values are too short for the damage tolerance based life prediction to be cost effective.

The PFM analysis, on the other hand, which randomly uses the distribution of undetected crack sizes for a given NDI technique to choose an a_i value for fracture mechanics calculations, demonstrates that the worst case combinations of a_i and FCGR do not occur during 7000 disc simulations. The PFM results also indicate that it may be possible to obtain cost effective SIIs if the sensitive ECI and the automated ULW techniques are used. However, the behaviour of short cracks would have to be characterized prior to obtaining usable PFM based SIIs.

1. INTRODUCTION

Damage tolerance based life prediction (DTLP) procedures are receiving attention for establishing turbine disc design life limits in new engines and for extending the usable service lives of discs whose life limits have been established conventionally[1-5]. The concepts have already been considered for several new generation engines, including the F100-PW-220, F110-GE-100 and F109-GA-10 engines. They have also been applied to existing engines such as PW F100, GE TF34 in the US and to GE J85-CAN40/15 in Canada for extending the usable service lives of discs[5].

In theory, DTLP procedures assume that the fracture critical locations of a component contain cracks of a size just below the detection limit of the nondestructive inspection (NDI) technique. The crack is then assumed to grow during service in a manner that can be predicted by linear elastic fracture mechanics or other acceptable methods, until a predetermined dysfunction limit* is reached beyond which the risk of failure due to rapid crack growth becomes excessive. The rates of crack growth and the dysfunction crack sizes are established analytically based on best estimates of service loads and material

*Note dysfunction crack size is not necessarily a critical crack length for catastrophic failure.

properties. The time or number of cycles required to grow the assumed crack (a_i) to its dysfunction size (a_d) is then used to define a safe inspection interval (SII) usually by dividing the life to dysfunction by a safety factor of 2[6]. This life cycle management concept is illustrated schematically in Fig. 1 which shows that at the end of one SII, all components are inspected and crack free components are returned to service for another SII and the procedure repeated until a crack is found. In this manner, components are retired on an individual basis when their condition dictates. In order to implement the DTLP procedure of Fig. 1, it is imperative to determine the detection limits of the candidate NDI techniques and to ensure that the selected NDI technique does not miss a dysfunction crack size under any circumstances. The United States Air Force (USAF) MIL-STD-1783 specifies that initial flaws shall be assumed to exist as a result of material manufacturing and processing operations and these flaw sizes shall be based on the intrinsic material defect distribution, manufacturing process and the NDI methods to be used during manufacture of the component[7].

In practice, however, the SII is computed either by using deterministic fracture mechanics (DFM) or probabilistic fracture mechanics (PFM) approaches[6,8-12]. The DFM approach assumes that an initial flaw size a_i already exists in the critical location of a component, where a_i is defined as the maximum crack size that might be missed by the NDI technique used[7]. Fracture mechanics analysis is carried out to plot the curve of worst case crack size (a) versus the number of fatigue cycles as shown in Fig. 1. The cyclic stress intensity factor (ΔK) ahead of the crack tip is given by:

$$\Delta K = \Delta\sigma\sqrt{\lambda\pi a} \tag{1}$$

where λ is a factor that depends on the crack shape, structure and gradient of stresses and $\Delta\sigma$ is the stress amplitude. Assuming that stable fatigue crack growth conditions prevail, the fatigue crack growth rate (FCGR) is given by:

$$\frac{da}{dN} = C(\Delta K)^n \tag{2}$$

where C and n are experimentally determined material constants. Upon substituting for ΔK from equation (1) in equation (2) and integrating, the number of fatigue cycles (N_d) required to grow a crack from the assumed initial size a_i to the dysfunction size a_d is given by:

$$N_d = \frac{1}{C(\Delta\sigma\sqrt{\pi})^n} \int_{a_i}^{a_d} (\lambda a)^{\frac{n}{2}}\, da \tag{3}$$

However, the DFM approach can be overly conservative since SII is calculated by using worst case values of n, C, $\Delta\sigma$, a_i and a_d, where:

$$SII = \frac{N_d}{2} \tag{4}$$

It has been suggested that the worst case situation for each and every variable in equation (3) may never occur in real life and these assumptions therefore impose unrealistic constraints on SII calculations[13,14].

The PFM approach also uses deterministic equations (1) to (4) for calculating a SII but input parameters such as a_i, a_d, C, n and $\Delta\sigma$ are treated as random variables with known or assumed distributions to generate a N_d distribution curve[10,12,13]. Therefore, rather than calculating a single SII value and using a safety factor based on good engineering judgement, a range of SIIs is calculated and appropriate values are selected to maintain a sufficiently low but cost effective failure probability (F)[15]. For example, the observed scatter in $\frac{da}{dN}$ in equation (2) could be simulated by random variation in C where C is assumed to show a log-normal distribution[10],

or
$$\log C = Gau(\mu_c, S_c) \tag{5}$$

where μ_c depicts the mean and S_c is the standard deviation. Similarly, a normal $\Delta\sigma$ variation can be represented by:

$$\Delta\sigma = Gau(\mu_{\Delta\sigma}, S_{\Delta\sigma}) \tag{6}$$

where $\mu_{\Delta\sigma}$ represents the mean and $S_{\Delta\sigma}$ is the standard deviation. Finally, the a_i and a_d distributions can also be assumed to be log-normal,

or
$$\log a = Gau(\mu_a, S_a) \tag{7}$$

where μ_a represents the mean and S_a is the standard deviation. The number of cycles (N_d) required to propagate a_i to a_d can be represented by:

$$N_d = f(C, \Delta\sigma, a_i, a_d) \tag{8}$$

Equations (5) to (7) can be combined with equation (3) to generate an N_d distribution and a SII value can be picked from this N_d distribution at an appropriate failure probability, such as, for example 0.1% F. It has been suggested that in accordance with the central limit theorem, a large N_d data base will follow a log-normal distribution providing a single random variable does not dominate the product of the variables in equation (8)[16]. The log-normal N_d distribution is represented by:

$$f(N_d) = \frac{1}{\sqrt{2\pi}\zeta N_d} \exp\left[-\frac{1}{2}\left[\frac{\ell n N_d - \lambda_1}{\zeta}\right]^2\right] \quad (9)$$

where λ_1 and ζ are related to the mean and standard deviation of the variate. Some researchers, on the other hand, prefer to use a Weibull distribution for N_d, because it is independent of the underlying distributions of the random variables and biased theoretical opinions are less likely to influence the overall results. The equation for the Weibull distribution is of the form[17]:

$$F(N_d) = 1 - \exp - \left[\frac{N_d}{\eta}\right]^{\beta} \quad (10)$$

where η is the characteristic life and β is the slope.

Whether DFM or PFM approaches are used to calculate N_d, equations (3) and (8) clearly indicate that N_d predictions will be strongly influenced by the crack length values used for a_i and a_d. Usually a single (worst case) a_d value is specified for a given batch of components using the best estimates of service loads and material properties. In contrast, the a_i value chosen for calculating N_d through equations (3) and (8) will depend upon the detection and sizing capabilities of the NDI technique used to inspect the components. This dependence requires that a number of NDI techniques should be quantified in terms of crack detection capabilities (sensitivity) and reliability (probability of detection) in order to select the most suitable NDI technique for implementing the DTLP procedures for a given set of components. One way of assessing the suitability of a given NDI technique is through a statistically valid demonstration programme.

In a demonstration programme, a statistically significant number of flawed and flaw free parts are inspected by NDI procedures that essentially duplicate proposed maintenance inspections and statistically significant crack growth rate data bases are generated on coupons or components in environments that duplicate the engine operating environment. The essential elements of a demonstration programme involve the assessment of the sensitivity and reliability of various NDI procedures for selecting a_i values and performing fracture mechanics calculations for predicting SIIs. The objectives of a demonstration programme are to assess the feasibility of implementing DTLP procedures and to use the predicted SII values for selecting the most cost effective NDI technique for a given set of components.

This paper presents the results of a programme that was conducted to determine the influence of the sensitivity and reliability of several NDI techniques, available for detecting turbine disc bolt hole cracks, on DFM and PFM based SII predictions for J85-CAN40 5th stage compressor discs. The NDI techniques evaluated included the conventional liquid penetrant inspection (LPI), manual eddy current inspection (ECI) and an ultrasonic leaky wave (ULW) inspection carried out in an automated C-scan system.

2. EXPERIMENTAL MATERIALS AND METHODS

J85-CAN40 5th stage compressor discs were selected for this demonstration programme because a large number of retired discs, containing service induced cracks, were available. In all cases, the low cycle fatigue cracks initiated in the tie bolt holes and then grew radially inward towards the bore of the discs[6]. The discs are fabricated from AM-355 material, a precipitation hardened martensitic stainless steel.

2.1 FRACTURE MECHANICS TESTING

To generate a crack growth data base for use in DFM and PFM calculations, FCGR testing was performed on compact tension (CT) specimens machined from retired 5th stage compressor discs. The CT specimens were machined as close to the bolt holes as possible. In order to simulate the fatigue crack growth behaviour of service cracks, the CT specimens were machined such that the direction of crack propagation through the specimen was radial towards the bore of the disc. This orientation is illustrated in Fig. 2. The geometry of the CT specimens is illustrated in Fig. 3. The CT specimen met the ASTM standard E-647 minimum size recommendations in all dimensions excepting the specimen thickness[18]. The specimen thickness was limited by the minimum disc thickness in the bolt hole regions. The CT specimen required a precrack of 6.67 mm and had a valid final crack length of 17.6 mm. These crack lengths correspond to a ΔK range of 30 to 85 MPa $\sqrt{m}$ at a stress ratio (R) of 0.1. The CT specimen also met the elasticity requirements of ASTM E-647[18].

The FCGR testing was carried out at 200°C in the laboratory air environment using a sawtooth waveform at a frequency of 1 Hz and an R value of 0.1. The maximum applied load was 1 kN. The 200°C testing temperature was selected to simulate the disc service temperature and a sawtooth loading cycle was selected because it was deemed more severe than a comparable sine wave form[19]. An automated direct current potential drop technique was used to monitor the crack length during the testing and the details of this technique can be found elsewhere[20]. The data acquisition time for the potential drop technique was limited to 1 second per reading in order to eliminate creep contributions to crack growth. Six CT specimens from the same disc were tested.

2.2 NONDESTRUCTIVE INSPECTION AND CRACK VERIFICATION PROCEDURES

Ten severely cracked, 5th stage compressor discs were used in this study. Each disc contains forty bolt holes which are used to assemble the compressor section, Fig. 4. These discs had been inspected by qualified NDI personnel at the engine overhaul and maintenance (EOM) facility using a production LPI technique with a 30 minute dye penetrant soaking period (called LPI30). The LPI maps were supplied for further analysis. All discs were sent to the Aircraft Maintenance and Development Unit (AMDU) of the Canadian Forces for laboratory nondestructive inspections. Two sets of inspections were carried out by qualified NDI personnel using conventional LPI as well as the manual ECI techniques. Two AMDU technicians certified at Level II in LPI carried out the inspections in accordance with the MIL-STD-6866[21], Type I, Method D specifications using 45 and 60 minute dye penetrant soaking periods (called LPI45 and LPI60 respectively). The crack lengths were measured with a digital readout vernier caliper with an accuracy of ±0.02 mm.

The manual ECI at AMDU was also carried out by two technicians certified at level I. The ECI was conducted using a Nortec Reichii instrument equipped with a 4.76 mm diameter rotating probe scanner (3000 rpm) which is specifically designed for fasterner bolt hole (4.84 mm diameter) inspections. The ECI unit operated at a test frequency of 500 Hz and at this frequency, the maximum eddy current penetration depth for AM-355 material is ∿6mm[22]. Two gain setting levels were used for ECI. One inspector used a gain setting of 2 (called ECI2) whereas the other inspector used a more sensitive gain setting of 5 (called ECI5). In the present investigation, however, the eddy current signals were not processed to size the cracks. Only an indication of whether a crack existed or not was noted for each bolt hole.

A further inspection was carried out on all discs using an ultrasonic leaky wave (ULW) technique, which is described in reference 23. This method is not an approved NDI technique for crack detection in engine components but it was felt that the technique had potential for detecting disc bolt hole cracks. The inspections were performed automatically using the California Data Corporation C-scan system at NAE, which produced an image of cracks indicating the location and the size of the cracks. The compressor discs were mounted on a turntable immersed in a water tank and a 10 MHz (25.4 mm focal length) probe was positioned at ∿20° to the surface of the disc for sending and receiving the ultrasonic waves. The disc was rotated while the probe moved radially towards the bore until the required area of the disc was covered. The ULW inspections were performed by two students who were trained for approximately one month on the instrument. The students did not have any formal training in NDI and the C-scan images were individually interpreted by the students.

After the nondestructive inspections were completed, the material surrounding all bolt hole areas were cut out into coupons as shown in Fig. 5(a). The bolt hole coupons in which cracks were detected by ULW were pried open along the crack faces, Fig. 5b, allowing crack lengths and crack geometries to be measured by scanning electron microscopy (SEM), Figs. 5(c) and 5(d). The remaining coupons were mounted in bakelite and mechanically polished for examination under an optical microscope. Care was taken to avoid excessive grinding which would efface small corner cracks. Again, the bolt hole coupons, where cracks were detected optically, were pried open along the crack faces and the crack lengths were measured by SEM. Finally, all remaining bolt hole coupons were broken out of the bakelite mounts and fractured in accordance with the procedure shown in Fig. 5(b). It was felt that an embedded crack would not be visible optically, and if a crack was indeed present, then the bolt hole coupon would fracture along the embedded crack surface. Therefore, all fractured bolt hole coupons were examined by SEM and a typical thumbnail profile with some fatigue striations ahead of the thumbnail (usually showing dark fracture surface due to service exposure) was considered as a service induced crack, Fig. 6. This procedure revealed approximately 100 additional cracks that were not detected optically[24].

3. RESULTS AND DISCUSSION

In order to calculate a SII through DFM or PFM analysis, statistically significant information must be available on:

(a) sensitivity and reliability of NDI techniques used for detecting cracks, i.e. a maximum a_i value for DFM calculations or an a_i distribution for PFM calculations,

(b) FCGR data, i.e. da/dN scatterband as a function of ΔK.

(c) operational loads, i.e. ΔK varying as a function of crack length for the component,

(d) dysfunction crack size, i.e. a_d, and

(e) a typical engine mission profile.

A dysfunction crack size, a_d, of 4.5 mm was specified for the 5th stage compressor disc bolt hole cracks by the engine manufacturer[4]. This a_d limit was apparently derived on the basis of fracture mechanics testing, vibration analysis and field experience[4]. Between a_i and a_d, however, the stress distribution ahead of the crack tip would be expected to change since disc dimensions and the distance between the crack tip and the disc rotational axis are continuously changing. A three dimensional finite element stress analysis was therefore carried out on the 5th stage compressor disc where the disc was assumed to rotate between zero and 16,500 rpm[25]. The stress distribution ahead of the crack tip of a bolt hole thru-crack was then computed under plane stress conditions. The values of ΔK computed in this manner for various bolt hole crack lengths have been plotted in Fig. 7, where ΔK is noted to increase with increasing crack length.

The FCGR data from CT specimens showed a large amount of scatter, Fig. 8. The Paris relationship, Eq. (2), was fitted to the data using a least squares method of linear regression. The mean line equation was found to be:

$$\frac{da}{dN} = 2.14 \times 10^{-12} (\Delta K)^{3.16} \text{ m/cycle} \tag{11}$$

where ΔK is in MPa$\sqrt{m}$. The conditional standard deviation (Sy/x) was calculated in order to account for the scatter in FCGR results. Figure 8 shows a mean solid line drawn through the data points and two parallel dashed lines drawn at ±3 conditional standard deviations of log C (±0.0711) from the mean line. The upper bound of the scatterband was calculated by drawing a line parallel to the mean line at +3 conditional standard deviations and the equation for the upper band was found to be:

$$\frac{da}{dN} = 10^{+(3\times0.0711)} \times 2.14\times10^{-12}(\Delta K)^{3.16} \text{ m/cycle}$$

or

$$\frac{da}{dN} = 3.497 \times 10^{-12}(\Delta K)^{3.16} \text{ m/cycle} \tag{12}$$

In order to determine a_i values for DFM calculations, the longest crack missed (a_i longest) by each NDI technique was noted, Table 1. The longest crack missed by the ULW technique was 1.48 mm in length whereas the LPI techniques missed cracks that were 3.69 to 4.33 mm in length. The most sensitive ECI technique (ECI5) detected almost all cracks above 1.27 mm in length although it missed one crack that was 2.7 mm in length. It will be recalled that the ECI in this study was carried out manually and it is likely that the 2.7 mm long crack missed by ECI5 could be due to an operator error. The less sensitive ECI technique (ECI2), on the other hand, consistently missed cracks longer than 4 mm. The USAF MIL-STD-1783, however, provides an approximate guideline for selecting a_i values stating that 0.8 mm and 0.4 mm uncovered surface flaw length should be assumed in the case of LPI and ECI/ultrasonic techniques respectively[7].

The USAF MIL-STD-1783 also recommends that the selected a_i value based on the NDI method used to inspect the component should be demonstrated to have a POD and confidence level of 90% and 95%, respectively[7]. In order to determine the POD as a function of crack length for our NDI data, the crack lengths were grouped into intervals since only one inspection per crack was performed for a given NDI procedure. Several crack length intervals between 0.2 mm and 1 mm were tried and the best compromise between the number of crack length intervals and the maximum number of cracks contained in each interval was obtained for a crack length interval of 0.5 mm[26]. The POD data points were calculated by dividing the number of cracks detected in a given crack length interval by the total number of cracks contained in that interval. Following the suggestion of Berens and Hovey[27], the middle of each crack length interval was assigned the calculated POD value rather than the maximum crack length in that interval. For reasons explained elsewhere[26], a log-logistic curve was fitted through the POD data points using the equation:

$$P_i = \frac{\exp(\beta_o+\beta_1 \ell n a_i)}{1 + \exp(\beta_o+\beta_1 \ell n a_i)} \tag{13}$$

where P_i is the POD value for a given crack length interval, β_o is the slope parameter and i varies between 1 and n_1, where n_1 is the total number of crack length intervals used to plot the POD curve. The curve fitting procedure involves the transformation of (P_i, a_i) pairs into a regressible format of the form:

$$Y_i = \alpha + \beta x_i \tag{14}$$

where $Y_i = \log[P_i/(1-P_i)]$ and $x_i = \log(a_i)$ and α is the intercept of the regressed line. In situations where all or no cracks are detected within a given crack length interval, P_i is given by $[1/(n_1+1)]$ or $[n_1/(n_1+1)]$ respectively)[27].

The POD data for LPI30, LPI45, LPI60, ECI2, ECI5 and ULW techniques were regressed in accordance with equations (13) and (14) and the mean log-logistic curves are plotted on a linear scale in Figures 9, 10, 11, 12, 13 and 14 respectively. Additional regression analysis was performed on ECI5 data assuming that the 2.7 mm long crack missed by this technique was an operator error (from now on depicted by ECI5*) and this crack was considered detected while analyzing the NDI data. The mean POD versus crack length curve for ECI5* is presented in Fig. 15. A set of a_i values was picked from Figs 9 to 15 at 90% POD. These 90/mean a_i values are compared with the longest crack missed data ($a_{i_{longest}}$) in Table 1. There is no direct correlation between $a_{i_{longest}}$ and 90/mean a_i, although for a given NDI procedure, both methods of selection yield similar a_i values, Table 1. It should, however, be recognized that the 90/mean a_i value is a reflection of the sensitivity of a given NDI technique because this value indicates that 90% of the cracks, i.e. a large proportion, of this size were detected in the demonstration programme. The smaller the 90/mean a_i value, the more sensitive is the NDI technique. It is therefore evident that ECI5 proved most sensitive in detecting LCF cracks (90/mean a_i = 1.65 mm), closely followed by ULW (90/mean a_i = 1.85 mm), whereas LPI techniques were less sensitive (90/mean a_i = 3.45 to 3.75 mm), Table 1. Out of all LPI procedures examined in this demonstration programme, LPI60 was marginally more sensitive than LPI30 and LPI45.

However, the calculated a_i value at a given POD or POD as a function of crack length for a given NDI procedure are known to show statistical variations from one demonstration programme to another[26,27]. These variations arise from a number of uncontrollable factors such as the ability and the attitude of the inspector, material type and component geometry and the location, orientation and the size of the flaw. Standard statistical methods are therefore used to plot confidence bounds on top of the mean POD data and a lower 95% confidence POD line is used to assess the reliability of various NDI techniques. The closer the 95% confidence line to the mean-POD line, the more reliable is the NDI technique. Following similar logic, the smaller the a_i value at 90% POD with 95% confidence (90/95 a_i) the more sensitive and reliable is the NDI technique.

A number of distributions were used to calculate the 95% confidence bounds on the mean log-logistic POD curves presented in Figs. 9 to 15. The distributions tried included the F-distribution, the normal distribution, the student t-distribution and the binomial distribution. Results comparing their suitability for realistically describing various types of NDI data can be found elsewhere[26]. In the present investigation, however, the normal and the student t-distributions resulted in the 95% confidence bounds that were closer to the mean POD curves for longer crack lengths relative to those given by the binomial and the F-distributions[26]. The criterion for selecting the most suitable distribution for computing the 95% confidence bound is based on the closeness of the 95% confidence-curve to the mean POD curve at longer crack length values. This procedure is considered to be a realistic approach. It is logical to assume that the larger the crack size, the higher should be the chance of its detection. Between the normal and the student-t distributions, the 95% confidence bounds were closer to the mean POD line in the case of the normal distribution[26]. The 95% confidence bound in the case of the normal distribution was determined by:

$$POD_{95\%\ confidence} = POD_{mean} \pm 1.96\ Sy/x \qquad (15)$$

where 1.96 is the normal standard variate for a confidence interval of 0.95 and Sy/x is the conditional standard variance[26]. This assumption leads to a lower bound 95% confidence curve which also takes a log-logistic form with the same slope as the mean POD line but with a different intercept value in equation (14), Figs. 9 to 15. A set of 90/95 a_i values was picked from Figs. 9 to 15 and these data are compared with the $a_{i_{longest}}$ and 90/mean a_i values in Table 1. It is evident from Table 1 that a 90/95 a_i value for a given NDI procedure is considerably larger than the respective $a_{i_{longest}}$ and 90/mean a_i values. It is also clear that the ULW technique appears superior to the ECI5 technique when compared on the basis of combined reliability and sensitivity, i.e. the 90/95 a_i for ULW is 2.90 mm versus 4.10 mm for ECI5. However, assuming that the 2.7 mm long crack missed by ECI5 may have been an operator error, the ECI5* technique comes out to be more reliable and sensitive than the ULW technique, Table 1.

Having compared the reliability and sensitivity of various NDI techniques, the following sections describe their influence on DFM and PFM based SII calculations for the 5th stage compressor discs.

3.1 DFM ANALYSIS

A number of "worst case" fracture mechanics calculations were performed to determine N_d values upon selecting different a_i values from Table 1, i.e. $a_{i_{longest}}$, 90/mean a_i and 90/95 a_i, for various NDI techniques and allowing the cracks to grow up to a predetermined a_d limit of 4.5 mm. Each N_d calculation was performed in a stepwise fashion using a

computer programme. The initial stress intensity range (ΔK_i) was computed for a selected a_i value from Fig. 7 and the ΔK was allowed to vary from ΔK_i to the dysfunction stress intensity (ΔK_d) in $2MPa\sqrt{m}$ intervals. The upper bound crack growth rate equation (Eq. (12)) was iteratively used in conjunction with Fig. 7 to calculate the cumulative number of fatigue cycles (N_d) required to grow the disc bolt hole crack from a_i to a_d. In order to convert the deterministic N_d data into engine operating hours, the calculated N_d values could be divided by a factor of 3 to 5 since it was previously established that 3 to 5 major throttle excursions can occur per flight hour in the J85-CAN40/15 engines[6]. The number of fatigue cycles to dysfunction computed through this procedure were further divided by a safety factor of 2 to obtain the SII's.

The SII's computed in cycles, using different inspection procedures and a_i selection criteria, are compared in Table 2. It is evident that all a_i selection criteria yield extremely low SII values in the case of LPI30, LPI45, LPI60 and ECI2 techniques. In fact, when a 90/95 a_i selection criterion is used in DFM calculations, the SII's equal zero in all four cases because 90/95 a_i values are greater than the predetermined a_d values of 4.5 mm, Table 1. Using the 90/95 a_i selection criteria, the longest SII obtained was of the order of 1623 cycles for the ECI5* technique.

The SII's calculated on the basis of $a_{i_{longest}}$ and 90/mean a_i were of the same order of magnitude for all NDI procedures with the exception of ECI5, Table 2. The deviation of ECI5 from this general trend is caused by the single incident of missing a 2.7 mm long crack. The longest SII's (2285/2293 cycles) were obtained for the ECI5* technique upon using $a_{i_{longest}}$ and 90/mean a_i in the DFM calculations.

3.2 PFM ANALYSIS

The primary aim of the PFM analysis was to simulate the consequences of missing a crack during inspection and/or of material degradation during service. In this paper, however, we will only present the PFM results dealing with the consequences of missing a crack. A computer programme, using Monte-Carlo simulation technique, was written to perform the analysis and the flow diagram of the programme is presented in Fig. 16.

The programme used LCF cycles-to-crack-initiation (also known as time-to-crack-initiation (TTCI)) distribution as a starting condition because TTCI provides an identifiable crack for inspection by state-of-the-art NDI techniques and it also permits the use of fracture mechanics models for propagating the crack from a_i to a_d[28]. In addition, the crack initiation as well as the crack propagation life of a disc is completely utilized through this approach. A Weibull distribution with known β and η values (similar to that represented by equation (10)) is used to describe the TTCI distribution of the high strain LCF damaged discs. The programme randomly chooses a TTCI value for a disc from the specified Weibull distribution, Fig. 17, and simulates the NDI of the disc. Since, by definition, the disc contains a crack approximately 0.8 mm in length at TTCI, the NDI simulation for a given technique is performed by comparing the POD value at a specified confidence level for a 0.8 mm crack (Figs. 9 to 15) with a computer generated uniform random number between the values of 0 and 1, which represents the probability of missing a crack. If the random number generated is smaller than the POD value, then the crack is detected and vice versa. In practice, however, if a crack is detected in a disc during inspection it will be retired and for this reason the simulations indicating crack detection were not used in the PFM analysis. If the crack at TTCI goes undetected by the NDI simulation procedure, the programme randomly sizes the crack, i.e. a_i, using the experimentally determined log-normal distribution of the crack sizes undetected by a particular NDI technique, Fig. 18.

Although, intuitively, one would expect the crack to be 0.8 mm in length at TTCI, an estimated crack length of 0.8 mm by a given NDI technique could actually be considerably different if the crack is measured accurately with the help of SEM. In fact, linear regression analysis between NDI estimated and SEM measured crack lengths was carried out on results from four of the six NDI techniques during the course of this demonstration programme, Table 3 and Fig. 19. The ECI2 and ECI5 techniques were excluded from this part of the programme since they did not estimate a crack length but simply indicated whether a crack was present or not. Given an NDI estimated crack length of 0.8 mm, the measured crack lengths were assumed to vary normally about the mean and these normal distributions were computed by using the conditional standard deviation across the mean regressed line in Fig. 19. The measured crack length distributions for an estimated crack length of 0.8 mm are plotted in Fig. 20 for LPI30, LPI45, LPI60 and ULW techniques. The ±95% confidence bounds of the measured crack lengths for an estimated crack length of 0.8 mm, using different NDI techniques, are also presented in Table 3. In the case of LPI30 and ULW techniques, the SEM measured ±95% confidence bounds for an NDI estimated crack length of 0.8 mm are seen to vary from a negative to a positive value. It is obviously not possible to have a negative crack length but, theoretically, this is a solution since the normal distribution extends from negative to positive infinity. Given this type of a statistical guideline for determining the size of an undetected crack at TTCI, the random use of 'the undetected crack size distribution' was considered more appropriate for PFM analysis. This is because, first, all cracks have a positive length, secondly, statistically significant

data bases were available for all NDI techniques including ECI2 and ECI5, and thirdly it provides a common basis for simulating the uncertainties associated with various NDI techniques. In addition, the use of the undetected crack size distributions as a starting condition for PFM analysis would always be best suited for simulating the behaviour of new discs, thus making the programme more versatile[29].

Having determined an a_i value, the programme computes the ΔK_i from Fig. 7 and allows the crack to grow from ΔK_i to ΔK_d in 2 MPa$\sqrt{m}$ intervals. To calculate N_d, the programme uses the experimentally determined da/dN versus ΔK scatterband, Fig. 8, in a random fashion. The crack growth rate equation is randomized following the method proposed by Yang and his co-workers[30,31] such that:

$$\log \frac{da}{dN} = Z + \log C + n \log \Delta K \qquad (16)$$

where Z is a normal random variable with zero mean and a standard deviation equal to the conditional standard deviation of the log $\frac{da}{dN}$ in Fig. 8. For simplicity, 'n' is assumed to have a constant value (e.g. 3.16 for the 5th stage compressor discs, see equations (11) and (12), for all discs and the scatter in da/dN is taken into account by varying 'C' from one disc to another. Typically, in 100 computer simulations da/dN varies between ±2 conditional standard deviations. The programme finally subtracts the original TTCI low cycle fatigue cycles to yield purely N_d data that can be compared with DFM results. The N_d data computed for a large number of discs are sorted numerically and given a cumulative probability plotting position using both log-normal and Weibull distribution functions. Both least squares and maximum likelihood lines are drawn through the cumulative probability of failure data to calculate the correlation coefficients for the PFM generated N_d distribution. Finally, the computer programme calculates a SII at 0.10% F using the Weibull or the log-normal distributions.

It will be recognized that, while generating an N_d distribution through PFM analysis, a sufficient number of simulations must be carried out to adequately represent the distribution. Therefore, a stability and convergence test was carried out where 10, 50, 100, 200, 500, 1000, 2000 and 5000 simulation runs were repeated a number of times and a statistically significant SII data base was generated for each type of simulation run. A normal distribution was then fitted through each set of SII data in order to determine the mean and the standard deviation for the SII. If the mean SII values are close to one another for all simulations, the data indicate good convergence whereas very small standard deviations about the mean indicate good stability. It was found that 5000 simulations gave stable SII estimates and the maximum likelihood SIIs converged better than the least squares estimates. Above 500 simulations, however, the least squares SII estimates also showed good convergence.

A total of 7,000 simulations were carried out for each NDI technique using the mean and the 95% confidence POD data in separate computer runs. All N_d data bases were plotted in accordance with the Weibull and the log-normal distributions and the least squares lines were drawn through the PFM generated data to determine the SII values from these plots. Typical Weibull and log-normal plots for LPI60, ULW and ECI5* are shown in Figs. 21, 22 and 23 respectively. The results of all PFM simulations are presented in greater detail in Tables 4 and 5. These tables list the number of cracks missed by each NDI technique, the least squares line correlation coefficients for the Weibull and the log-normal distributions and the SII values at 0.1%F. It is evident from Tables 4 and 5 that LPI and ECI2 techniques missed the greatest number of cracks followed by the ULW technique whereas the ECI5 missed the least number of cracks of all NDI techniques. As expected, the number of cracks missed by a given NDI technique increases significantly when 95% confidence POD data is used instead of the mean POD data in PFM simulations. These data therefore indicate that for a crack length of 0.8 mm the ECI5 technique is more sensitive and reliable than any other technique considered in this demonstration programme.

A comparison of the correlation coefficients for the Weibull and the log-normal distributions in Tables 4 and 5 indicates that the Weibull distribution provides a slightly better fit to the N_d data bases in the case of LPI30, LPI45, LPI60 and ECI2 techniques. In contrast, the log-normal distribution marginally fits the data better in the case of ULW and ECI5 techniques. These observations suggest that the underlining log-normal distribution for the undetected crack sizes is not unduly biasing the overall N_d distribution, thus proving the randomness of the PFM analysis in this demonstration programme.

The highest SII values were obtained for the ECI5 technique, closely followed by the ULW technique, whereas the SII values were considerably lower for ECI2 and LPI techniques, Tables 4 and 5. This is because ECI5 and ULW techniques primarily miss a large number of smaller cracks which results in smaller a_i values, and in turn a larger number of fatigue cycles are required to grow the crack from the randomly chosen a_i value to a fixed a_d value of 4.5 mm. In contrast, the LPI and ECI2 techniques miss a large number of longer cracks thus decreasing the number of fatigue cycles required to grow a large a_i to a fixed a_d. It should also be noted that the mean and the 95% confidence POD data do not appear to influence the SII values significantly, Tables 4 and 5. It will, however, be recognized that the 95% confidence POD data only increases the number of cracks undetected relative to the mean POD data during PFM simulations, whereas the same 'undetected crack size distribution' is used to size the cracks in both cases. Therefore, as long as a statistically signifi-

cant number of cracks go undetected in both cases, one should expect these similarities in SII values for a given NDI technique.

The PFM results also indicate that for a given NDI technique, the SII value computed on the basis of the log-normal distribution is considerably larger than the value predicted on the basis of the Weibull distribution, Tables 4 and 5. This discrepancy arises from force fitting the log-normal distribution which does not take into account a number of data points with lower N_d values. In contrast, the Weibull distribution takes the whole data base into account while predicting a SII value.

4. CONCLUDING REMARKS

Traditionally, a binomial distribution has been used to specify the confidence bounds for POD data because it is said to provide an optimum fit to the experimental results[32]. The major problem with the binomial distribution in terms of the type of inspection data generated in the present work, i.e. one observation per crack, is related to the fact that the confidence bounds are significantly influenced by the number of cracks contained in a crack length interval, Fig. 24, and therefore the method used to choose this interval. In addition, the USAF 'Have Cracks Will Travel' NDI programme on aircraft structural components[27], where multiple observations per crack were carried out, demonstrated that cracks of the same length could have different POD values. The binomial distribution on the other hand assumes that a specific crack length will always reveal the same POD for a given NDI procedure. Because of these limitations Berens and Hovey[27] concluded that a log-logistic curve was the most suitable method for describing POD data. Having used the log-logistic POD analysis method in the present work, it was found that the 90/mean and 90/95 a_i values for the most sensitive NDI techniques, e.g. the ECI5 and the ULW, do not even come close to the a_i guidelines provided in the USAF MIL-STD-1783, Table 1. The USAF MIL-STD-1783 suggests that uncovered surface flaw lengths of 0.4 mm shall be assumed to be present in the case of the ECI and ultrasonic inspection techniques. The smallest 90/mean and 90/95 a_i values, 1.25 mm and 1.75 mm respectively, were obtained in the case of ECI5* assuming that the 2.7 mm long crack missed by the manual ECI5 technique was the result of an operator error. It is therefore likely that the ECI5 technique would have to be automated to reliabily obtain the a_i values listed in Table 1 in a production environment. It may also be possible to use more sensitive probes in the case of the ECI technique in order to obtain smaller 90/mean and 90/95 a_i values. Increasing the eddy current probe sensitivity could, however, lead to a greater number of 'false calls'. In this demonstration programme, the ECI5 technique resulted in the maximum number of 'false calls' relative to the other NDI techniques considered, Table 6.

The DFM analysis indicates that $a_{i_{longest}}$ and 90/mean a_i criteria yield similar SII values for a given NDI procedure, Table 2. On the other hand, USAF MIL-STD-1783 suggests that, from a reliability point of view, the 90/95 a_i criterion should be used for SII calculations and this criterion is shown to reduce the SII values dramatically for all NDI techniques, Table 2. It could, however, be argued that once an engine is disassembled at inspection, the discs can be inspected as many times as deemed necessary to meet a specific reliability requirement. Under these circumstances, therefore, the use of the 90/mean a_i criterion may prove to be a better choice since it would yield a longer SII value. Use of the 90/mean a_i criterion is feasible only if the inspection procedure is fully automated because the inspection costs for a labour intensive technique could otherwise prove uneconomical.

The DFM calculations also indicate that out of all NDI techniques, the ULW and ECI5* techniques yield the largest SII values (2000 and 2300 fatigue cycles respectively), Table 2. However, depending upon the operational role of a military engine, a safe inspection interval should typically be of the order of 4000 to 8000 cycles for the DTLP procedure to be cost effective. These results therefore indicate that the DFM based SIIs may not prove to be cost effective in the case of J85-CAN40 engines. In contrast, the PFM results in Table 4 suggest that cost effective SIIs can be obtained provided that either the ECI5 or the ULW techniques are used to inspect the discs. The large differences in the DFM and PFM predicted SII values simply reflect the fact that the worst case combination of a_i and $\frac{da}{dN}$, used in DFM calculations , did not occur during 7000 disc simulations in any PFM computer run.

However, the PFM predicted SII values, listed in Table 4, should not be accepted at face value. This is because the a_i distributions used in the PFM calculations (Figure 18) comprise of a large number of short cracks and, for simplicity, we have assumed that the growth rate of the these short cracks can be depicted by the CT specimen data within the Paris regime of crack growth. There is now increasing evidence to show that short crack behaviour differs considerably from long crack behaviour and that evaluation of lifetimes based on long crack data can be nonconservative especially at lower stresses[33]. Therefore, the front end of the PFM computer programme used in the present analysis, Fig. 16, would have to be modified to incorporate a short crack growth rate model instead of the TTCI data base. Assuming that an appropriate analytical model along with a statistically significant short crack growth rate data base are available to meet these requirements, an engineer is still faced with the dilemma of drawing a boundary condition between the short and the long crack, i.e. when does a short crack begin to behave like a long crack.

5. REFERENCES

(1) A. Coles, 'Material Science Considerations for Gas Turbine Engines', Proc. 3rd *International Conference on* Metals, Vol. 1, Cambridge, England, August 1979, pp. 3-11.

(2) R.H. Jeal, 'Damage Tolerance Concepts for Critical Engine Components', Proc. AGARD-SMP Conference on Damage Tolerance Concepts for Critical Engine Components', AGARD-CP-393, San Antonio, Texas, 1985, pp. I-1 to I-12.

(3) C.G. Annis Jr., M.C. VanWanderham, J.A. Harris Jr. and D.L. Sims, 'Gas Turbine Engine Disk Retirement-For-Cause: An Application of Fracture Mechanics and NDE', Trans. ASME, Vol. 103, January 1981, pp. 198-200.

(4) A.K. Koul, W. Wallace and R. Thamburaj, 'Problems and Possibilities for Life Extension in Gas Turbine Components', Proc. AGARD-PEP Conference on Engine Cyclic Durability by Analysis and Testing, AGARD-CP-368, Lisse, Netherlands, 1984, pp. 10-1 to 10-32.

(5) A.K. Koul, J.P. Immarigeon and W. Wallace, 'Emerging Technologies for Life Cycle Management of Turbine Engine Components', CASI Journal, 1988, in press.

(6) A.K. Koul, R. Thamburaj, W. Wallace, M.D. Raizenne and M.C. de Malherbe, 'Practical Experience with Damage Tolerance Based Life Extension Concepts for Turbine Engine Components', Proc. AGARD-SMP Conference on Damage Tolerance Concepts for Critical Engine Components, AGARD-CP-393, San Antonio, Texas, 1985, pp. 23-1 to 23-22.

(7) MIL-STD-1783 Military Standard, Engine Structural Integrity Program (ENSIP), 30 Novembr 1984, Department of Defense, Washington, D.C., 20360

(8) R. Thamburaj, A.K. Koul, W. Wallace and M.C. de Malherbe, 'Life Extension Concepts for Canadian Forces Aircraft Engine Components: J85-CAN40 Compressor and Turbine Materials', National Research Council of Canada, NAE Report, LTR-ST-1585, 1986.

(9) P.M. Besuner, K.G. Sorenson, and D.P. Johnson, 'A Workable Approach for Extending the Life of Turbine Rotors', ASME Publications on Fatigue Life technology, Eds. T. Cruse and J. Gallagher, 1977, pp. 53-71.

(10) P.M. Besuner and A.S. Tetelman, 'Probabilistic Fracture Mechanics', Journal of Nuclear Engineering and Design, Vol. 43, 1977, pp. 99-114.

(11) J.A. Harris, D.L. Sims and C.G. Annis Jr., 'Concept Definition: Retirement for Cause of F100 Rotor Components', AFWAL-TR-80-4118, 1980.

(12) C.H. Cook, C.E. Spaeth, D.T. Hunter and R.J. Hill, 'Damage Tolerant Design of Turbine Engine Disks', ASME 82-GT-311, 1982.

(13) C.A. Rau Jr., 'The Impact of Inspection and Analysis Uncertainty on Reliability Prediction and Life extension Strategy', DARPA/AFML Review of Progress in Quantitative NDE, San Diego, July 1978.

(14) C.A. Rau Jr. and P.M. Besuner, 'Quantitative Decisions Relative to Structural Integrity', Trans. ASME, Vol. 102, Jan. 1980, pp. 56-63.

(15) C.A. Rau Jr. and P.M. Besuner, 'Probabilistic Fracture Mechanics', Product Engineering, Vol. 50, October 1979, pp. 41-47.

(16) A. Ang and W.H. Tang, Probability Concepts in Engineering Planning and Design, Volume 1 Basic Principles, John Wiley and Sons Inc., New York, 1975.

(17) W.J. Daub, Weibull Analysis for Aircraft Engine Components, General Electric (J85 Project).

(18) A.S.T.M. Method E647-83, 'Constant Load Amplitude Fatigue Crack Growth Rates Above 10E-08 m/cycle', 1983.

(19) A.J.A. Mom, 'Working Document for the AGARD Cooperative Test Programme on Titanium Alloy Engine Disk Material', NLR-TR-84022L, March 1984.

(20) G.F. Akers and T. Terada, 'The Calibration and Implementation of the Direct Current Potential Drop Technique on CT Specimens', National Research Council of Canada, NAE Report, LTR-ST-1599, 18 August, 1986.

(21) MIL-STD-6866 Military Standard, Inspection, Liquid Penetrant, 30 September 1985, Department of Defense, Washington, D.C., 20402, (AFWAL/MLSE).

(22) Nortec RECH11 I. Rotating Eddy Current Hole Inspection Instrument. Operating Manual, 1981, Revised 1982..9, 421 N Quay, Kennewick, Washington, 99336.

(23) A. Fahr, N.C. Bellinger, P. Stoute and A.K. Koul, 'Inspection of Compressor Discs by Ultrasonic Leaky Waves Using an Automated C-scan System', to be published.

(24) N.C. Bellinger, P. Stoute, G. Gould, A. Fahr, and A.K. Koul, 'The Nondestructive and Destructive Inspection Data for J85-CAN40 Compressor Discs for Detecting Bolt Hole LCF Cracks', National Research Council of Canada, NAE Report, ST-490, January, 1988.

(25) J.J. Kaprzynski, 'Determination of Stress Intensity Factors in a J85 CAN40 Fifth Stage Compressor Disc by Finite Element Analysis', National Research Council of Canada, NAE Report, to be publilshed.

(26) N.C. Bellinger, A. Fahr, A.K. Koul, G. Gould and P. Stoute, 'The Reliability and Sensitivity of NDI Techniques to Detect LCF Cracks in Fastener Bolt Holes of Compressor Discs', National Research Council of Canada, NAE Report, LTR-ST-1651, May 1988.

(27) A.P. Berens and P.W. Hovey, 'Characterization of NDE Reliability', Review of Progress in Nondestructive Evaluation, Vol. 1, Eds. Thompson and Chimenté, Plenum Press, NY, 1982, pp. 579-585.

(28) J.N. Yang and S. Chen, 'Fatigue Reliability of Gas Turbine Engine Components Under Scheduled Inspection Maintenance', J. Aircraft, Vol. 22, No. 5, May 1985, pp. 415-422.

(29) G. Gould, 'Damage Tolerance Based Life Extension of Turbine Discs: A PFM Approach', *Masters Thesis, Department of Mechanical and Aeronautical Engineering*, Carleton University, Ottawa, November 1987.

(30) J.N. Yang, R.C. Donath and G.C. Salivar, 'Statistical Fatigue Crack Propagation of IN100 at Elevated Temperatures', ASME International Conference on Advances in Life Prediction Methods, April 1983, pp. 241-247.

(31) J.N. Yang, W.H. Hsi, S.D. Manning and S.L. Rudd, 'Stiochastic Crack Propagation in Fastener Holes', J. Aircraft, Vol. 22, No. 9, September 1985, pp. 810-817.

(32) M. Zako, T. Kawashima, H. Aono, K. Jimbok, H. Ohnabe and T. Méyoski, 'Residual Life Prediction of Jet Engine Rotor Disks', Design of Fatigue and Fracture Resistant Structures, ASTM STP 761, 1982, pp. 408-423

(33) T. Lankford and S.J. Hudak Jr., 'Relevance of the Small Crack Problem to Life time Prediction in Gas Turbines', Int. J. of Fatigue, Vol. 9, No. 2, 1987, pp. 87-93.

6. ACKNOWLEDGEMENTS

The financial support for this work was provide by the Office of the Chief of Research and Development of the Department of National Defence, Canada. The authors would like to thank the staff of the Aircraft Maintenance and Development Unit (AMDU) of the Department of National Defence for conducting parts of the nondestructive inspection programme on retired discs. In particular, the contributions of Capt. D. Masters and Maj. R. Drummond in executing the NDI programme at AMDU are much appreciated. The contribution of Dr. J.J. Kacprzynski of NAE in conducting the finite element analysis on the 5th stage compressor disc is also appreciated. Thanks are extended to the staff of the Orenda Division of Hawker Siddley Canada Inc. for making the retired discs and their LPI results available to the authors. Thanks are also due to Dr. R. Thamburaj, Mr. P. Stoute and Mr. G. Akers (previously with Carleton University) for conducting some parts of the experimental programme. The authors gratefully acknowledge the constant encouragement of Dr. W. Wallace of NAE in completing the programme and this manuscript. Special thanks are due to Mrs. H. Cuccaro of the Stenographic Services of NRC and her staff for the expedient typing of the manuscript. Thanks are also due to Mrs. Shirley Dodds of NAE and her staff for the expedient processing of the manuscript.

Table 1: Comparison of a_i values selected for use in DFM calculations using different selection criteria.

NDI Technique	a_i values in mm		
	longest crack missed	at 90% POD from mean log-logistic curve	at 90% POD from log-logistic curve with 95% confidence
LPI30	3.98	3.75	6.40
LPI45	4.33	4.25	8.35
LPI60	3.70 (0.8)	3.45	6.20
ECI2	4.43	5.60	>10.00
ECI5	2.70	1.65	4.10
ECI5*	1.27 (0.4)	1.25	1.75
ULW	1.48 (0.4)	1.85	2.90

*assuming that the 2.7 mm log crack missed by ECI5 was an operator error.
( ) A guide for selecting a_i values from MIL-STD-1783 prior to in-service verification.

Table 2: Influence of the sensitivity and combined sensitivity plus reliability of NDI techniques on DFM based SII calculations.

NDI Technique	SII in cycles using different a_i selection		
	$a_{i_{longest}}$	90/mean a_i	90/95 a_i
LPI30	183	278	0
LPI45	53	80	0
LPI60	295	405	0
ECI2	20	0	0
ECI5	815	1773	135
ECI5*	2293	2285	1623
ULW	1973	1989	695

* Assuming that the 2.7 mm long crack missed by ECI5 was an operator error.

Table 3: Correlation between NDI estimated and SEM measured crack lengths for different NDI techniques.

NDI Techinque	Regression analysis results for estimated versus measured crack lengths ($a_{measured}$ = slope×a_{NDI}+ intercept) in mm.			Measured crack length in mm for an estimated crack length of 0.8 mm.		
	Mean Line Slope	Mean Line Intercept	Conditional Standard Deviation	Mean	-95% confidence	+95% confidence
LPI30	0.470	1.460	1.05575	1.84	-0.23	+3.91
LPI45	0.760	1.220	0.85384	1.83	+0.16	+3.50
LPI60	0.820	0.660	0.59043	1.32	+0.16	+2.48
ULW	0.990	-0.200	0.55908	0.59	-0.51	+1.69

Table 4: The PFM analysis results for 7000 simulations using a Weibull distribution to calculate SII at 0.1% F N_d.

NDI Technique	No. of cracks undetected upon using		Safe inspection interval in cycles upon using		Least squares correlation coefficient (r^2)	
	Mean POD	95% confidence POD	Mean POD	95% confidence POD	Mean POD	95% confidence POD
LPI30	6140	6787	1740	1871	0.95	0.94
LPI45	5822	6721	1627	1584	0.95	0.94
LPI60	4695	6069	2374	2282	0.96	0.94
ECI2	4929	6211	1554	1491	0.96	0.93
ECI5	1503	3066	4465	4615	0.87	0.89
ECI5*	1514	2326	4685	4768	0.87	0.87
ULW	3801	5620	3652	3580	0.92	0.91

* Assuming that the 2.7 mm long crack missed by ECI5 was an operator error.

Table 5: The PFM analysis results for 7000 simulations using a log-normal distribution to calculate SII at 0.1% F N_d.

NDI Technique	No. of cracks undetected upon using		Safe inspection interval in cycles upon using		Least squares correlation coefficient (r^2)	
	Mean POD	95% confidence POD	Mean POD	95% confidence POD	Mean POD	95% confidence POD
LPI30	6140	6787	3397	3606	0.94	0.94
LPI45	5822	6721	3215	3175	0.93	0.93
LPI60	4695	6069	4139	4199	0.94	0.94
ECI2	4929	6211	3046	3052	0.94	0.91
ECI5	1503	3066	6961	7121	0.88	0.89
ECI5*	1514	2326	7235	7321	0.87	0.88
ULW	3801	5620	5846	5893	0.92	0.93

* Assuming that the 2.7 mm long crack missed by ECI5 was an operator error.

Table 6: The 'false calls' data for all NDI techniques.

NDI Technique	% false calls = $\frac{\text{no. of nonexistent cracks detected}}{\text{Total no. of cracks present}}$
LPI30	0.9
LPI45	0.0
LPI60	0.6
ECI2	0.9
ECI5	2.4
ULW	0.6

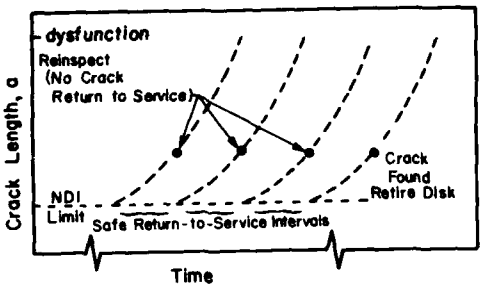

Fig. 1. Schematic representation of the damage tolerance based life prediction methodology for discs where fracture mechanics is used to predict a safe inspection interval.

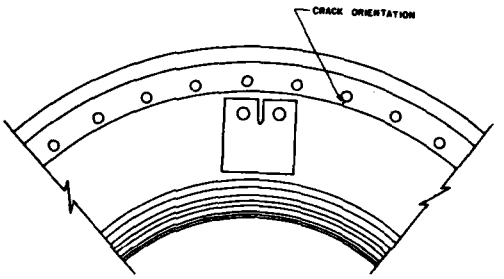

Fig. 2. Orientation of the compact tension specimens as machined from the J85-CAN40 5th stage compressor discs.

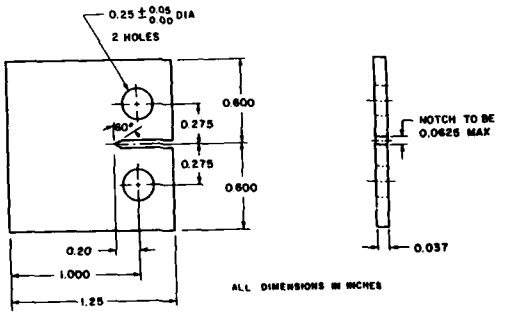

Fig. 3. Geometry of the compact tension specimen used to generate fatigue crack growth rate (FCGR) data at 200°C.

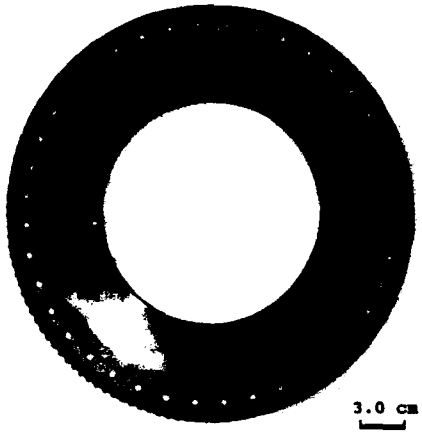

Fig. 4. A photograph of the 5th stage compressor disc showing 40 tie bolt holes.

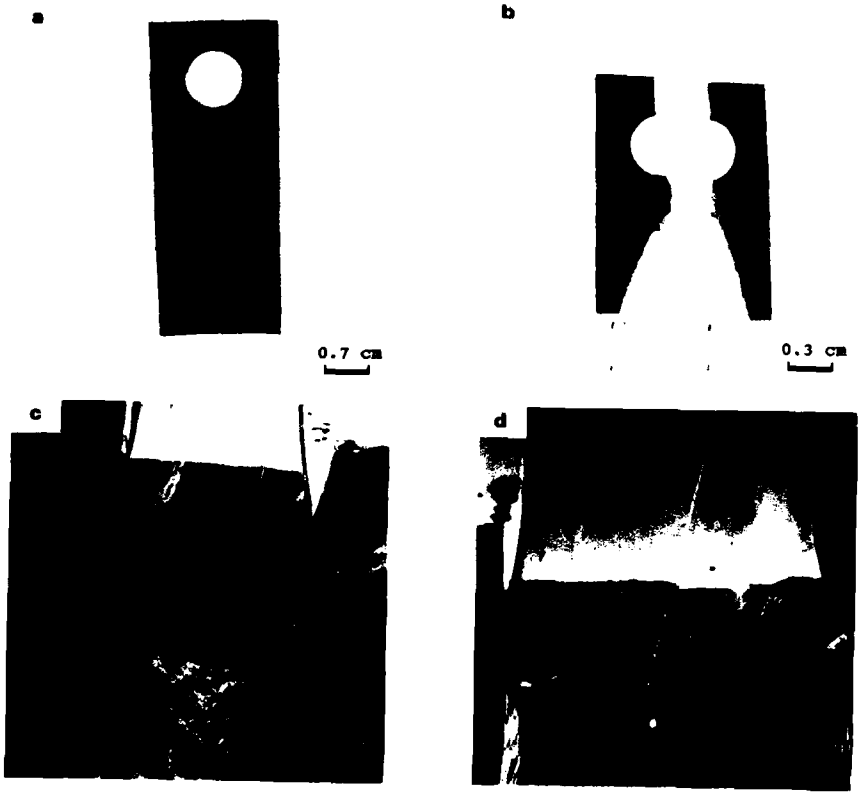

Fig. 5. Destructive procedures followed for prying the cracks open and measuring the crack lengths: (a) a typical bolt hole coupon; (b) a coupon with a V-notch prior to fracturing the specimen through the crack; (c) a typical example of a crack front, and; (d) an example of multiple crack initiation sites.

Fig. 6. Scanning electron micrograph showing the typical thumbnail profile of a crack that was missed by all NDI techniques.

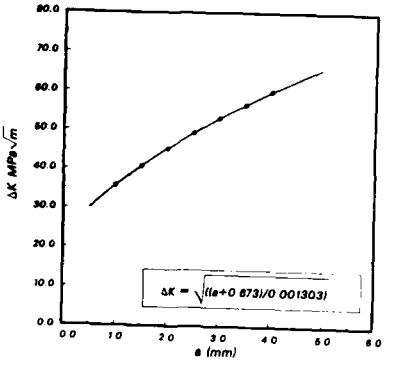

Fig. 7. Three dimensional finite element analysis results for the 5th stage compressor disc showing stress intensity range varying as a function of crack length. (Ref. 25).

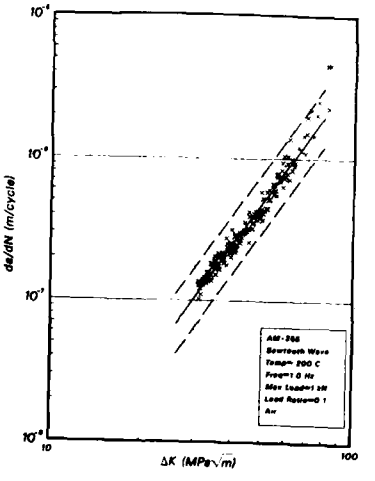

Fig. 8. Fatigue crack growth rate data from six compact tension specimens showing the upper and lower confidence bounds at ±3 conditional standard deviations.

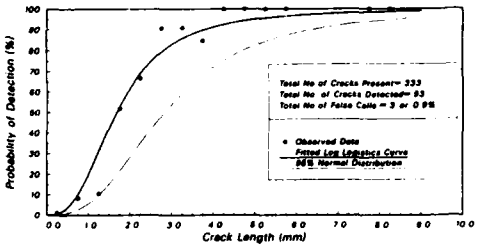

Fig. 9. Probability of detection data for the liquid penetrant inspection technique using a 30 minute dye penetrant soaking period (LPI30).

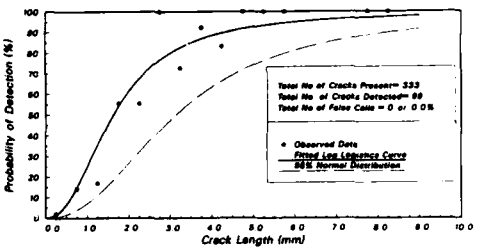

Fig. 10. Probability of detection data for the liquid penetrant inspection technique using a 45 minute dye penetrant soaking period (LPI45).

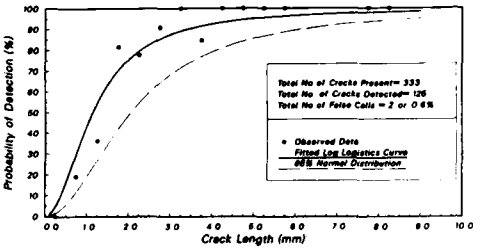

Fig. 11. Probability of detection data for the liquid penetrant inspection technique using a 60 minute dye penetrant soaking period (LPI60).

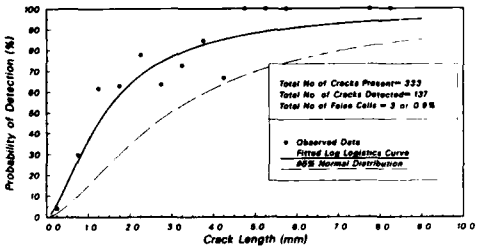

Fig. 12. Probability of detection data for the manual eddy current inspection technique using a low gain setting (ECI2).

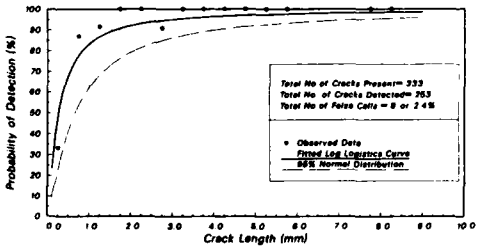

Fig. 13. Probability of detection data for the manual eddy current inspection technique using a high gain setting (ECI5).

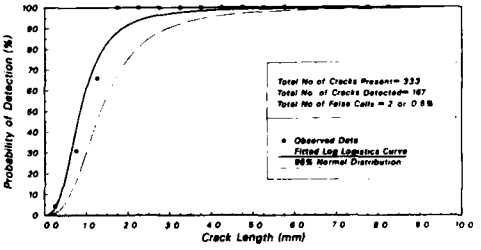

Fig. 14. Probability of detection data for the ultrasonic leaky wave (ULW) inspection technique using a C-scan system.

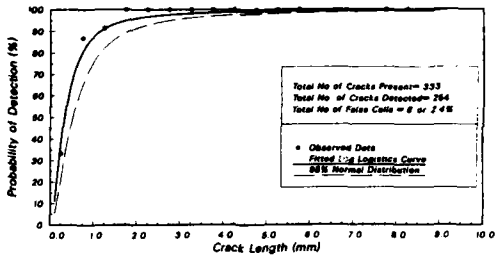

Fig. 15. Probability of detection data for the manual eddy current inspection technique using the high gain setting and assuming that the 2.7 mm long crack missed by ECI5 was an operator error (ECI5*).

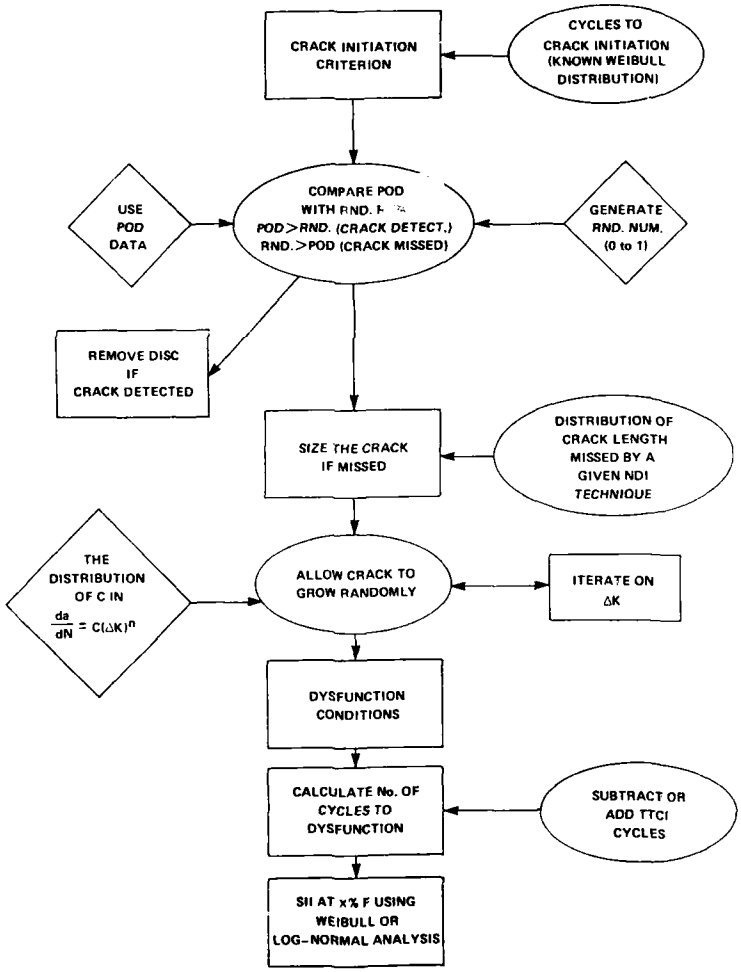

Fig. 16. The flow diagram of the NAE computer programme for simulating the nondestructive inspection and allowing the cracks to grow randomly from a_i to a_d.

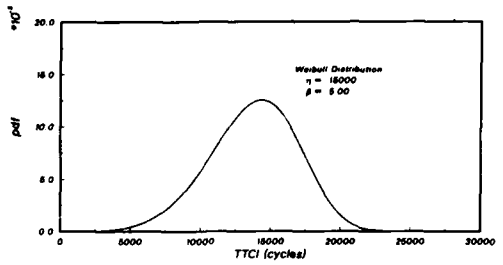

Fig. 17. The LCF cycles to crack initiation distribution for the 5th stage compressor discs. (Ref. 6.)

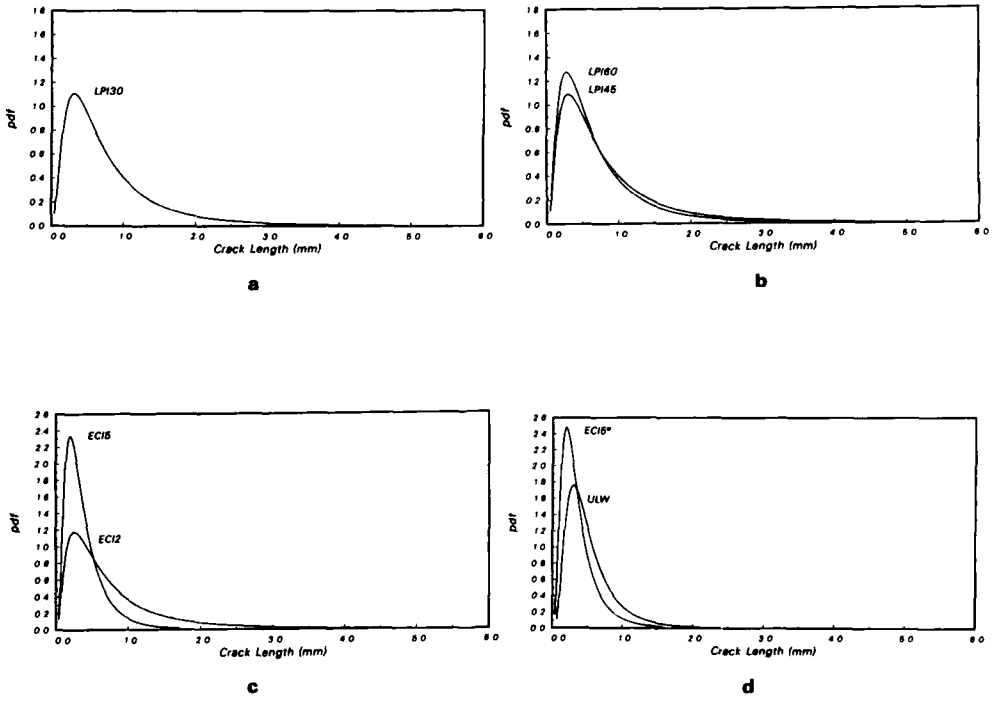

Fig. 18. Log-normal distributions for the undetected crack sizes for (a) LPI30, (b) LPI45 and LPI60, (c) ECI2 and ECI5 and (d) ULW and ECI5*, techniques.

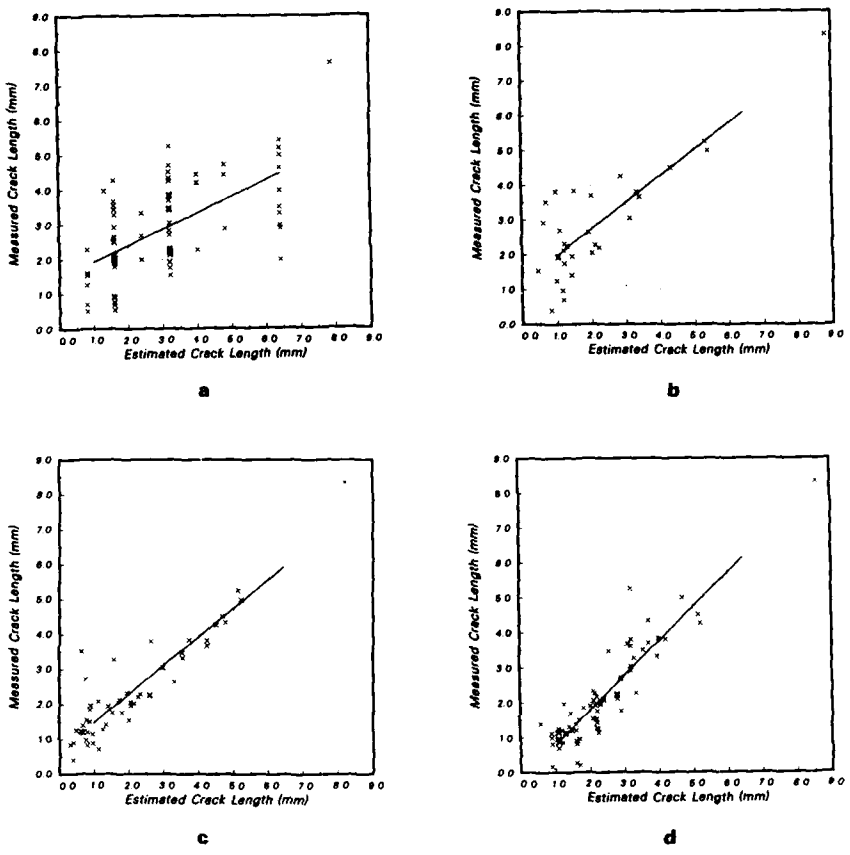

Fig. 19. Estimated versus SEM measured crack size data for (a) LPI30, (b) LPI45, (c) LPI60 and (d) ULW, techniques.

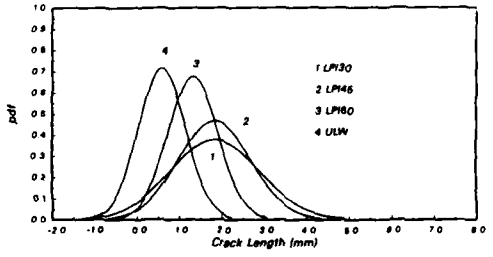

Fig. 20. SEM measured crack length distribution for an estimated crack length of 0.8 mm for LPI30, LPI45, LPI60 and ULW techniques.

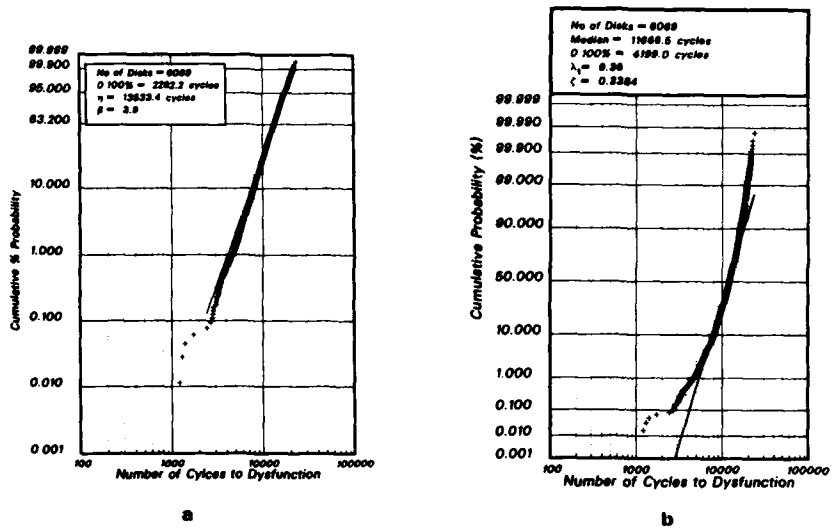

Fig. 21. The PFM based N_d data for the LPI60 technique using the lower 95% confidence bound to generate the POD data and the undetected crack size distribution to size the missed cracks: (a) Weibull analysis results, and; (b) Log-normal analysis results.

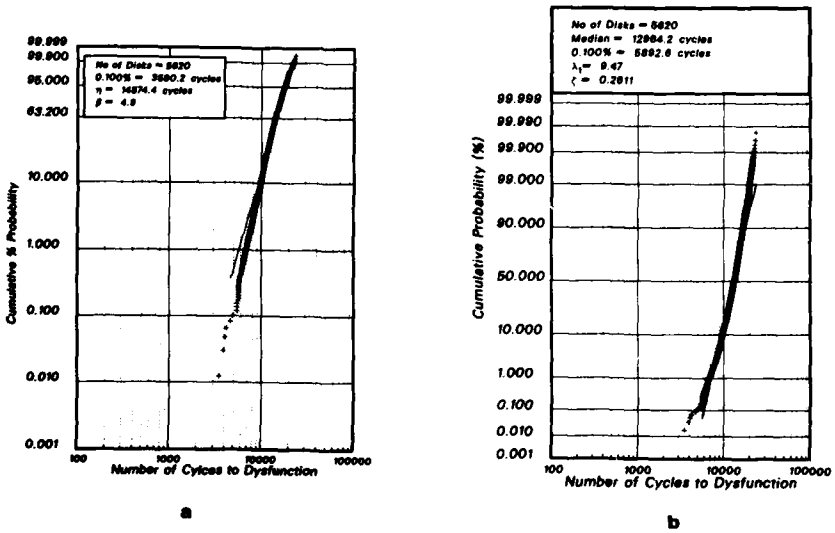

Fig. 22. The PFM based N_d data for the ULW technique using the lower 95% confidence bound to generate the POD data and the undetected crack size distribution to size the missed cracks: (a) Weibull analysis results, and; (b) Log-normal analysis results.

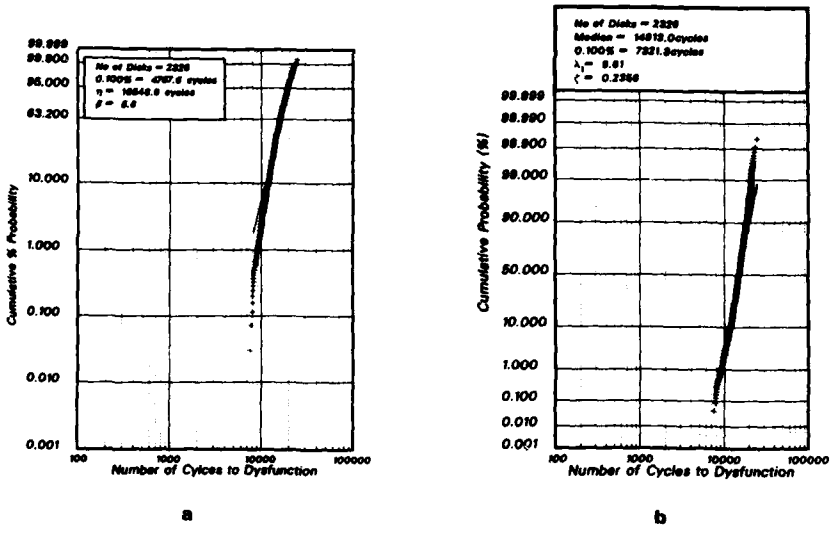

Fig. 23. The PFM based N_d data for the ECI5* technique using the lower 95% confidence bound to generate the POD data and the undetected crack size distribution to size the missed cracks: (a) Weibull analysis results, and; (b) Log-normal analysis results.

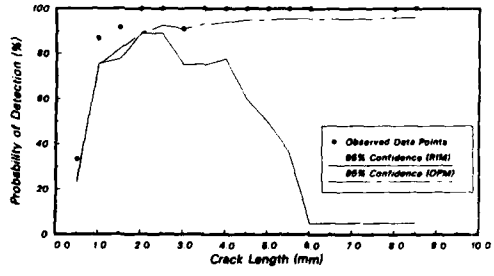

Fig. 24. The lower 95% confidence bounds varying as a function of crack length for the ECI5 technique determined with the help of the binomial distribution. The dotted line represents results obtained by the optimized probability method (OPM) whereas the solid line represents the results obtained by the range interval method (RIM).

LES DEVELOPPEMENTS A COURT TERME DES CONTROLES NON DESTRUCTIFS APPLICABLES AUX PIECES DE TURBOMACHINES

par

J.Vaerman
SNECMA Corbeil
B.P. 81
91003 Evry Cedex
France

1. INTRODUCTION

Les contrôles non destructifs sont et demeureront un des facteurs déterminants de la qualité et de la sécurité des turbomachines aéronautiques.

Il est désormais unanimement admis que l'intégrité structurale de celles-ci doit être assurée en tenant compte de la présence éventuelle de défauts de fabrication ou d'endommagements en service restant dans des limites définies "acceptables", qui tendent à devenir de plus en plus faibles en valeur et en tolérance de dispersion. L'absence de défauts internes ou superficiels supérieurs à ces limites nécessite la mise en oeuvre de contrôles non destructifs de plus en plus efficaces et fiables.

Pour améliorer l'efficacité et la fiabilité des contrôles non destructifs, quel que soit le principe physique exploité, il est indispensable de les structurer sur la base d'une organisation en phases élémentaires qui sont présentes dans tous les cas.

Le schéma de principe de la figure 1 présente de manière synoptique l'organisation de ces phases élémentaires.

Jusqu'à un passé récent, ce type de processus de fonctionnement d'un contrôle non destructif était considéré de manière globale. Il était admis que le résultat du contrôle soit fluctuant et que l'évaluation des défauts demeure qualitative ou semi quantitative.

Les besoins nouveaux en caractérisation quantitative des défauts ainsi qu'en fiabilité de détection justifient les actions de progrès qui sont maintenant menées de manière spécifique, au niveau de chaque phase du processus relatif à chaque principe physique exploité.

2. LES PHASES ELEMENTAIRES

2.1. Génération de l'énergie d'excitation

2.1.1. Principes communs à l'ensemble des techniques

Pour la plupart des techniques CND appliquées, l'énergie d'excitation est générée par transformation d'une énergie de sollicitation primaire (énergie de sollicitation d'un élément piézoélectrique par exemple) elle-même issue d'un courant électrique d'alimentation (secteur).

Les sources d'énergies d'excitation proprement dites (rayonnement électromagnétique, vibrations US, Courants de Foucault) sont généralement définies par les caractéristiques essentielles suivantes :

- dimensions : ponctuelle étendue,
- forme du faisceau de radiation émis : divergent, parralèle ou convergent
- le type d'émission continu ou impulsionnel,
- l'intensité,
- la fréquence temporelle de la source ou spatiale du faisceau émis.

Certaines de ces caractéristiques sont définies par construction, d'autres ajustables par réglages manuels et plus récemment par commande automatique programmée des énergies de sollicitation primaires.

Les exigences de performances et de qualités des sources sont sans cesse croissantes ; fonction de transfert, précision des réglages, stabilité de fonctionnement, insensibilité à l'environnement.

Les besoins prévisibles à court terme nécessitent des développements dont quelques exemples sont donnés ci-après :

2.1.2. Traducteurs ultrasonores

Les traducteurs appliquent le principe de la piézoélectricité réversible.

2.1.2.1. Amortissement de l'élément vibrant

La sensibilité d'un traducteur sollicité par impulsions croît avec le niveau d'énergie émise. Sa résolution est moins bonne lorsque la durée de vibration de l'élément vibrant est plus longue. Actuellement, l'amortissement de la vibration de la céramique est réalisée en changeant sa face arrière (Backing) ce qui réduit l'énergie émise donc sa sensibilité.

Du fait des fortes ruptures d'impédance entre milieux successifs (céramique, couplage, pièce, défaut) traversés deux fois (contrôle par réflexion), le signal de défaut recueilli par la céramique représente une faible part de l'énergie émise (Fig. 2).

Une étude récente * a montré qu'une solution à ce problème principal de rupture d'impédance entre céramique et milieu de couplage consistait à utiliser des couches d'adaptation d'impédance entre ces deux milieux de manière à amortir les vibrations de la céramique par sa face avant, augmenter l'énergie émise, donc améliorer simultanément la sensibilité de détection et de résolution du traducteur. L'adaptation de l'impédance électrique d'entrée est aussi un facteur à considérer.

Les modèles réalisés dans le cadre de cette étude ont été validés expérimentalement, leurs prise en compte par les fabricants de traducteur devrait aboutir à la fonction de bande passante la plus large possible donc à un progrès sensible dans l'efficacité des contrôles ultrasons (figure 3).

2.1.2.2. Caractéristiques acoustiques du faisceau

La mesure de la pression acoustique en différents points d'un faisceau ultrasonore et le tracé des isobares permettent d'en définir la forme. La sensibilité maximale de détection des défauts se situe dans la zone où la pression acoustique est maximale. Cette zone habituellement centrée sur l'axe longitudinal du faisceau constitue la tache focale lorsqu'il est focalisé, sa distance nominale par rapport au traducteur étant généralement définie dans l'eau.

Lorsqu'un faisceau focalisé traverse perpendiculairement un dioptre plan (milieu de couplage-matériaux à contrôler) la distance focale est modifiée par effet de réfraction (incidence oblique des rayons s'écartant de l'axe en faisceau) mais la tache focale reste approximativement symétrique. Lorsque la géométrie du dioptre devient une surface cylindrique (contrôle de barres ou de fond d'alvéoles, etc.) la symétrie géométrique du volume de la tache focale est détruite d'autant plus que le rayon du cylindre est faible. On constate une augmentation du diamètre de la tache focale et de sa profondeur dans le plan perpendiculaire à celui comprenant la génératrice du cylindre. Cette défocalisation entraîne une perte de sensibilité de détection.

Pour les contrôles à haute performance, il est nécessaire de corriger cette aberration géométrique. Cette correction est maintenant possible en utilisant des éléments de focalisation de forme bifocale. Les gains constatés en sensibilité de détection sont significatifs (Fig. 4 et 5).

En conclusion de ce chapitre, nous pouvons retenir que :

- les recherches scientifiques dans le domaine de la physique des traducteurs sont désormais bien actives,
- les progrès seront d'autant plus sûrement et rapidement réalisés que les besoins seront plus rigoureusement définis et que les fabricants de chaînes de mesures ultrasonores et de traducteurs coordonneront leurs efforts.

2.1.3. Sondes à Courants de Foucault

La détection des défauts de surface ou sous-jacents par Courants de Foucault repose sur l'induction électromagnétique. L'excitation est générée par une bobine alimentée par un courant alternatif. On mesure l'impédance de la bobine qui est modifiée par la proximité de la surface de la pièce et les variations de cette proximité liées à :

---

* Université de technologie de Compiègne.

- des imprécisions de déplacement de sonde par rapport à la surface,
- la microgéométrie de surface, la présence de traces de chocs,
- les variations locales de caractéristiques électriques ou magnétiques,
- l'instabilité en température,
- la présence des criques, inclusions.... à détecter.

Lorsque la fréquence du courant d'alimentation de la bobine est augmentée, la pénétration de l'excitation décroit mais la densité de Courants de Foucault de surface croit.
Si la sonde est constituée d'une simple bobine et que la fréquence est inadaptée, les anomalies des 4 premiers points énumérés ci-dessus peuvent donner des indications plus importantes que les défauts à détecter (dernier point).
Afin d'accroître l'efficacité des contrôles par Courants de Foucault, les améliorations déjà réalisées ou en cours portent sur :

- la focalisation du champ d'excitation qui accroit la sensibilité de détection et la résolution latérale,
- la division des bobines en deux parties (avec ou sans blindage intercalaire) afin d'améliorer encore la focalisation.
- l'utilisation de deux bobines montées en opposition afin d'améliorer la stabilité en température par compensation de l'effet de ses variations. Ce montage est aussi favorable pour l'utilisation de champs magnétiques plus intenses.

- le balayage en fréquence (projection multifréquence ou multiparamètres) qui permet une optimisation de la sensibilité de détection sur une profondeur plus étendue, une meilleure discrimination entre perturbations parasites et celles à prendre en compte.
- l'excitation pulsée générée par des impulsions à large bande d'un spectre de fréquence continu.
  L'amplitude du signal est évaluée en fonction du temps (similitude avec l'échographie ultrasonore). Cette méthode encore au stade des études favoriserait une haute sensibilité de détection, une résolution améliorée ainsi qu'une bonne fiabilité. Le progrès serait particulièrement sensible au niveau de la précision de mesure :
  . de la profondeur des défauts,
  . des épaisseurs notamment lorsqu'elles sont inférieures à 0,5 mm.

2.1.4. Générateurs de rayons X

La courbe caractéristique d'un film radiographique est tracée à partir de la relation entre le logarithme de l'exposition et la densité optique du film. Il est donc nécessaire de bien déterminer les valeurs d'exposition, ce qui n'est pas courant et encore difficile.

Afin de connaître et optimiser les caractéristiques d'une irradiation issue d'un générateur de rayons X, les paramètres essentiels à prendre en compte sont les suivants :

- valeur de la haute tension,
- spectre d'émission,
- répartition angulaire de la fluence des photons dans le faisceau utile,
- dimension du foyer.

La valeur de la haute tension est généralement inaccessible directement. C'est plutôt la reproductibilité en fonction des mises en service successives et du vieillissement qui est actuellement considérée. L'écart de la valeur de la haute tension peut atteindre :

- quelques % pour des générateurs anciens à réglages analogiques,
- mieux que 1 % pour des générateurs plus récents à commande numérique, 0,05 % pour les meilleurs.

Ces résultats révèlent un progrès sensible dans l'amélioration de la reproductibilité des valeurs de haute tension propres à chacun des générateurs récents.

Cependant, l'absence de référence commune induit un doute certain dans l'évaluation des écarts entre appareillages.

Etant donné que la tension d'accélération (HT) détermine l'énergie des photons et les coefficients d'absorption associés, des écarts d'exposition consécutifs à ceux de la HT sont donnés ci-après à titre indicatif.

ECARTS DES VALEURS DE HT EN %	ECARTS D'EXPOSITION % A LA SORTIE DE L'ABSORBANT
1	4 à 7
2	8 à 15
5	20 à 40

L'influence des écarts peut donc être importante.

A noter encore que :

- la sensibilité d'une émulsion photographique est réduite d'un facteur 20 lorsque l'énergie des photons croit de 40 à 200 keV,
- l'irradiation d'un tube Rx varie d'un facteur 2 lorsque l'épaisseur du filtre interne varie de 0,4 à 0,7 mm, variation encore accentuée si le spectre contient beaucoup de photons de basse énergie.

  Il parait donc nécessaire d'avoir des tolérances plus sévères pour l'épaisseur des filtres propres aux tubes et une meilleure connaissance des spectres d'émission particulièrement pour le contrôle des épaisseurs et masses volumiques faibles (composites).

- La forme et l'orientation relative anode cathode peut avoir une influence sensible sur la répartition des fluences (densité de flux) des photons dans le faisceau utile d'un générateur de rayons X. L'écart peut atteindre 75 % entre la zone des valeurs maximales et celles des valeurs minimales sur des appareils commercialisés.

- A signaler enfin l'intérêt des générateurs à microfoyer pour l'amélioration de la sensibilité de détection des petits défauts (microporosités). Les tensions d'accélération et débits encore faibles limitant l'emploi aux pièces d'épaisseur ou de masse volumique faible, mais des progrès sont en cours afin d'étendre le champ d'application notamment dans le domaine des Rx temps réel.

Nous venons de souligner qu'en contrôle par Rx la plupart des caractéristiques ne peuvent être directement mesurées. Les conditions de fonctionnement des processus sont généralement évaluées de manière globale, à l'aide d'IQI (indicateur de qualité d'images). Ayant constaté comme beaucoup d'autres, la sélectivité insuffisante de ces IQI, la SNECMA, par exemple, a réalisé et évalué un indicateur de sensibilité de détection beaucoup plus sélectif (figure 20).

En résumé, des progrès sont en cours (stabilité HT), d'autres sont nécessaires (spectres d'émissions, répartition de la fluence). La pression des besoins sera sans doute un élément moteur, ne serait-ce que dans le domaine des applications en tomodensitométrie.

2.2. Perturbation

La propagation d'une énergie dans un milieu donné est "perturbée" par la présence d'hétérogénéités éventuellement présentes au sein de ce milieu (absorption, diffusion, réflexion, diffraction...).

La présence d'une pièce à contrôler dans ce milieu remplit évidemment ces conditions.

A la perturbation par la pièce se superposent :

- une perturbation par un défaut à détecter situé en surface ou au sein de la pièce,
- l'environnement de la pièce à contrôler et celui du défaut à détecter en surface ou au sein de l'objet qui constituent une autre cause de perturbation de l'énergie reçue par le capteur (Fig. 6).

Dans le but de ne prendre en compte que les informations significatives de la présence de défauts à détecter et de les optimiser, il est nécessaire de procéder à une étude préalable et à une définition rigoureuse des conditions de contrôle, particulièrement lorsque les performances à atteindre sont élevées (quantifier des petits défauts de manière reproductible).

A l'origine, les définitions des processus de CND pour applications industrielles étaient recherchées par une approche presqu'exclusivement expérimentale longue et coûteuse conduisant à une solution parfois éloignée de l'optimum dans les cas difficiles.

Depuis 1960 environ, les nouvelles exigences des clients, la pression de la concurrence, l'accroissement de sécurité nécessaire dans certains secteurs industriels (nucléaire, automobile, aéronautique) ont imposé que les méthodes expérimentales soient complétées par des approches analytiques ; des spécialistes sont apparus, des laboratoires spécialisés dans l'étude de CND (anoblis en END) ont été créés et les END sont devenus une technologie à part entière.

La méthode analytique nécessite encore de nombreux essais souvent à l'aide de plusieurs appareils et diverses "sondes" (émetteur capteur) et dans tous les cas de nombreux échantillons d'essais. Au cours de ces dernières années, la recherche de solutions par modélisation des processus END a fait son apparition d'abord dans les laboratoires universitaires puis dans ceux de l'industrie. Le déroulement des processus possibles d'inspection sont représentés par leurs modèles physiques formulés par des équations introduites dans des programmes informatiques qui les traitent.

Sans avoir à réaliser de sondes prototypes onéreuses, d'éprouvettes représentatives avec défauts artificiels, d'essais réels, ces modèles permettent :

- de prédire si une solution imaginée pour résoudre un problème de CND sera valable,
- de comparer les résultats de solutions différentes,
- de résoudre des cas de matériaux difficiles, de géométries complexes impossible à traiter par méthode analytique.

La solution retenue doit bien évidemment être validée expérimentalement, mais comparativement aux approches précédentes, les réductions de coûts et délais peuvent être très importantes pour aboutir à une solution du problème plus performante dans la plupart des cas.

Le développement des outils mathématiques et moyens informatiques adaptés, l'extension en cours du champ des applications (Courants de Foucault-Ultrasons-Magnétoscopie-Thermographie infrarouge) amènent à considérer que la modélisation mathématique des techniques CND est maintenant un outil réel et valable qui sera de plus en plus largement utilisé dans le futur (exemples d'applications, (Fig. 7 et 8).

2.3. Révélation

2.3.1. Analyse par capteurs

2.3.1.1. Objectif

L'objectif est de détecter des défauts et de les caractériser en nombre et respectivement en nature, forme, dimension, position, orientation et relation d'interface dans le volume contrôlé.

Selon la technique et l'état de l'art, le capteur réagit de manière plus ou moins fidèle par des "signaux" porteurs d'informations spécifiques de défauts situés :

- en surface (visuel, ressuage, magnétoscopie, Ultrasons, Courants de Foucault, Rayons X ...),
- au voisinage immédiat de la surface (Magnétoscopie, Courants de Foucault),
- dans le volume :

  . sans information de profondeur (Rayons X, Thermographie IR classique),
  . avec information de profondeur (Ultrasons, Thermographie IR en cours d'évolution).

Selon sa nature, le capteur élémentaire peut réagir de manière quasi instantanée à des informations d'origine :

- ponctuelle (CdF),
- linéaire dans la direction du sondage (US),
- surfacique (photographie de surfaces, caméras vidéo, CCD),
- volumique (films Rx, Rx temps réel, caméras IR).

Par déplacement relatif capteur/pièce à contrôler, donc par balayage linéaire et juxtaposition des lignes de balayage, il est possible de passer d'une information :

- ponctuelle à une information linéaire dans la direction du balayage puis surfacique (CdF).
- linéaire dans la direction du sondage à une information volumique (US). (Voir Fig. 9).

Pour détecter et caractériser automatiquement les défauts, il est actuellement indispensable qu'à chaque point (pixel) de la surface ou du volume de l'objet à contrôler, soient affectées les grandeurs physiques qui le caractérisent. Il s'agit de la fonction ANALYSE réalisée par le capteur.

Etant donné que ces grandeurs physiques n'ont de valeur significative que par comparaison avec celles des points voisins, considérés à plus ou moins longue distance, cette comparaison ou synthèse sera le résultat d'une action complémentaire distincte située au niveau de la fonction traitement de signaux.

En résumé, la démarche est donc :

- de procéder à une ANALYSE par le capteur de la surface ou du volume à contrôler (grandeurs physiques spécifiques de chaque pixel),
- de réaliser la SYNTHESE des résultats précédents par comparaison et établissement des relations entre grandeurs physiques des pixels plus ou moins proches.

2.3.1.2. Les capteurs

La détection visuelle des indications de défauts et l'interprétation des résultats par des opérateurs différents induit une fluctuation dans l'efficacité des contrôles qui, si elle était admise ou subie jusqu'à présent, devient inacceptable pour les applications futures. L'évolution s'oriente donc vers la généralisation de l'utilisation de capteurs au sens physique du terme, c'est-à-dire d'appareils transformant une énergie de nature quelconque en ENERGIE-ELECTRIQUE. Cette énergie doit, dans certains cas, être adaptée au domaine de sensibilité du capteur utilisé par l'action préalable d'un traducteur qui transforme la grandeur physique de sortie adaptée au domaine de sensibilisation du capteur.

Pour couvrir l'ensemble des besoins en CND, la nature physique des excitations mises en jeu sont diverses (thermique, vibratoire, capillarité, magnétique, électromagnétique...). Le tableau I révèle cependant qu'actuellement, c'est l'intéraction rayonnement électromagnétique/capteur qui est la plus utilisée et qui tend à se généraliser ou à se développer.

Cette évolution convergeant vers l'utilisation de capteurs sensibles à la détection d'un seul type d'énergie présente des avantages décisifs :

- depuis Huygens (1629-1695), la connaissance de la physique du rayonnement électromagnétique est l'une des plus avancées et progresse constamment.

- les systèmes de "manipulation" de ces rayonnements sont en constant développement et les techniques de fabrication correspondantes bien maîtrisées (optique géométrique de précision, interféromètres, laser, systèmes optoélectroniques intégrés, fibres optiques...)

- les capteurs optoélectroniques multiéléments (barrettes, matrices) constituent une interface particulièrement bien adaptée aux systèmes d'acquisition et de traitements d'analyse et de synthèse.

La figure 1 montre que, quelle que soit la technique de contrôle appliquée, le principe du processus et l'objectif sont identiques.

Cette unité constitue une situation favorable et il serait dès à présent opportun de choisir une voie, définir les moyens adaptés à celle-ci, y canaliser les efforts de créativité, y concentrer les applications, les investissements de manière à accélérer le progrès, réduire les coûts et enfin favoriser sans difficultés la standardisation et la normalisation.

2.3.2. Synthèse

2.3.2.1. Les traitements de signaux

Comme indiqué précédemment et considérée de manière simplifiée, l'analyse aboutit à l'enregistrement d'une répartition dans un plan (2D) ou dans un volume (3D) des valeurs de grandeurs physiques mesurées point par point.

La synthèse est le résultat d'une comparaison des grandeurs ponctuelles avec celles des points voisins considérés à plus ou moins longue distance. Elle suppose que les valeurs mémorisées pour chaque point sont représentatives des points objets correspondants (Signal 2D ou 3D homothétique de l'objet).

En fait, il n'en est rien, et même dans l'hypothèse où toutes les phases antérieures ont été réalisées correctement, les signaux "significatifs" enregistrés sont altérés par de nombreux phénomènes physiques réels mais considérés comme parasites et ayant pour origine :

- le capteur (y compris barrettes et matrices) : sensibilité, réponse spectrale, linéarité du gain (si amplificateur), stabilité, caractéristiques temporelles, bruit électronique (figure 19).

- la pièce à contrôler, le défaut à détecter et leur environnement :
  variation d'épaisseur, proximité défaut surfaces limites, effets d'absorption, diffusion, réfraction, diffraction, réflexion....

D'autre part, à quelques exceptions près une représentation en "niveaux de gris" de la répartition 2D 3D des grandeurs physiques mesurées ne permet pas une extraction directe des "objets" (défauts) à analyser. Une amélioration et une simplification préalable doit être réalisée afin d'aboutir à une représentation binaire des résultats. Il est aussi nécessaire de réaliser une réduction des effets parasites, une optimisation des contrastes et de la résolution.

Sans entrer dans le détail des méthodes de traitement, rappelons cependant les deux principaux types de traitement :

- le filtrage temporel,
- le filtrage spatial.

Dans le filtrage temporel, la sommation de N acquisition d'une même zone (capteur fixe) entraîne un écart d'amplification des indications significatives (stables) par rapport aux indications aléatoires (bruit) d'autant plus important que N est élevé.

Le niveau de contraste souhaité détermine le N nécessaire donc la durée de l'intégration. C'est la seule méthode qui améliore le contraste sans altérer la définition.

La conséquence industrielle a priori pénalisante des temps d'intégration tend à se réduire en utilisant des multicapteurs (barrettes, matrices) à chaque fois que la technique de contrôle le permet. Parallèlement, les fabricants de capteurs cherchent à optimiser la vitesse d'acquisition afin d'accroître le nombre d'intégrations en durée constante.

En réalité, l'amélioration du rapport signal sur bruit ne suffit pas à rendre significative la grandeur physique mesurée en chaque point.

La zone d'action efficace du capteur n'étant pas rigoureusement ponctuelle, elle prend aussi en compte l'influence des points voisins. Le filtrage spatial d'une "image" intégrée et mémorisée permet l'amélioration de sa définition, d'aboutir à une classification des objets et généralement à une comparaison à des références pour décisions.

Les principaux types de filtres spatiaux sont :

- les filtres linéaires ou non (élimination bruit de fond),
- les filtres morphologiques (simplification de la forme des objets).

L'opération finale de seuillage transforme une image en niveaux de gris (sur n bits) en image binaire (sur 1 bit).

L'accroissement des besoins pousse les chercheurs à imaginer de nouvelles méthodes de reconnaissance de formes plus puissantes mais aussi très consommatrices de temps de calcul ce qui est contraire à l'objectif temps réel.

Afin de résoudre ce dilemme, l'évolution en cours tend à :

- créer des systèmes spécialisés en marge des calculateurs et de l'informatique classique,
- accélérer les logiciels d'application en les affectant à des unités de calcul rapide utilisant des composants électroniques spéciaux microprogrammés,
- créer des primitives microprogrammées puissantes de reconnaissance de forme et ce, plus particulièrement pour la morphologie mathématique.

(Le synoptique d'un système avancé est donné par la figure 10).

- concevoir des interfaces électroniques spécifiques pour les capteurs car les progrès possibles en traitement d'"images" sont dépendant de l'adaptation respective des technologies des capteurs et calculateurs. L'interdépendance est déjà essentielle pour des applications médicales telles la Tomographie X, le Scanner infrarouge, les sondes ioniques et les analyseurs à ultrasons.

  Des exemples plus concrets d'interdépendance (et d'intégration) capteur traitement sont donnés ci-après.

2.3.2.2. *Capteurs intelligents*

De l'interdépendance forte entre capteurs et systèmes de traitement, le secteur médical est allé plus avant dans la miniaturisation et l'intégration en plaçant sur la même pièce le capteur et une électronique intégrée comportant en particulier le microprocesseur et des mémoires.

Ces capteurs intelligents présentent les avantages suivants :

- amélioration du rapport signal sur bruit par adaptation d'impédance et amplification,
- prétraitement du signal : compensation en température et en variation d'alimentation, remise à zéro automatique, filtrage des signaux parasites et correction de non linéarité,
- traitement du signal, codage et modulation des signaux de sortie, moyennage pour extraire le signal de bruit, redondance et alarmes intégrées signalant les défauts de capteurs,
- logique de décision : tendance d'un signal et corrélation entre plusieurs signaux, calculs multiparamètres, reconnaissance d'un signal et réjection.
- réduction de consommation.

Les applications médicales sont multiples notamment celles qui nécessitent un "monitorage ambulatoire".

D'une manière générale, l'industrie et plus particulièrement l'industrie aéronautique a aussi ce type de besoins à satisfaire en contrôle in situ d'aéronefs en cours d'utilisation. Plus directement, les avantages cités précédemment, associés aux capteurs intelligents, apportent tous une réponse aux questions qui pour l'essentiel restent posées dans notre secteur d'application. Un simple effort de transfert de technologie est à faire.

2.3.2.3. *Sondes incohérentes*

Autre résultat de la liaison forte entre capteurs et systèmes de traitement, l'analyse spectrale d'un écho ultrasonore se fait sur le bruit échographique du milieu multidiffuseur (speckle acoustique).

Ce bruit :

- résulte de l'interface entre tous les échos élémentaires situés dans la cellule de résolutions (sources induites dans l'objet par le champ incident).
- empêche de distinguer des structures spéculaires de faible contraste dans des milieux diffuseurs (fissures dans les aciers à gros grains).

L'analyse spectrale de ce bruit dans une porte temporelle donne des allures de spectre très chahutées.

Afin d'obtenir des spectres plus lissés de ces milieux, on effectue jusqu'à présent un moyennage spatial sur de nombreux "tirs" ultrasonores décorellés (N positions décorellées) d'où perte de résolution spatiale.

Plus récemment, afin d'augmenter le nombre d'informations décorellées pour une position donnée de la sonde, des essais ont été réalisés à l'aide de sondes :

- annulaires (6 anneaux) : un déplacement de sondes sur environ 20 positions étant encore nécessaire.
- multi-éléments (36) : technique très lourde du fait de la connectique à développer.

Une solution très prometteuse en cours d'étude consiste à intercaler dans le faisceau d'un seul traducteur un écran de phase aléatoire mis en rotation rapide.

Au cours du déplacement du décohéreur, une série de tirs ultrasonores est effectuée. Pour chaque position du décohéreur les relations de phases entre échos des différents diffuseurs sont modifiées.

- Le signal échographique résultant présente des minima et des maxima, fonctions de la position du décohéreur dans le signal.

- On étudie la moyenne des enveloppes échographiques et des densités spectrales de puissance (figure 21).

L'application de cette dernière méthode au contrôle ultrasonore des milieux diffuseurs permettra l'accès à des informations intéressantes en séparant les échos spéculaires du bruit de speckle échographique.

3. L'EVOLUTION ET ADAPTATION DES CRITERES

3.1. Etat actuel

Acutellement, les critères limites d'acceptation en CND sont définis de manière spécifique dans chaque type d'industrie (aéronautique, automobile, nucléaire ...) en fonction :

- Du type de pièce - produits, demi produits, pièces.

- Des matériaux métalliques, céramiques, composites organiques.

- Du mode d'élaboration, pièces forgées, coulées, Métallurgie des Poudres.

- Du stade d'application : - contrôle spécifique des phases critiques de fabrication, usinage par rectification, soudage, traitement thermique ou de surface ... et pièces finies.
  - Contrôle après utilisation
  - Maintenance
  - Réparation

- Des méthodes de contrôle appliquées : - visuelles, Ressuage, Magnétoscopie, Ultrasons, Radiographie X.

- Du type de défaut cherché : - aspect, criques, porosités, inclusions, ségrégations.

- Des méthodes de comparaison défaut/seuil limite d'acceptation : - systèmes avec seuils automatiques (ultrasons, Courants de Foucault), interprétation visuelle (humaine) d'un résultat global.

Dans ce contexte, les critères définissant les défauts sont très divers et dans certains cas la complexité d'application entraîne des incertitudes sur l'efficacité de leur application.

Le tableau synoptique n° II présente, à titre indicatif, l'ensemble des stades d'application des CND relatifs à la fabrication et à l'exploitation d'un moteur d'aviation.

De manière synthétique, la définition actuelle et l'application des critères peuvent être considérées comme présentées ci-après :

- <u>Défauts individuels quantifiés selon</u> :

  . Une grandeur qui mesure <u>directement</u> les caractéristiques du défaut : longueur surface orientation position espacement entre deux défauts (exemple : criques, cavités, inclusions présentes en surface de pièce et évaluées en examen visuel avec aide optique le cas échéant).

  . Une grandeur indirectement liée aux caractéristiques du défaut ; amplitude-temps (ultrasons, Courants de Foucault).

- <u>Défauts non quantifiables individuellement</u>

  . Il s'agit de défauts dont la représentation est complexe et pour lesquels la caractérisation individuelle est visuellement impossible ou non réalisable industriellement.

L'évaluation est faite soit :

- Directement par rapport à des classes d'échantillons types,

- Indirectement par rapport à des documents de référence (répliques, photographies, clichés radiographiques type ASTM).

3.2. Evolution et adaptation

L'évolution des CND vers le tout automatique a engendré une évolution sensible des moyens au cours des dernières années au niveau de l'acquisition et du traitement des signaux :

- Utilisation plus fréquente des capteurs sensibles aux rayonnements ionisants (voir tableau I),
- Systèmes de traitements puissants et rapides (proches du temps réel),
- Algorithmes de traitement évolués à la veille de traiter la majeure partie des cas industriels courants au moins en ce qui concerne l'aptitude à isoler et à caractériser la forme des "objets" significatifs (défauts) tout en éliminant ou en réduisant actuellement à un niveau proche de l'acceptable la prise en compte des artefacts (fausses alarmes).

Le nombre d'applications industrielles est encore limité et il a été tenté dans la plupart des cas d'appliquer avec plus ou moins de succès les critères limites d'acceptation initialement définis pour des conditions de diagnostic et de sanction classique.

Afin d'optimiser les nouvelles possibilités, une remise en cause de la définition des critères est nécessaire et paraît possible par une approche plus synthétique des problèmes posés.

Le tableau 2 présente aussi :

- les différents types de défauts recherchés aux différents stades du contrôle,
- les grandes classes de forme type des défauts cherchés.

Ce tableau de synthèse révèle que l'ensemble des principaux défauts classiques connus recherchés aux différents stades de la fabrication des pièces et de la maintenance ou de la réparation de machines rentrent dans 4 classes de forme de défauts dont :

- ponctuels
- linéaires (filiformes)
- surfaciques (2D)
- volumiques (3D)

Selon la manière dont ces défauts sont représentés sur le plan d'analyse, la synthèse peut consister en l'extraction et la quantification de lignes ou de surfaces de géométries plus ou moins complexes.

Considérés individuellement, les objets peuvent être définis par tout ou partie de l'ensemble des caractéristiques géométriques possibles (Fig. 11)

dont pour l'essentiel :

- la plus grande dimension,
- facteur de forme (identification défaut plans),
- barycentre,
- surface,
- périmètre,
- orientation,
- position,
- etc.

Pris dans leur ensemble et les uns par rapport aux autres, les défauts peuvent être considérés en :

- nombre total,
- nombre par unité de surface (densité),
- distance entre barycentres de 2 proches voisins en fonction de la plus grande dimension de l'un d'eux,
- relations de continuité entre particules isolées (alignement de soufflures ou porosités).
- la répartition par classe de l'une des caractéristiques individuelles,
- etc.

Sur cette base, des images de clichés radiographiques de référence (ASTM) ont été quantifiées et des clichés radiographiques de pièces réelles automatiquement comparées avec succès à ces références.

Il est souhaitable que les spécialistes en la matière se concertent afin de :

- sélectionner les grandeurs caractéristiques à retenir pour satisfaire l'essentiel des besoins en critères,
- codifier cette sélection et l'introduire dans des standards de niveau international,
- favoriser le développement, l'optimisation et la commercialisation des capteurs et de l'électronique rapide d'acquisition et de traitement

- favoriser la normalisation de ces éléments,
- favoriser une automatisation efficace du diagnostic et de la sanction proche du temps réel à moindre coût.

4. LES DEPLACEMENTS RELATIFS EMETTEURS CAPTEURS PIECES

Ce qui vient d'être présenté permet d'imaginer sans difficulté ce que doit être la partie "support" d'une installation de contrôle.

La détection et la caractérisation dimensionnelle de défauts fins, leur situation précise en surface ou dans le volume d'une pièce qui peut être de géométrie complexe, impose des exigences au niveau des conditions des déplacements des émetteurs récepteurs et de la pièce à contrôler.

Dans la plupart des cas, ils sont séparés mais interdépendants.

Le niveau des performances du contrôle et la complexité de la géométrie des pièces imposent :

- le nombre de degrés de liberté (jusqu'à 6 ou 7 voire plus),
- la précision et la reproductibilité :
  . des positions relatives (de l'ordre de 0,01 mm pour les translations et de quelques secondes d'arc pour les rotations),
- . des vitesses de déplacement.

Dans le but d'atteindre ces performances mécaniques, l'automatisation devient inévitable et la fiabilité des programmes est un point aussi essentiel.

Les installations sont ou vont devenir de véritables machines-outils capables de performances métrologiques véritables)

5. LA PRATIQUE INDUSTRIELLE

5.1. Microscopie acoustique

Les progrès récents réalisés dans l'élaboration de matériaux "Hautes températures" par métallurgie des poudres ou céramiques frittées et les gains en performances qui leur sont associés ont naturellement engendré des applications sur moteurs d'aviation.

La nécessité de fabriquer et contrôler industriellement les pièces correspondantes s'est alors présentée.

Sur ces matériaux, la taille critique des défauts est de 10 (MDP) ou 100 (céramiques) fois plus faible que sur pièces de même type (disques, aubes) réalisées jusqu'à présent par méthode conventionnelle (forge, fonderie). Dans le but de détecter ces défauts de très petites dimensions, de 10 à 100 µm, les premières études lancées il y a environ 10 ans se sont orientées vers la réalisation de systèmes ultrasonores à très haute fréquence (plusieurs GHz) dans la perspective de performances équivalentes à la microscopie optique (x 1000) mais permettant des "observations" sous les surfaces des objets.

Ces systèmes conçus pour des applications en laboratoires présentent des inconvénients qui en limitent les applications industrielles :

- échantillon de faible dimension,
- exigences critiques d'alignement sonde/surface de pièce,
- très faible pénétration : quelques µm.
- résolution limitée,
- champ d'examen limité à quelques mm^2.

Plus récemment, des systèmes fonctionnant à des fréquences inférieures à 100 MHz ont été conçus et réalisés de manière à réduire les inconvénients précités. Certains d'entre eux restent cependant des appareils de laboratoire (CGE Marcoussis - Université de Valenciennes, France).

D'autres sont actuellement capables du contrôle de pièces de production. Deux d'entre eux peuvent être signalés sans donner le détail du principe de fonctionnement :

- Système développé par General Electric Company, Schenectady

  - Capable du contrôle des disques de turboréacteurs (ou de pièces cylindriques),
  - Fréquence de 0,5 à 100 MHz (habituellement 50 MHz),
  - Méthode par impulsion et réflexion (écho),
  - diamètre tache focale 0,137 mm dans l'eau (0,147 dans un superalliage base Nickel),
  - grandissement jusqu'à X 20 par accroissement proportionnel sur C-Scan du pas lignes, et de la vitesse de balayage,
  - image 16 niveaux de gris : affichage direct de l'amplitude des échos,
  - pénétration dans super alliage base Nickel
    F = 50 MHz = 3,8 mm
    F = 25 MHz = 6,35 mm

- Système basse fréquence développé par l'université de Stanford (USA)et l'Aérospatiale France

  - Capable pièces (plaques composites) 200 mm x 1000 mm,
  - Fréquence de 3 à 20 MHz,
  - Méthode par train d'ondes monofréquence et écho,
  - Diamètre tache focale dans l'eau 0,1 mm (10 MHz) 0,3 mm (5 MHz),
  - Signaux recueillis : résultat de phénomènes d'interférences entre onde de Rayleigh, de compression, de surface.

  Il paraît cependant possible de :

  - focaliser en surface = relevé de la topologie de surface,
  - refocaliser à une profondeur voisine d'une longueur d'onde de Rayleigh = contrôle efficace de quelque 0,1 mm sous la surface,
  - faire une pseudofocalisation en ondes transversales (particulièrement intéressant pour contrôle des composites sur plusieurs millimètres de profondeur)
  - vitesse de balayage 200 mm/seconde.

5.2. Chaîne de mesure ultrasonore

Les applications en contrôle ultrasonore dans l'industrie en général et plus particulièrement dans l'aéronautique se sont multipliées de manière impressionnante au cours des 30 dernières années.

Au cours de cette période, des progrès importants ont été réalisés au niveau des équipements. Cependant, avec les nouveaux concepts de tolérance au dommage, parallèlement à l'introduction de nouvelles technologies de fabrication sur de nouveaux matériaux, les performances nécessaires en contrôle ultrasonore sont plus élevées et les exigences plus précises.

Dans l'industrie aéronautique internationale, cette situation est générale de même que le constat d'inaptitude des appareils à ultrasons, y compris les plus récents, pour satisfaire ce nouveau besoin.

Afin de résoudre cette difficulté technique, des sociétés aéronautiques (1) se sont regroupées pour rédiger des spécifications techniques d'une nouvelle génération de "CHAINE DE MESURE ULTRASONORE", présentée ci-après à titre d'exemple. Cette mise en commun a pour but de faciliter l'étude et la réalisation de cette chaîne grâce à la perspective d'un marché plus étendu.

Les points essentiels de cette spécification sont les suivants :

5.2.1. Objectif

Application sur installation de contrôle ultrasonore automatique par immersion à haute performance de pièces métalliques, céramique, composites.

Cette chaîne doit constituer la tête d'une nouvelle génération apte à satisfaire les besoins pour les 10 prochaines années.

Spécifications techniques :

5.2.2. Emetteur

- Modulaire, multivoies, multiplexables (possibilité commande des impulsions en temps décalé).
- Pilotage numérique.

5.2.2.1. Impulsions

Sinusoïde carré bipolaire amortie (Fig. 12).

Nombre, largeur et amplitude des arches programmables, tension première arche ajustable de 50 à 500 V crête à crête.
Impédance de sortie 50 Ω ± 5 Ω, quelle que soit la fréquence.

---

(1) Document AAST 001 éd. 1 du 4 juin 1987.

5.2.2.2. Fréquence de récurrence

100 Hz à 10 kHz par voie par pas progressifs de 10 Hz (autour de 100 Hz) à 1000 Hz (vers 10 kHz),
Fréquence spécifique d'une voie en mode multiplexé.

5.2.3. Récepteur

5.2.3.1. Préamplificateur

- gain de 0 à 24 dB par pas 6 dB. Commutation manuelle ou pilotée prise en compte automatiquement
- par l'amplificateur numérique (voir § 5.2.3.3.).

- linéarité < 0,5 % (écart par rapport à la valeur absolue).
- prise en compte automatique en complément des 24 dB, d'une préamplification primaire de 12 dB éventuellement, située près du traducteur mais intégrée au cable de liaison (connexion séparée et spécifique du raccordement à un câble avec ou sans préamplificateur primaire).

5.2.3.2. Fréquences

- Sans filtre bande passante à - 6 dB de 0,2 à 100 MHz,
- Filtre ajustable
  - filtre passe bande symétrique et fenêtre de fréquence mobile pour analyses spectrales et études de structures.

5.2.3.3. Amplificateur

- Numérique (28 bits mini)
- Linéaire et logarithmique
- Gain mini 114 dB en dynamique totale
- Précision ± 0,5 dB en absolu.

5.2.3.4. Corrections amplitude distance

Base de temps découpée en :

- 300 segments de 300 ns sur la dynamique totale,
- segments de 50 ns sur une dynamique de 10 dB,
- dans tous les cas à partir de l'écho d'entrée.

5.2.4. Moniteur

5.2.4.1. Forme du signal

Type RF pour traitement, le cas échéant.
RF redressé à 1 ou 2 alternances UNIQUEMENT pour visualisation sur écran.

5.2.4.2. Echelle de temps

- Codage sur 21 bits
- Etendue de l'échelle possibilité limite :
  - Contrôle 500 mm d'acier,
  - Colonne d'eau 1 mètre,
  - incrément maxi 10 ns,
  - Résolution 1 ns

5.2.4.3. Portes de surveillance (figure 13)

3 portes de surveillance :

- débuts et fins de portes ajustables par CN ou synchronisées sur échos permanents,
- synchronisation possible entre deux portes avec coïncidence ou décalage positif ou négatif entre début de l'une et fin de la précédente.
- 2 seuils symétriques de détection par porte (positif et négatif) programmables par incrément de 1 bit (résolution de l'amplification) avec une précision de niveau du seuil de 1 bit.

5.2.4.4. Visualisation

- Ecran numérique,
- Représentation
  - A scan temps réel
  - B - C scan en temps pseudo différé,
- Affichage paramètres de réglage de la chaîne et résultats de contrôle.

5.2.5. Données

Trois options possibles de numérotation et stockage
- Signal complet (A,t) situé dans la porte pour chaque récurrence,
- Signal complet (A,t) situé dans la porte pour chaque récurrence ou A maxi > seuil,
- de la valeur de l'écho d'amplitude Max (A) et profondeur correspondante (t) parmi les échos dépassant le seuil.

5.2.6. Auto-contrôles

- Tension de référence calibrée pour autocontrôle de la totalité des fonctions de la chaîne.

- Emetteur :
  - tension,
  - accord d'impédance,
  - mesure de bruit par rapport à la tension de référence,
  - contrôle de chaque changement de paramètre,

- Récepteur :
  - linéarité du préamplificateur analogique,
  - fidélité de la courbe d'amplification du préamplificateur,
  - détermination de la prise en compte d'une courbe de correction,
  - sorties de points tests groupés et repérés.

5.2.7. Traducteurs

Deux configurations possibles :

- fixé directement au porte traducteur machine,
- fixé sur l'étage de préamplificateur primaire lui-même fixé au porte traducteur machine (coaxialité ≤ ± 0,05 mm, parallélisme ≤ ± 0,05°).

Dans les deux cas, possibilité de changement automatique traducteur et étanchéité à l'eau garantie.

5.2.7.1. Exigences standard (Fig.14)

Affichage fréquence contrôle f_c à - 6 dB et - 12 dB (Précision ± 5 %) et bande passante LB.

Ecart entre fréquence dominante (fm) et fréquence centrale $\left| 1 - \frac{fm}{fc_{6dB}} \right| \leq 5\ \%$

Ecart entre amplitude respective des composantes
fm et fc ≤ 1 dB.

5.2.7.2. Caractéristiques acoustiques

Exploration du champ acoustique à l'aide d'un hydrophone aiguille étalonné (Pression absolue affichée en Pascals) :

- au pas de 0,1 mm pour les pressions acoustiques comprises entre la pression Maximale et -3 dB,
- au pas de 1 mm en dehors des valeurs précédentes et ce jusqu'à la limite de - 18 dB.

Représentation graphique des volumes selon deux types de coupes longitudinales et transversales
Définition des paramètres relatifs aux désalignements et excentration selon figure 15.

5.2.8. Caractéristiques des câbles de raccordement appareil de mesures/traducteurs

5.2.8.1. Electriques

- Impédances 50 Ω ± 2 Ω,
- Taux d'ondes stationnaires

$$S = \frac{1 + (K)}{1 - (K)} < 1{,}2\ \%$$

avec $K = \frac{ZL - ZC}{ZL + ZC}$ ZL = impédance selfique, ZC = impédance capacitive

5.2.8.2. Mécaniques

Le câble doit pouvoir supporter 5 10^6 pliages de rayon 25 mm sans altération des caractéristiques.

Inspection automatique par Courants de Foucault de pièces de turbomachines en exploitation

L'inspection par Courants de Foucault est bien adaptée à la détection de criques de fatigue oligocyclique prenant éventuellement naissance dans des zones soumises à des contraintes élevées.

L'aspect critique des zones est souvent associé à une forte sollicitation de parties de pièces de géométrie localement complexe (alvéoles, festons, rayons de raccordement, trous).

Jusqu'à un passé recent, le contrôle par Courants de Foucault des pièces de turbomachines en exploitation était effectuée manuellement ou à l'aide d'équipements mécanisés : sonde fixée à un support déplacé radialement par rapport à un disque en rotation motorisée. Depuis environ 10 ans, un effort important a été réalisé par les motoristes pour développer des systèmes automatiques de contrôle par Courants de Foucault de pièces tournantes.

Plusieurs d'entre eux ont développé des installations qui peuvent être considérées comme tête de génération des équipements futurs pour ce type d'application, par exemple : ECII de G.E. (figure 16), ROBINSPEC 1 de F.M. Industrial System (figure 17), KHD.

Globlement, ces systèmes fonctionnent sur le même principe avec des caractéristiques voisines.

Mouvements

- Pilotage automatique des déplacements de pièces et/ou sondes selon 7 (ou 8) axes indépendants (translation ou rotation).

  La partie mécanique est conçue et réalisée pour atteindre un niveau élevé de précision (25 à 50 µm pour les translations ; 0,03 à 0,003° pour les axes de rotation) et de répétabilité (0,02m en translation) et présente la capacité dimensionnelle permettant le contrôle de l'ensemble des disques des moteurs actuels ou futurs, militaires ou commerciaux. Ils sont conçus pour une maintenance aisée.

Pilotage des mouvements, réglage des appareils et réalisation des contrôles

Les séquences successives d'étalonnage et de contrôle par balayage des différentes zones critiques d'une pièce sont commandées par programme informatique. Pour créer ces programmes, l'opérateur est guidé pas à pas par un menu interactif en tenant compte des sondes et étalons spécifiques éventuellement nécessaires au contrôle de chaque zone. Les programmes réalisés sont ensuite stockés en mémoire puis appliqués autant de fois que nécessaires pour réaliser les contrôles.

La fonction de l'opérateur se limite au changement des sondes et des pièces et la rentrée d'informations relatives à l'identification de celles-ci et des zones à contrôler.

Des standards de référence permettent de vérifier automatiquement que le système est en état de fonctionnement et que le niveau de sensibilité est capable de détecter les défauts dans les zones à contrôler.

En contrôle de pièces les amplitudes du signal Courants de Foucault sont acquises et font l'objet d'un traitement automatique limité actuellement à l'utilisation d'un seuil qui permet de déclencher une alarme, d'effectuer un enregistrement de l'indication détectée ou d'effectuer un arrêt ou retour sur défaut.

Limites actuelles et améliorations nécessaires

Dans leur état actuel de développement, les systèmes présentent certains inconvénients :

- Les problèmes d'accessibilité pour les pièces de géométrie complexe nécessitent l'utilisation d'une robotique et d'algorithmes de déplacements complexes, ce qui explique en partie le coût élevé des systèmes et rend la mémorisation des trajectoires par apprentissage très lourde à réaliser ou impossible dans des cas extrêmes.

- Le taux de fausse alarme sur pièce neuve et surtout sur pièces après fonctionnement est élevé (effets géométriques, présence de rayures ou de pollution superficielle), d'où appel fréquent de l'opérateur et risque de mauvaise interprétation des résultats pouvant compromettre la fiabilité du contrôle.

  La résolution de ces problèmes nécessitera :

  - La possibilité pour les systèmes d'utiliser les données CAO/FAO,

  - Le développement et l'utilisation de traitements de signaux permettant de séparer les indications de défauts des indications non significatives.

5.4. Tomographie RX

5.4.1. Rappel du principe

La tomographie par rayons X permet de réaliser de manière non destructive des vues en coupe d'objets. Elle est utilisée dans le domaine médical et dans le domaine industriel (contrôle *non destructif*).

Le principe de la tomographie est le suivant :

On mesure l'atténuation d'un pinceau de rayons X à travers l'objet à étudier et on obtient ainsi l'intégrale du coefficient d'absorption suivant un trajet appelé projection. On acquiert l'ensemble des projections suivant un grand nombre de directions et on reconstruit par calcul l'image de la coupe de l'objet.

5.4.2. Constitution des tomographes, modes d'utilisation et paramètres critiques

Un tomographe industriel est constitué :

- D'une source de rayons X,
- D'un ou plusieurs détecteurs de rayons X avec l'électronique associée,
- D'un système mécanique permettant de déplacer l'objet examiné dans le faisceau,
- D'un système de traitement et de reconstruction d'image.

En utilisant différemment les mouvements un tomographe peut réaliser de simples vues en projection du type de ce que l'on obtient en radiographie classique sur film.

Les principaux paramètres déterminant la qualité d'un tomographe sont :

- Paramètres jouant sur la résolution spatiale :

  taille du foyer du tube, longueur et hauteur de l'élément de détection, pas d'acquisition (système pluridétecteur) ou pas du détecteur (système multidétecteur), position relative foyer/pièce/détecteur, dimension de l'élément d'image, ces paramètres devant former un ensemble cohérent.

- Paramètres jouant sur la résolution en densité :

  fréquence d'alimentation et stabilité du générateur RX, stabilité de l'ensemble de détection, précision des mesures.

- Paramètres jouant sur les épaisseurs contrôlables :

  tension du générateur RX, dynamique de l'ensemble de détection.

- Paramètres jouant sur les cadences de contrôle :

  Flux de photons émis par le tube RX, efficacité du détecteur, temps de réponse du détecteur, rapidité du système de reconstruction d'image (pour que la reconstruction d'une image soit plus rapide que le temps d'acquisition et puisse être réalisée en temps masqué), chargement et déchargement des pièces automatiques si l'application le nécessite.

5.4.3. Application au contrôle des aubes de turbine

SNECMA a lancé l'acquisition d'un tomographe destiné au contrôle des aubes de turbine creuses à noyau céramique.

Les défauts recherchés sont des défauts métallurgiques (inclusions, microporosités ...) et géométriques en particulier épaisseur de paroi non conforme à cause d'une déformation du noyau céramique pendant la coulée). Un contrôle d'aube nécessite typiquement 1 vue en projection et 3 coupes tomographiques réparties sur la hauteur de la pale, complétées éventuellement par des coupes tomographiques passant par les défauts métallurgiques pour lever de doute.

Le tomographe retenu est du type multidétecteur et a les caractéristiques suivantes :

- Générateur RX : tension maxi : 420 kv
  foyer 1,5 mm.
- Détecteur à gaz (Xénon sous pression)
  pas 0,15 mm
  hauteur des éléments de détection : 0,25 mm
  efficacité : 75 % à 420 kv.

- Objet limite : diamètre 170 mm
  hauteur 450 mm
  épaisseur d'acier : 50 mm.

- Etalonnage automatique.

- Chargement des aubes dans la chambre de contrôle et déchargement automatiques par convoyeur chargé en dehors de la cabine anti X (capacité : 25 à 50 aubes selon leur taille).

Pour le contrôle des épaisseurs de parois des aubes, 3 modes sont utilisables :

Mode manuel : le système calcule la distance entre 2 points sélectionnés par l'opérateur.

Mode semi-automatique : le système calcule l'épaisseur de la paroi le long d'une ligne droite joignant 2 points sélectionnés par l'opérateur en dehors et de part et d'autre de la paroi.

Mode automatique : le système calcule les épaisseurs correspondant aux minimum locaux par zone et prononce automatiquement la sanction par comparaison à des critères, les zones et les critères ayant été préalablement définis pour chaque type de pièce.

Les cadences de contrôle sont de 12 à 24 aubes mobiles/heure selon leur taille, sur la base d'une vue par projection et 3 coupes tomographiques par pièce.

Un exemple de coupe tomographique est donné Figure 18.

CONCLUSIONS

Nous avons tenté d'analyser et de présenter l'ensemble des techniques de contrôle d'une manière synthétique.

La décomposition en phases élémentaires facilite la mise en facteur au niveau de chacune d'elles des exigences communes à la plupart des techniques si ce n'est l'ensemble.

La différenciation le plus marquée semble se situer au niveau des générateurs d'excitation dont les principes physiques restent assez spécifiques.

La similitude des principes physiques va croissante à partir de la perturbation.

La phase révélation nous montre que la plupart des capteurs utilisés sont sensibles aux rayonnements électromagnétiques. La conséquence est la bonne unité qui apparaît aux stades de l'analyse, de la synthèse et plus particulièrement au niveau de l'évolution des critères où l'ensemble des défauts, quelle que soit la technique appliquée ou le stade d'intervention du contrôle, peuvent être considérés sous 3 ou 4 géométries élémentaires de base.

Ces analogies et simplifications constituent une situation favorable pour harmoniser les orientations, les choix, les investissements, concentrer les efforts de créativité, de manière à accélérer les progrès et leur industrialisation, réduire les coûts de développement et de contrôle.

Dans ces évolutions, il se confirme que l'informatique est un élément fondamental qui nous situe très près des débouchés industriels en ce qui concerne la sanction basée sur la géométrie des défauts. Un dernier pas difficile à franchir sera celui de la nature réelle des défauts.

TABLEAU N° I

		FORME D'ONDE(S) EXCITANT LE CAPTEUR			DETECTABILITE ET DEFINITION POSITION X Y Z DES DEFAUTS REPRESENTES SUR FIGURE 8 EN FONCTION DE LA METHODE APPLIQUEE													
					A			A			C			B			E		
					X	Y	Z	X	Y	Z	X	Y	Z	X	Y	Z	X	Y	Z
Visuel		X			R	R		R	R										
Ressuage fluorescent		X			R	R		R	R										
Magnétoscopie	Rev. flue Magnétomètre) sonde de Hall)	X	X		R R	R R		R R	R R		R R	R R							
C & F			X		R	R		R	R		R	R							
R x	film temps réel	X X			T T	T T		T T	T T		T T	T T		T T	T T		T T	T T	
Thermo IR	Transmission Réflexion	X X			T R	T R		T R	T R		T R	T R		T R	T R		T R	T R	
Ultrasons	Transmission Réflexion	X (1) X		X X	T R	T R	R	T R	T R	R	T R	T R	R	T R	T R	R	T R	T R	R

(1) Laser.

TABLEAU N° II

	STADES D'APPLICATION DES CND																	
	Approv.	Pièces brutes		En cours de fabrication						Après fonct.			FORME REELLE DES DEFAUTS			
	Matériaux Demi-produits	Billettes	Lingots	Usinage	Soudage	Traitt thermique	Traitt surface	Peinture	Autres	Fissuration	Corrosion	DEFAUTS TYPES	Ponctuelle	Linéaire (filiforme)	Surfacique (2D)	Volumique (3D)
Autres défauts							X		X	X	Adhérence revêtements			X	
Mélange matière Etat de TT Echauffement après fonctionnement Déformations Usures Mesures épaiss.		X	X	X	X		X	X	X	X	Aspect	X	X	X	
				X		X		X	X	X	Corrosion	X	X	X	
	X	X	X	X	X	X	X	X	X	X	Criques (tapures, replis)			X	
	X		X		X			X		X	Inclusions volumiques, lamellées				X
		X						X					X	X	
					X					X	Manque de pénétration			X	X
			X								Microretassures			X	X
			X								Retassures				X
	X		X					X			Ségrégations		X	X	X
			X		X					X	Soufflures porosités				X

Si la représentation du défaut au stade de la synthèse correspond à :
- une coupe du défaut par le plan d'analyse, sa forme apparente peut être décalée d'une classe vers la gauche (ponctuel excepté)
- une projection du défaut sur le plan d'analyse, sa forme apparente peut rester du même type ou être décalée d'une classe vers la gauche (ponctuel excepté).

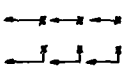

FIGURE 1

PROCESSUS DE FONCTIONNEMENT D'UN CONTROLE NON DESTRUCTIF

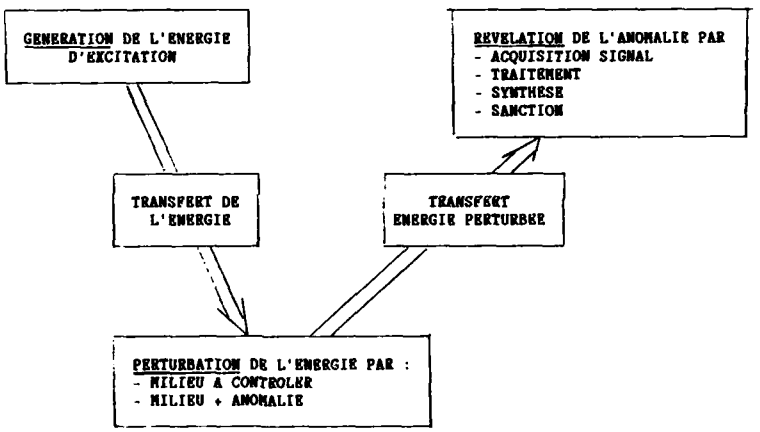

FIGURE 2

INFLUENCE DE L'IMPEDANCE ACOUSTIQUE Z DES MILIEUX: COUPLAGE ET ALLIAGE A CONTROLER

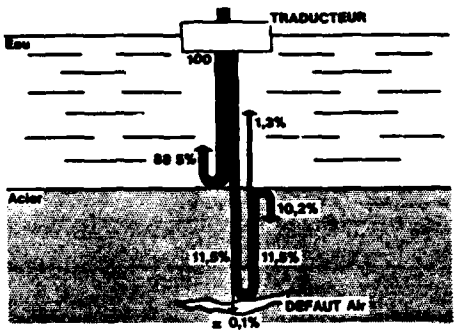

FIGURE 3

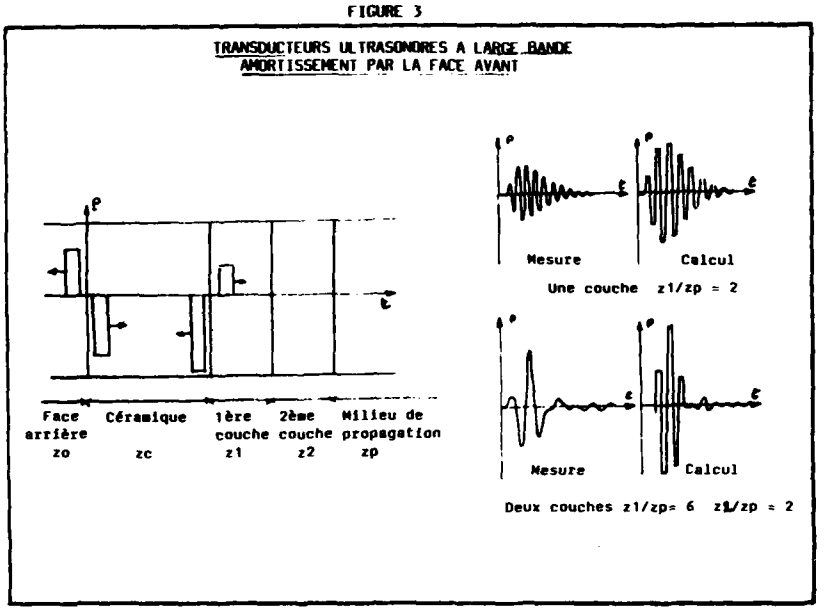

FIGURE 4

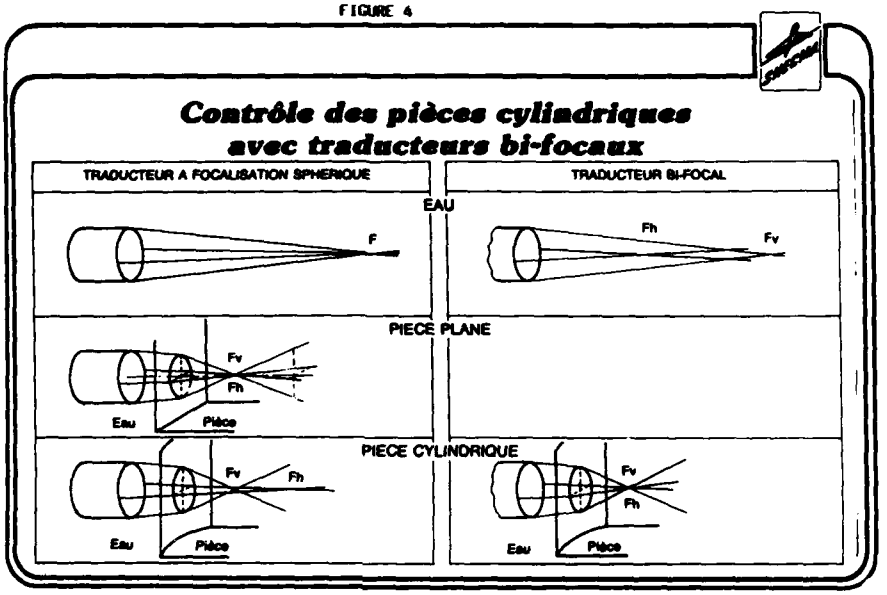

FIGURE 5

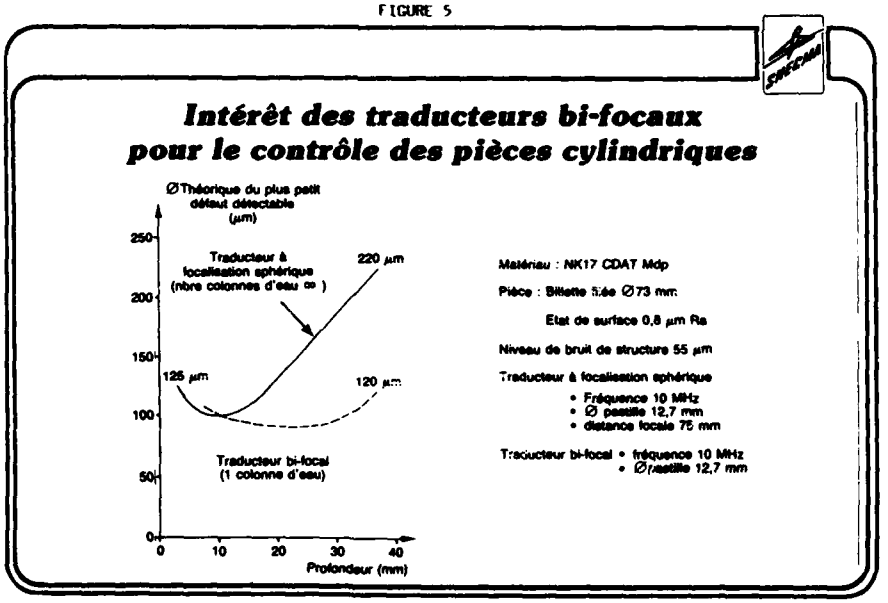

FIGURE 6

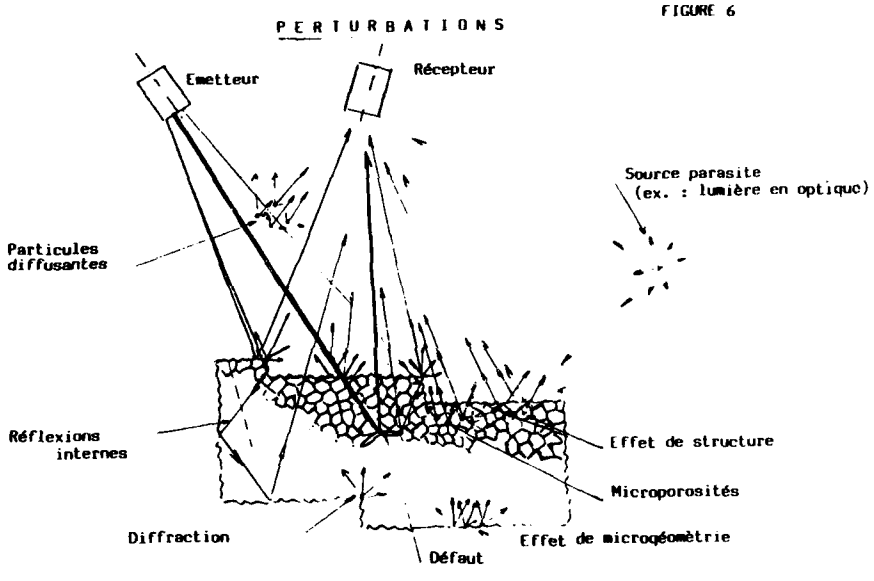
PERTURBATIONS
Emetteur
Récepteur
Source parasite
(ex. : lumière en optique)
Particules
diffusantes
Réflexions
internes
Effet de structure
Microporosités
Diffraction
Effet de microgéométrie
Défaut

FIGURE 7

EXEMPLE DE MODELISATION EN CONTROLE PAR COURANTS DE FOUCAULT

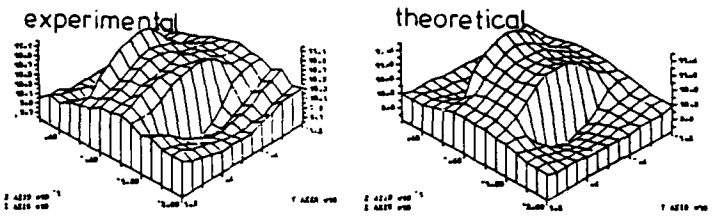

Signaux obtenus pour une entaille circulaire (d'après HARWELL)

FIGURE 8

EXEMPLE DE MODELISATION EN CONTROLE ULTRASONORE

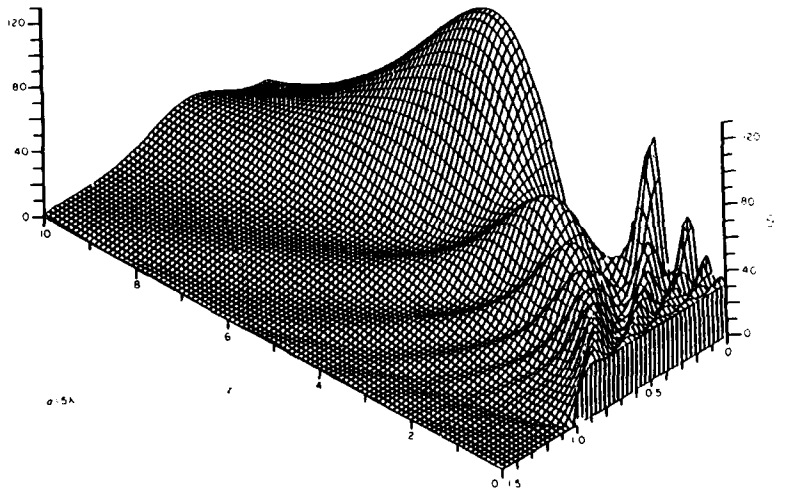

Pression acoustique calculée pour un traducteur ultrasonore
(d' après SHARPE)

FIGURE 9

ANALYSE PAR CAPTEUR

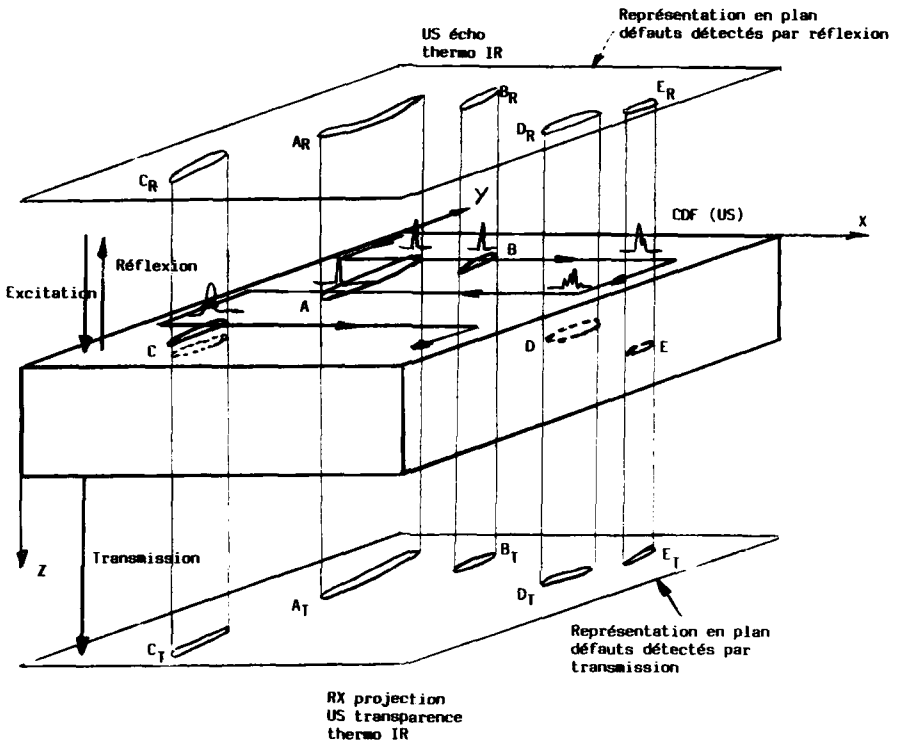

FIGURE 10

SYNOPTIQUE D'UN SYSTEME AVANCE

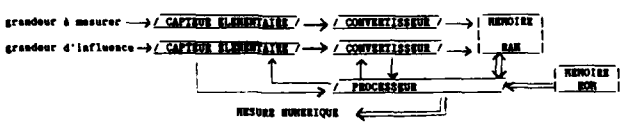

FIGURE 11

GEOMETRIES BINAIRES PARAMETRABLES

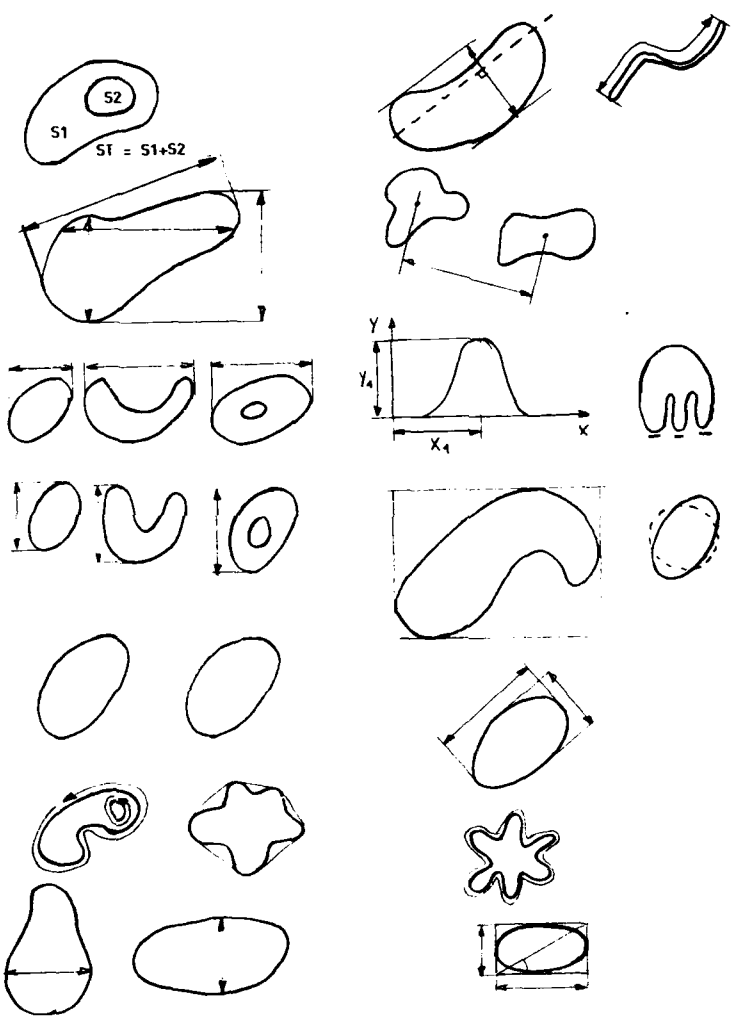

FIGURE 12

EXEMPLE DE SINUSOIDE CARREE BIPOLAIRE AMORTIE

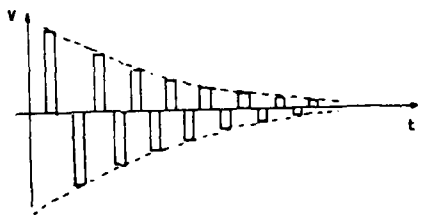

FIGURE 13

FONCTION TYPE PORTE DE SURVEILLANCE

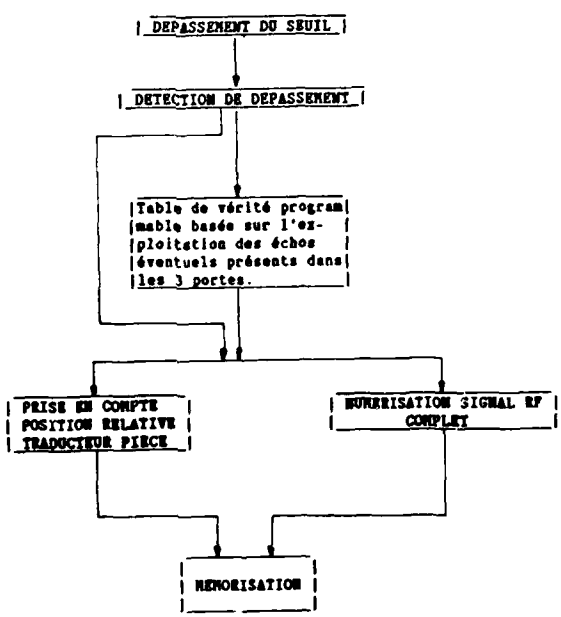

FIGURE 14

CARACTERISTIQUES DU SIGNAL D'EXCITATION GENERE

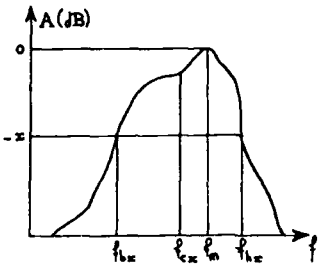

Fréquence centrale à - x dB

$$fcx = \frac{fbx + fhx}{2}$$

Largeur de bande à - x dB

$$LB_x \ (\%) = \frac{fhx - fbx}{fc_x} \times 100$$

FIGURE 15

TRADUCTEURS ULTRASONORES
DEFINITION DES PARAMETRES RELATIFS AUX DESALIGNEMENTS
ET EXCENTRATIONS

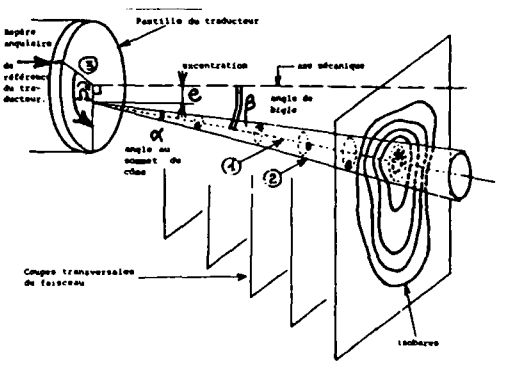

FIGURE 16

CONTROLE AUTOMATIQUE PAR COURANTS DE FOUCAULT
DE PIECES DE TURBOMACHINES EN EXPLOITATION

SYSTEME ECII DE GENERAL ELECTRIC

FIGURE 17

CONTROLE AUTOMATIQUE PAR COURANTS DE FOUCAULT
DE PIECES DE TURBOMACHINES

SYSTEME ROBINSPEC 1 DE FN INDUSTRIAL SYSTEM

FIGURE 18

COUPE TOMOGRAPHIQUE D'UNE AUBE DE TURBINE

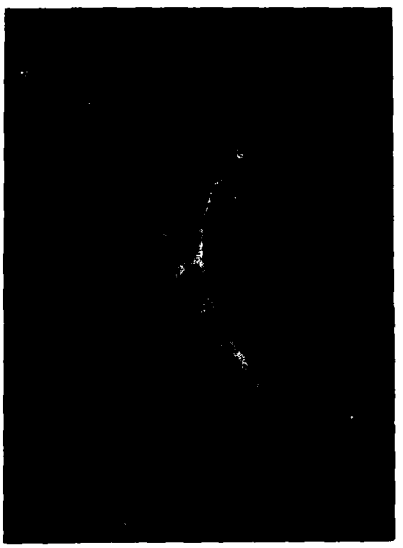

Aube mobile HP SNECMA (moteur LARZAC)

FIGURE 19

EXTRACTION PAR INTEGRATION D'UN SIGNAL REPETITIF MASQUE PAR DU BRUIT

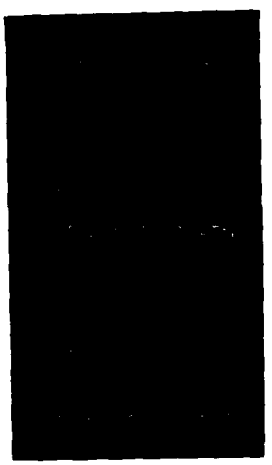

après 1 passage

après 100 passages

après 5000 passages

Exemple : numérisation d'une sinusoïde mélangée à du bruit

PLANCHE 20

CONTROLE RADIOGRAPHIQUE - INDICATEUR DE SENSIBILITE DE DETECTION
- Exemple d'influence de variation d'un paramètre -

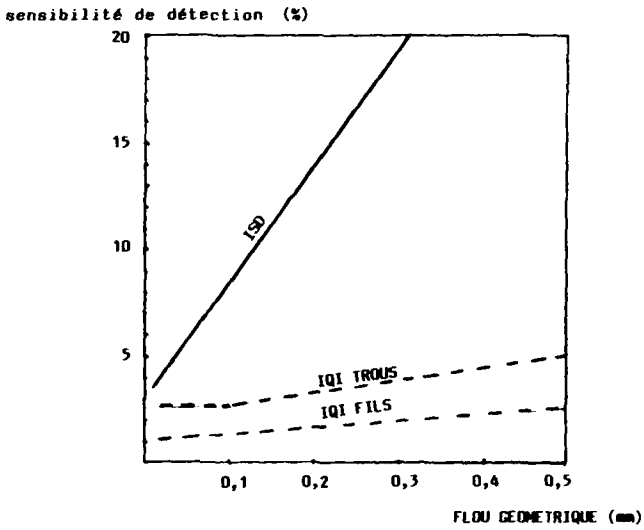

PLANCHE 21

CONTROLE ULTRASONORE - TRADUCTEURS INCOHERENTS

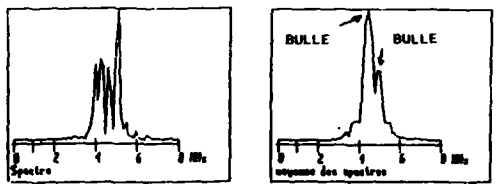

Détection de bulles dans une mousse diffusante
(résultats Groupe de Physique des Solides de l'ENS, Université PARIS 7)

LONG TERM POSSIBILITIES FOR NONDESTRUCTIVE EVALUATION FOR US NAVY AIRCRAFT

by W. R. Scott
Naval Air Development Center
Warminster, PA 18974
USA

ABSTRACT

The majority of Nondestructive Inspection (NDI) techniques currently in use for US Navy aircraft are labor intensive, operator dependent and result in excessive aircraft down-time. For this reason NDI R&D efforts currently are directed toward developing rapid automated systems capable of remote or unattended inspection of large areas and inaccessible structures.

Ongoing programs of this type to be discussed include Laser Ultrasonics, Acoustic Emission, and Quantitative Imaging. The primary thrust of the presentation will cover the advantages of each technique and the technical obstacles preventing its implementation.

LASER ULTRASONICS

Laser Ultrasonics is a nondestructive testing technique that has the potential to perform all of the same types of inspections as conventional ultrasonics except that instead of using piezoelectric probes to interrogate material defects it relies upon optical techniques. The principle of operation of this technique, shown schematically in figure 1, involves the use of a pulsed laser to generate thermoelastic waves which are then detected using a high sensitivity optical interferometer. For all practical purposes these thermoelastic waves are identical to ultrasonic stress waves. When such waves interact with defects or interfaces within a material they are scattered or reflected at points of material property discontinuity. Surface displacements resulting from the scattered waves reaching the component surface are detected by a high sensitivity optical interferometer and are converted into RF signals commonly referred to as a-scans.

This means of inspection has a number of obvious advantages over conventional ultrasonic techniques. First of all laser ultrasonics operates in a noncontact mode in contrast to conventional ultrasonics for which a coupling is required between the probe and the sample being tested. This coupling is normally accomplished in any of three ways:

1. a thin film of liquid couplant is placed over the surface of the part to be tested and a piezoelectric probe is placed in direct contact with the part,

2. the part is immersed in a liquid medium and the piezoelectric transducer radiates acoustic energy through the medium and into the part,

3. a piezoelectric transducer is placed inside of a nozzle which directs liquid couplant onto the surface of the part being tested; acoustic energy radiated from the transducer is waveguided along the liquid stream onto the surface of the part.

The purpose of the liquid couplant in all three cases is to provide an acoustic impedance match between the transducer and the part being tested, thereby allowing sufficient acoustic energy to reach the part and be returned to the transducer. Since laser ultrasonics generates the ultrasonic stress wave right at the surface of the part and detects ultrasonic displacements at its surface, the need for coupling is eliminated.

In addition to eliminating the need for couplant, laser transduction has the added benefit that it permits remote ultrasonic inspection in the absence of any intermediate medium. While squirter techniques do allow some distance to exist between the transducer and the specimen, they also require that a liquid medium be sprayed onto it. This spraying can adversely effect the ultrasonic signal especially at the higher squirter velocities needed for horizontal or inverted vertical probe attitudes.

In contrast, laser ultrasonic probes can work at any angle and only require the existence of a transparent path between the probe and the part being inspected. This

suggests the possibility of inspecting moving parts and parts functioning in hostile environments. Furthermore, the fact that laser ultrasonics uses a massless probe that can reach its target almost instantaneously opens up the possibility of scanning rates which far exceed those achievable with c-scanning or other servo-mechanical probe positioning schemes.

Despite the obvious advantages of laser ultrasonic inspection, it does have a number of drawbacks which have prevented its practical implementation. These include the following:

1. Lasers sufficiently powerful to produce usable ultrasonic intensities in highly reflecting metals may be capable of thermally damaging other materials such as plastics.

2. High laser light intensities associated with ultrasonic inspection are capable of producing eye damage. This means that inspections must be performed in limited access areas and operators will be required to use protective eyewear.

3. The interferometric sensing techniques used to detect ultrasonic displacements may be considerably less sensitive than corresponding piezoelectric techniques, especially at long distances.

Much of the current R&D work on laser ultrasonics is concerned with overcoming the above problems.

Three effects are involved in the conversion of light into ultrasonic waves. These are in order of increasing efficiency, radiation pressure, thermoelastic generation and ablation. Radiation pressure results in a low conversion efficiency and is of no practical importance. Thermoelastic generation can produce efficiencies between 10^{-7} and 10^{-4} or greater, while ablation may have efficiencies of 10^{-3} or above. The last mechanism while very efficient has the disadvantage that it may lack reproducibility and in extreme cases can produce material damage.

The above mechanisms rely on the rapid heating of an opaque material surface in order to produce a stress wave and produce large near surface displacements that are inefficient in generating stress waves in the bulk of the material. Von Gutfeld [1,2] and others have shown that by pinning the material surface much higher transduction efficiencies are obtained than are available from free surface excitation. A related effect may have been demonstrated by Rudd [3] who nondestructively produced large amplitude stress waves by exciting milar films with a pulsed CO2 laser. Although Rudd was not able to make absolute measurements of the amplitude of the resulting waves it was clear from his results that the amplitudes were up to an order of magnitude larger than are ordinarily obtained from piezoelectric transduction of similar waves. This suggests that light is being absorbed through the thickness of the plastic film producing a self pinning stress wave.

Plastic films of this type could readily be coupled to large surfaces using a liquid couplant as shown in figure 2. A laser could then be rapidly scanned over the surface producing a rapid non-damaging probe suitable for a number of structures.

In addition to better laser generation techniques, significant advances in detection techniques are necessary in order to realize the full potential of laser ultrasonic inspection systems. Most interferometric devices currently in use for detection of ultrasonic displacements are shot noise limited and exhibit significant losses in sensitivity when only low levels of coherent light reach the optical detectors. As a result working distance, surface roughness, surface reflectivity, and light source intensity are all variables which are important in determining interferometer sensitivity.

Recent studies [4] have demonstrated that with lasers of moderate power (on the order of milliwatts) sensitivities of .5 Angstrom at a 10 MHz bandwidth are obtainable. This level of sensitivity would would be acceptable for many ultrasonic inspection applications, if it could be maintained during an inspection of a conventional part. However, most designs for high sensitivity devices, such as the one shown in figure 3, rely on maintaining a focussed laser beam of a near diffraction limited spot size at the point of inspection. This normally implies very short working distances (<1mm.) and depths of field on the order of microns. Compromises involving higher power lasers and larger spot sizes may be necessary to maintain both acceptable resolution and practical working distances.

ACOUSTIC EMISSION (AE)

Acoustic emission is a nondestructive testing technique that detects the presence of defects in a structure by monitoring the sounds which that structure makes under mechanical or thermal loading. These sounds can range in frequency from the audible range up to the low megahertz range or possibly higher. Current US Navy thrusts in acoustic emission are in the area of in-flight monitoring of airframe structures to detect the presence of crack growth in critical components.

In principle AE is completely passive relying on signals received from arrays of sensitive piezoelectric transducers to detect and localize sounds emitted from growing cracks. A piezoelectric sensor is mechanically secured to the specimen and a liquid couplant is placed between them to improve the acoustic impedance match. As the specimen is loaded bursts of acoustic energy are emitted; they are counted and the rate of emission is plotted against load level. In many materials the presence of a high emission rate or the occurence of a number of emissions above a certain amplitude is indicative of the presence of a growing crack. Such techniques have been shown to work reliably in the laboratory for specimens with simple geometries; and in some practical applications such as monitoring of pressure vessels. Structures such as aircraft, on the other, hand present difficulties not encountered in these other applications.

The single largest problem in developing a practical in-flight monitoring system is how to discriminate between these benign noise sources and AE events associated with crack growth. The benign, spurious, events are mainly associated with following:

Electromagnetic noise induced in the sensors, lead wires and associated instrumentation,

Noise associated with engine vibration transmitted to the airframe,

Cavitation noise from aircraft hydraulic systems,

Noise associated with fretting of mechanically fastened structural components particularly around loose rivets.

The three main techniques used for noise discrimination are array source localization, emission/load analysis [5] and pattern recognition. Source localization is usually applied to components having a two dimensional surface of approximately constant thickness which can be instrumented with an array of transducers. For isotropic materials, plate and surface waves of a particular mode and frequency travel at a constant velocity independent of direction. Depending on the shape of the part, it is usually possible to uniquely locate the source of an emission by measuring the difference in arrival time at each of three or four transducers mounted on the component s surface.

The source localization technique can immediately eliminate events associated with electromagnetic noise, since these normally arrive at all sensors simultaneously. Also, signals associated with cavitation and engine vibration can be localized as coming from outside the area of interest.

The most difficult noises to discriminate from crack growth are those associated with fretting. This is particularly difficult when the source of the fretting is around a loose fastener. Since fastener holes are likely locations for crack initiation, locating an event at a fastener hole does not a priori rule out the presence of a crack. This leaves load level discrimination and pattern recognition as the two remaining techniques for discriminating between crack growth and fretting.

Load level discrimination works by observing the rate of acoustic emission as a function of the load being applied of the component. A basic phenomenon observed in acoustic emission is that a component under cyclic load does not produce acoustic emission until it reaches the load at which the last emission occurred(the Kaiser Effect). This law does not hold in general; however, it is significantly more likely that a crack will grow at maximum load than at some other point in the load cycle.

In addition, for some materials another kind of emissions associated with crack closure will occur at the lower end of a load cycle. Since the rate of emission associated with fretting does not seem to vary as strongly with load level, it is possible to use load level vs. emission plots to obtain strong statistical evidence for the presence of crack growth. This method is also useful in developing "training sets" for a third discrimination technique, i.e. pattern recognition.

Pattern recognition is a general term referring to mathematical techniques which can be used to categorize empirical data on the basis of certain "features" of that data. For example, electrical transients can normally be discriminated from crack growth signals purely on the basis of their duration or frequency content. Pattern recognition normally involves two sets of data each containing a number of separate events. The first is a training set used to develop a discrimination algorithm. A second independent test set is then used to evaluate the algorithm's effectiveness.

Figure 4 illustrates the results of one pattern recognition scheme constructed for separating events due to crack growth from those due to fretting. Two separate features are selected as being indicative of these conditions and their values are placed on the plot for each event observed. The source of the emission is obtained by another means such as load level analysis. Solid points are plotted for cracks and open circles for fretting. Since crack events cluster selectively in the lower right corner of the plot and fretting events in the upper left, it is possible to draw decision lines which separate either type of event with a given confidence level.

In recent studies Hutton et. al. [6] applied pattern recognition techniques to acoustic emission waveforms obtained from aluminum tensile specimens. Using load level discrimination, training sets of fretting and crack extension waveforms were developed and these were used to construct algorithms for discriminating between the two types of events. When these algorithms were applied to independently acquired data sets from the same specimens the results of load level discrimination were reproducible with a 90 percent confidence level or greater. These results are highly satisfactory, since load level analysis does not guarantee separation of crack growth signals from benign events.

However, when these algorithms were applied to different specimens the agreement dropped significantly and when specimen geometry was changed results were quite poor. This was interpreted as meaning that certain features of acoustic emission events were unique to the particular crack from which they originated and to the geometry of the specimens through which they propagate.

Later work showed that transfer functions could be developed which removed many of the specimen specific features of AE events. When events from various specimens were processed in this way, a number of "robust" features were recognized as discriminating between fretting and crack growth events. In laboratory evaluations the reliability of these algorithms was found to exceed 90 percent.

Successes of the above R&D efforts suggest that methodologies based on aircraft noise surveys and statistical estimates of crack detection probability within noise environments could reliably detect subcritical crack growth in some aircraft.

Work in progress involves flying an AE system on a P-3 aircraft while monitoring crack growth in a redundant structure. The flight rack mounted AE system to be used for these tests is shown in figure 5. The three channel acoustic emission system, shown in the upper right hand rack panel, capable of identifying events from the region of interest and acquiring their waveforms on the two Biomation recorders in the lower right rack. The 12 bit digitized waveforms can then be recorded on the tape recorder for post flight analysis. A redundant cracked structure will be independently monitored for crack size using resistive crack growth monitors suplemented by periodic visual examinations. Post processing of this data will permit optimization of discrimination algorithms and critical evaluation of their utility.

If this methodology is successful in developing algorithms suitable for detecting critical crack growth, future efforts will be directed toward developing smaller aircraft specific systems for monitoring critical areas of the P-3 and for developing smaller prototyping systems for use on smaller aircraft.

QUANTITATIVE IMAGING

Quantitative Imaging is a U.S. Navy program involved with ultrasonic imaging of defects in airframe materials, particularly composite materials. The work draws on a number of technologies including robotics, image enhancement, machine vision, and ultrasonic signal processing. The ultimate goal of this project is to develop automated systems which can directly measure those parameters relating to the criticality of a defect in a component. In addition, the systems must be able to continuously monitor changes in such parameters by storing defect information and comparing it to results obtained at a later time in the life of a component.

The primary element of the quantitative imaging system is a conventional ultrasonic pulser receiver which excites short duration stress waves in a piezoelectric transducer. These waves are coupled into a component of interest through a water jet or by immersing both the transducer and the component in a water bath.

The latter configuration is employed in standard c-scan systems that are used to produce ultrasonic images of planar samples. These systems usually operate by moving the ultrasonic transducer above the sample in a raster pattern while detecting the amplitude of an ultrasonic echo arriving at a particular delay time after the initial pulse. This amplitude is used to modulate the gray level of the recording pen which moves in synchronization with the transducer.

In order for these devices to function properly, the transducer must be kept normal to the surface of the sample and at a constant distance from its surface. A certain amount of shape variation can be accommodated in these systems through the use of special fixtures, servomechanical devices for probe articulation and the use of delayed triggers to electronically compensate for small variations in signal arrival time. In addition multiple electronic gates are available which allow flaw probing at several depths through the thickness. In general, however; the cost of such systems and their limited capability for scanning complex geometries make robotic manipulation preferable.

The robotic scanning capability being developed under this program has three main thrusts.

(1) Constructing the digital representation of the component to be scanned.

(2) Translating that representation into a set of instructions which will permit the robot move an ultrasonic probe at a constant distance from the surface of the component and at normal incidence to its surface.

(3) Registering the component's location within the coordinate system of the robot, scanning and collecting data. (Reconstructing an appropriate ultrasonic image of the component may also fall partially into the realm of this thrust.)

An example of a component suitable for robotic scanning is illustrated by results of scans being done on a graphite/epoxy sine wave spar. The particular spar shown in figure 6 is a segment of a reinforcing member from the wing of an AV8-B aircraft. It is not inspected in an optimal manner after fabrication because of the difficulty in following its contours.

The digital representation of this part was obtained by using an optical scanning device which moved a thin laser beam over the surface of the part in a raster pattern. The component was photographed with a television camera during the scanning process. By knowing the camera angle and the angle of the scanning beam a digital representation of the scanned surface was computed. This was used to construct the isometric projection shown in figure 6.

Subsequently, a best fit sine wave was constructed from the digital data and used to drive the robotic scanner. When a scan was performed it was found in fact that the spar was not sufficiently close in shape to a real sine wave to obtain good scans and a more detailed digital approach was needed.

In general the problem of producing a robotic scan pattern for a particular shape seems to have no general solution. The robot being used in these studies has six independent axes available for placing and orienting the ultrasonic probe. Although this hardware provides sufficient degrees of freedom for scanning most objects of interest their are a number of subtle problems which emerge in developing scanning algorithms:

The robot must be programmed so as not to pass through the object that it is scanning.

The robot arm must be programmed not to pass through itself.

The solutions to equations used to bring the robot to a given position and orientation are not single valued. Improper selection of such solutions can result in the robot moving large distances to reach adjacent points.

Robotic coordinates may not have metrics which provide uniform resolution on parts with complex curvatures.

Automating the process of generating robotic scanning instructions will be a major thrust in future work.

After the scanning process, acquisition and storage of data presents the next important area where advanced development efforts are being concentrated. The usual reason for the formation of an ultrasonic image is to provide a permanent record of the condition of a component which can readily be interpreted in terms of the location and size of various anomalies or defects. With such records it should be possible to re-examine a scan of a component many years after it was made and confirm its original integrity. In fact the techniques currently used to collect and display ultrasonic data may not serve any of the above purposes properly. The results of ultrasonic images such as c-scans yield results which are as much determined by the operator as they are by the characteristics of the component.

Figure 7 shows graphs of the ultrasonic amplitude (a-scan) as a function of time for a hypothetical material. These a-scans, which are the raw data from which ultrasonic images can be constructed, provide cross sectional information relating to the integrity of a component. The upper most scan corresponds to a material in which no ultrasonic defects can be detected. The two large pulses going from left to right correspond to the front and back surface of the component. The absence of significant features between these echoes indicates that no ultrasonically detectable flaw is present.

In contrast, the lower a-scan shows the presence of an interior echo which may be associated with a defect. The strength of the echo increases with the size of the defect while at the same time the size of the back echo decreases. By gating various time slices from the waveform and using the amplitude of the enclosed features to modulate a display an image may be built.

As the ultrasonic probe is scanned in a narrow raster pattern (c- scan) over a component surface, patterns of light and dark are synchronously produced on a display or hard copy. Figure 8 is an example of a c-scan of a laminated material in which the gray level is modulated by the amplitude of an echo from a delaminated region. If the back surface echo had been used instead, then a negative of the above scan would have been produced due to loss of back echo from the delaminated area; gating on the front surface echo would produce no flaw image at all.

Clearly the processing of the waveforms determines what information will be displayed. Early approaches to optimizing this processing used image histograms and level slicing as shown in figure 9. Imaging devices typically have a discreet number of gray levels and colors that can be used in displaying an image. By defining the level slices in such a way as to maximize contrast across the range of a-scan amplitudes corresponding to defect conditions it should be possible to produce a scan with optimized flaw sensitivity.

The markedly improved image quality and flaw definition achieved with this approach still does not guarantee their reproducibility or the completeness of the information which they contain. For this reason recent studies have emphasized a technique referred to as full volume ultrasonic imaging. The full volume technique records not just a single intensity level but a complete ultrasonic a-scan for each point on a part to be imaged.

Figure 10 shows the isometrically projected output of a full volume scan of a section of a graphite/epoxy laminated panel. From the data base acquired in the scan both isometric projections and arbitrary cross sectional images can be created which show the detailed distribution of porosity in the panel. Such images can be shown in real time and a-scans for any location can be displayed and examined.

Because of the mass storage demands necessary to implement this technique it is only now becoming practical. If a scan is to be made which has the resolution of the human eye (i.e., approx. .2 mm), then a four square centimeter full volume scan would require approximately 1.3 megabytes of storage. This means that an optical disk with a few gigabytes of memory would be required to store the scan of a one square meter area.

The resolution required in many ultrasonic inspection , such as those for composite wing skins is considerably coarser than visual resolution and a scan of an entire aircraft could probably be contained on a few optical disks. Even now this cost would not be prohibitive. It is anticipated that future improvements will make this technique the preferred method of data storage.

The full volume method clearly has the advantage that post processing of scan data can be performed at any time after the original scan. This permits scrutiny for

types of defects that may not have been of interest when the scan was made. New data processing algorithms not previously available can also be applied.

Full volume scanning, though feasible, still leaves technology gaps. The primary shortcoming is the data transfer rate. Most off the shelf instrumentation cannot transfer more than about 100 ultrasonic waveforms per second. In contrast analog sampling using older technology can process 10000 waveforms per second or more. This does not seem to be a fundamental limitation, since both digitizers and computer busses are now available to handle these data rates.

Areas for future research in quantitative imaging will involve calibration and instrument normalization needed to make full volume scans made on different instruments or at different times fully comparable.

REFERENCES

[1] J. Von Gutfeld, Vigliotti and Ih, "Thermoelastic Structures for High Density Ultrasound Energy", REVIEW OF PROGRESS IN QUANTITATIVE NONDESTRUCTIVE EVALUATION, Aug 78

[2] J. Von Gutfeld and R.L. Melcher, Applied Physics Letters 30,p.257 (1977)

[3] M. Rudd, "Laser Generation of Ultrasound" NADC Report No. N62269-82-C-0442, Feb 1983

[4] E. Bourkoff and H. Palmer, "NONCONTACT MATERIAL TESTING USING LOW ENERGY OPTICAL GENERATION AND DETECTION OF ACOUSTIC PULSES", REVIEW OF PROGRESS IN QUANTITATIVE NONDESTRUCTIVE EVALUATION, VOL 5A, P659, PLENUM 1986

[5] J.M.Carlyle and W.R. Scott, Acoustic Emission Fatigue Analyzer, EXPERIMENTAL MECHANICS, Vol. 16 No. 10, p.369-372, Oct 1976

[6] P. Hutton, "Develop In-flight Acoustic Emission Monitoring of Aircraft to Detect Fatigue Crack Growth Vol.1, NADC-81087-60 Aug. 83.

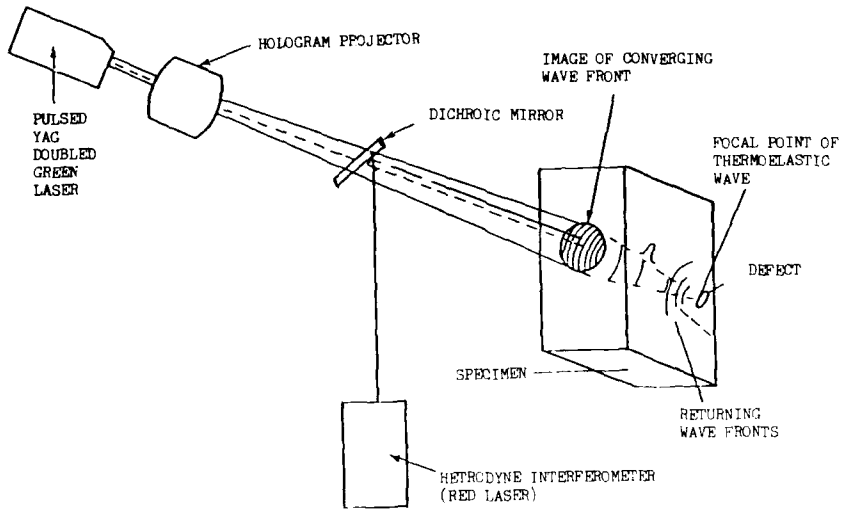

FIGURE 1 SCHEMATIC DIAGRAM OF A LASER ULTRASONIC SYSTEM

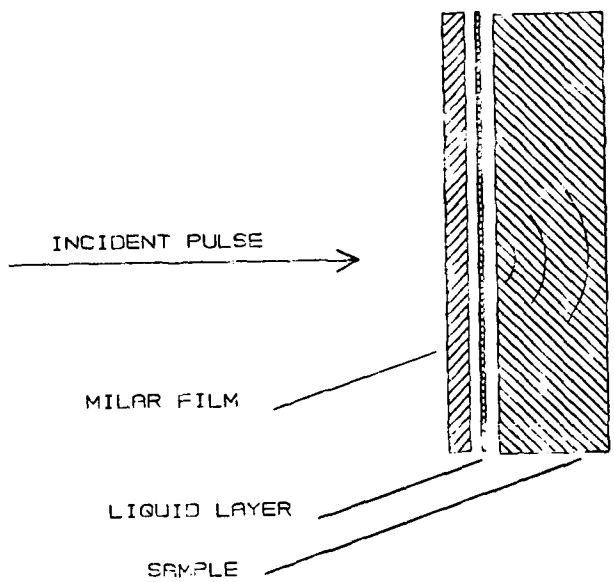

FIGURE 2 SCHEMATIC DIAGRAM OF THE INTERACTION OF A LASER BEAM WITH A LAYERED MEDIUM

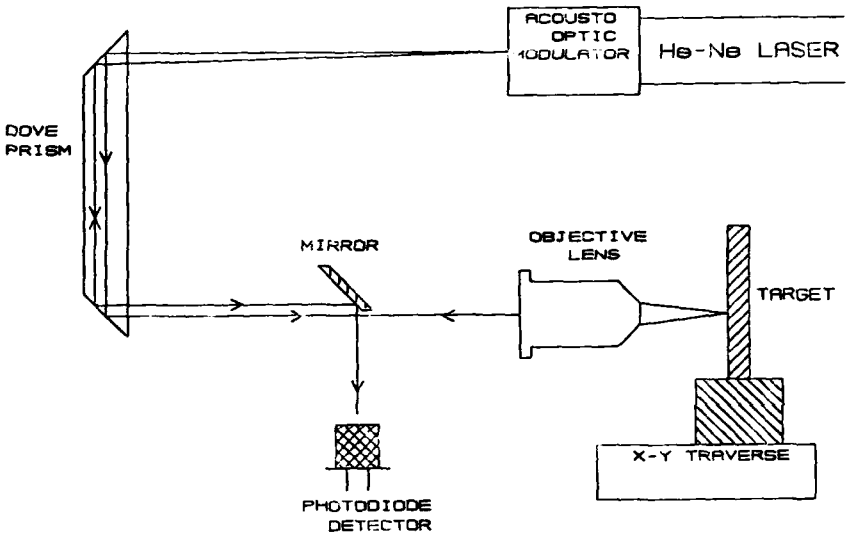

FIGURE 3 HIGH SENSITIVITY HETERODYNE INTERFEROMETER

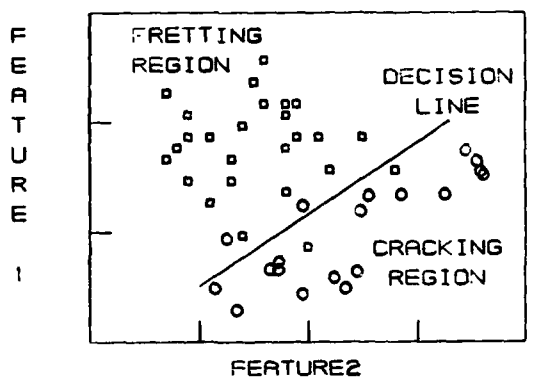

FIGURE 4 EXAMPLE OF A PATTERN RECOGNITION SCHEME FOR SEPARATING CLASSES OF DATA

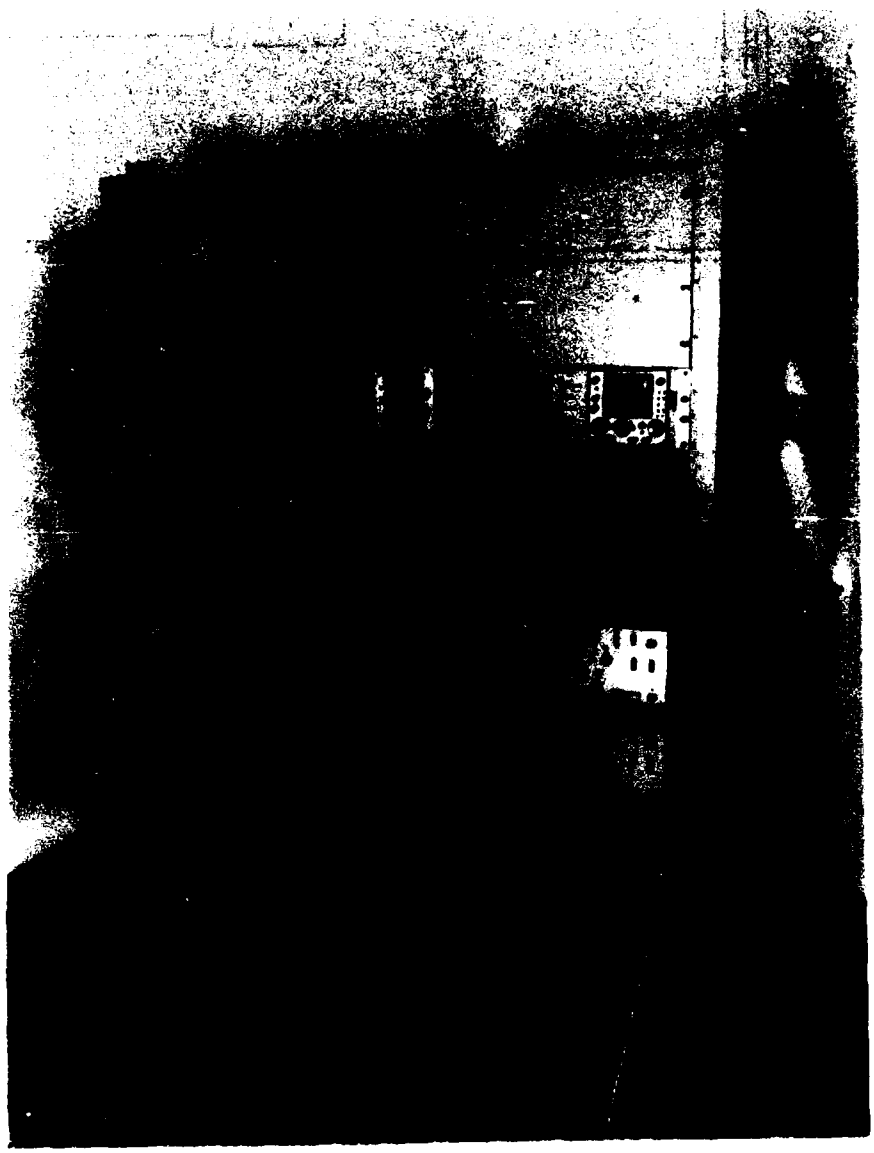

FIGURE 5 EXPERIMENTAL IN-FLIGHT MONITORING SYSTEM

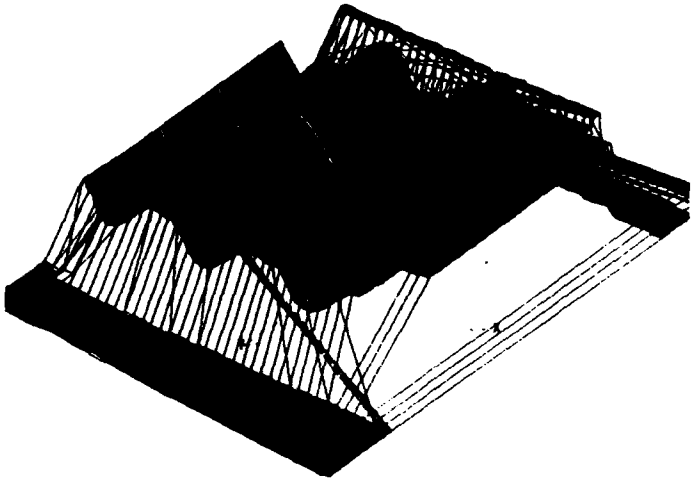

FIGURE 6 OPTICAL SCAN OF A SINE WAVE SPAR

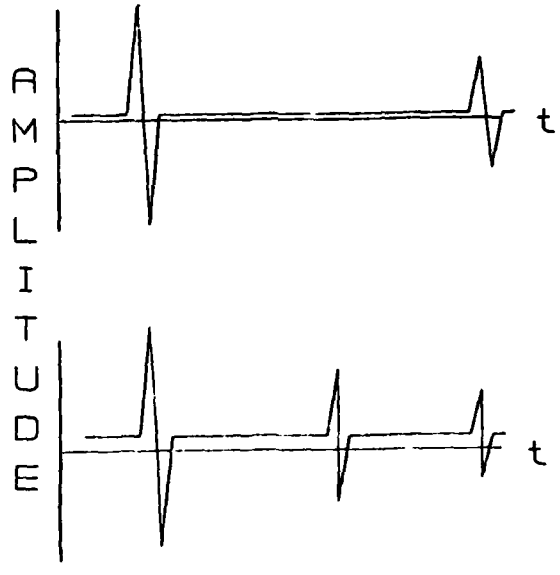

FIGURE 7 EXAMPLES OF ULTRASONIC A SCANS

FIGURE 8 C-SCAN OF A GRAPHITE EPOXY LAMINATE

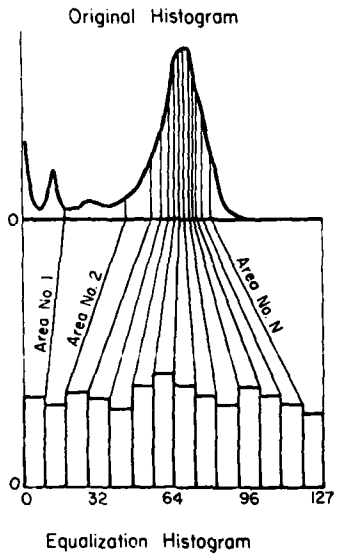

FIGURE 9 GRAPHIC ILLUSTRATION OF C-SCAN EQUALIZATION

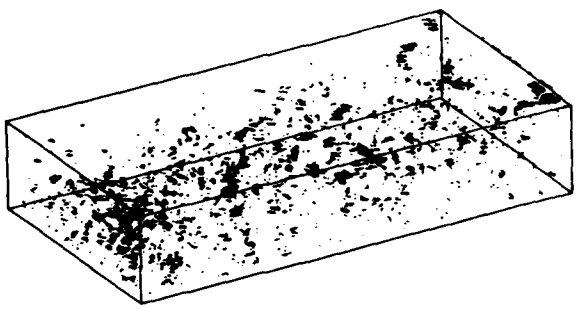

FIGURE 10 ISOMETRIC PROJECTION OF A FULL VOLUME C-SCAN SHOWING POROSITY IN A GRAPHITE EPOXY PANEL

NEED FOR COMMON AGARD APPROACH AND ACTIONS

R G TAYLOR
CHIEF OF NDT APPLICATIONS

ROLLS-ROYCE PLC
PO BOX 31
DERBY
UK

Introduction

During the past few years there has been a considerable increase in the inter-relationship between the major engine and airframe manufacturers, due to the need to collaborate on many airfraft projects, both within member countries and across international boundaries.

Whilst it may have been reasonable, over these years, to expect that these collaborations should have brought NDT Technology and methodology towards commonality, in reality it is perhaps disappointing to record that considerable differences still exist in both the application of NDT and other important aspects, such as the Training and Certification of personnel working in the Technology.

Whilst there is no direct evidence that the different approaches used in NDT have affected airworthiness, there are many pressures, both Technical and Commercial, for requiring a common approach within the community in the future. The Technical pressures arise from a need to achieve the same Technical standard of product, irrespective of the place of manufacture, in order to meet the stringent Damage Tolerance requirements now being placed on NDE, whilst the commercial pressures arise from the need for industry to rationalise the methodology, so that components are 'processed' in the same way, irrespective of the customer. An example of the problems associated with the lack of a common approach, is shown in the differing requirements of the major aero engine manufacturers, for the ultrasonic inspection of turbine discs. A study of the physics of the different methods demanded by the engine companies, shows that the same technical standard cannot be achieved, and the commercial problems are obvious when it is recognised that these different techniques are imposed on a common forging supplier.

As a result of recent collaboration activities with a number of other engine manufacturers, Rolls-Royce has carried out a survey of the differences that currently exist and these can be summarized as follows:-

Significant Differences - Technical

1. X-RAY

   - Penetrameters
   - Densities
   - Films

a) Penetrameters - These differ between Europe and the USA. In Europe it is normal to use DIN (wire) penetrameters for calibration, and step wedges are required in the USA.

b) Densities - Wide differences across the world, no international (or national) standards.

c) Films - One film manufacture produces a totally different range of film in the USA compared to its European Product.

2. ULTRASONIC - (Rotating Parts)

   - Scanning Philosophies, Angles Depth, Coverage.
   - Calibration Procedures
   - Grass, Attenuation

a) Ultrasonic Philosophies for rotating parts differs considerably from engine company to engine company, particularly in Probe Scanning angles which vary from 5^{o} scans to 45^{o} scans, although all companies do have a normal to surface scan requirement. In addition, considerable variation exists in the calibration procedures(one company still uses side-drilled holes in their test pieces), and

only one company appears to take into account the affects of grass,attenuation on detection sensitivity.

b) A significant influence on the different ultrasonic philosophies, is the various "opinions" on the likely orientation of sub-surfaces defects. In some cases it is the opinion that defects generally follow forging flow lines, and other opinions suggest that defects occur at a random orientation not necessarily associated with flow lines.

Clearly, in order to commonise on ultrasonic scanning, the defect orientation differences must be resolved.

3. MAGNETIC PARTICLE INSPECTION (MPI)

- Amperage Values
- Calibration and Control (Test Pieces)

The differences which exist in the MPI methodology are relatively few, but a major area which requires resolution is the amperage values used to calculate component magnetization requirements. These tend to differ largely between the USA and Europe although, some values differ within each continent.

4. PENETRANT INSPECTION

- Test Pieces
- Process Parameters (Dwell Times, Temperatures)
- Chemistry
- Part Preparation (Etch or no Etch)

A wide variety of differences exist in this technology, both in the application of the chemistry, and the preparation of the parts, in particular the penetrant contact time (varies from 10 minutes to 30 minutes), and whether to etch or not to etch as a pre-inspection surface preparation.

5. EDDY CURRENT - There appears to be very little differences in the application of this technology; however, there are considerable disagreements in the claims on the defect sizes that can be detected, this will be addressed later in the paper.

6. NEW AND EMERGING TECHNOLOGIES

- Real Time X-Ray
- Computer Tomography
- Fluorescent Detection etc

Whilst it is too early for significant differences to exist in the new and emerging technologies, a major problem requiring urgent resolution is to raise international calibration standards which will prevent the development of bad practices and technical differences.

SIGNIFICANT DIFFERENCES (GENERAL)

7. *TRAINING AND CERTIFICATION*

- Examination Requirements
- Operating Levels
- Periodic Examination or Assessment
- Eyesight - Tests and Frequency

In each of these areas there are major differences which need to be addressed, although there would seem to be more commonality in the training of NDT personnel across the world, than in the Certification & Approval methods used.

The main problem with Certification and Approval is concerned with who should carry this out. Some countries (and authorities) believe Certification should be carried out centrally; others suggest that this is the responsibility of the Employer, albeit to internationally agreed standards.

8. MULTI-NATIONAL NDE SPECIFICATIONS

The main approach to AGARD to achieve common standards is to work towards an Industry on Multi-National specifications for each NDT methodoly including the emerging techniques. Work is proceeding towards this end in Europe and in Penetrant Inspection alone, in the USA at present; however, there is no apparent effort to bring the USA and Europe together in this area. It is essential that this must be done to achieve the Common Approach goal.

9. PHYSICAL AND TESTING STANDARDS

One further essential step towards commonisation is to set up a 'Round Robin' testing programme to

a) determine the detection capability of facilities and methods and

b) to calibrate each facility against required standards.

This work has already been carried out on air frame components and could be duplicated on engine components. However, careful selection of test standards will be required before meaningful scientific studies can be carried out.

The use of inadequate test pieces with untypical defects (particularly artificially generated) may not be capable of distinguishing between a good or bad detection system.

One area where cross reference and calibration is vital, is in the application of Eddy Current for the detection of surface fatigue cracks. Dr L Bond's paper shows that considerable differences exist in the claims made for the detection capabilities of Eddy Current and since this will be the prime method for in-service inspections for life extension, we must have an AGARD agreement on the actual detection capabilities of the method. Including in this agreement must be the

- type of test piece
- defect morphology (real or seeded)
- Statistical method (miss calls, false calls)

and any other factor which must be taken into account to determine the probability of detection.

L'ETAT DE L'ART EN CONTROLE NON DESTRUCTIF DES PIECES DE TURBOMACHINE

par

JL.Meiffren
SNECMA Corbeil
Laboratoire R & D
B.P. 81
91003 Evry Cedex
France

1. INTRODUCTION

1.1. Durée de vie des pièces de turbomachines

La sécurité d'exploitation des turbomachines actuelles repose normalement sur une notion de durée de vie sûre, dûment calculée et démontrée.

L'application de méthodes de calcul élastoplastiques en fatigue oligocyclique permet le dimensionnement de la pièce considérée à partir de données acquises sur éprouvettes élémentaires ; ce dimensionnement est, le cas échéant, validé par des essais en fosse ou au banc.

Les contrôles non destructifs des fabrications sont un des éléments essentiels de l'assurance qualité : *ils permettent de garantir* la conformité des produits vis à vis de la référence technique pour laquelle la durée de vie sûre a été déterminée.

Il n'est pas rare que, tant pour conforter ou étendre la durée de vie sûre, que pour faire face à des événements fortuits, l'on soit amené à concevoir et appliquer des inspections non destructives pendant la durée d'exploitation du matériel.

Les performances des contrôles appliqués tant en production qu'en exploitation sont telles que les composants fabriqués ne présentent pas de défauts dont la taille est supérieure au seuil de détection affiché.

La situation actuelle peut être illustrée par le graphe ci-dessous :

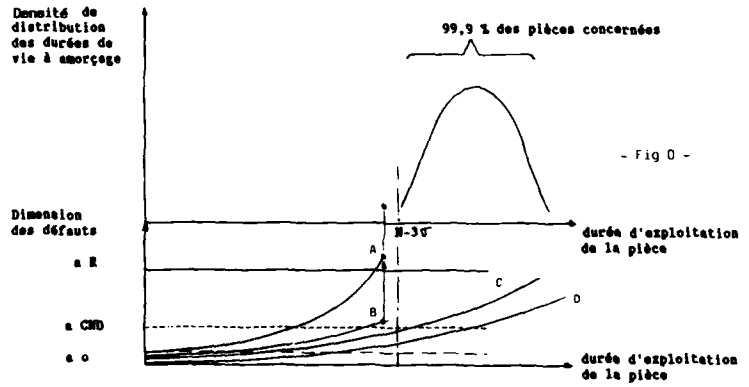

- Fig 0 -

$$DVA = \frac{N - 3\sigma}{a} \text{ où } a \in [1,3]$$

durée de vie sûre

a o représente la longueur initiale représentative de la qualité de production.

a CND représente le plus gros défaut non détectable par méthode CND.

a R représente la taille du défaut même entraînant la rupture statique

A représente le cas d'incident exceptionnel où une pièce est arrivée à rupture.

B représente la dépose d'une pièce contrôlée en maintenance après l'incident A.

L'ensemble de ces notions nous amène à préciser les performances des contrôles non destructifs.

1.2. **Efficacités comparées des différentes méthodes CND :**

Différentes études théoriques et expérimentales ont conduit un certain nombre de constructeurs aéronautiques à déterminer les niveaux de performances relatifs aux différentes techniques CND disponibles.

Des essais ont été réalisés sur des éprouvettes présentant des défauts type fissure de fatigue et représentatives de configurations géométriques réelles des pièces : alésage, alvéole, ...

La figure ci-dessous illustre les résultats obtenus.

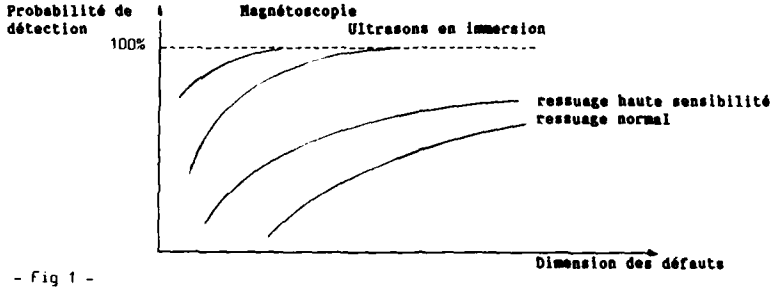

- Fig 1 -

Il est important de signaler que certains défauts présentés sur les pièces dont la taille est inférieure au seuil de détection garanti peuvent être détectés.

A ces courbes doivent être associées celles des "fausses alarmes", c'est-à-dire des détections d'anomalies sans rapport avec le défaut recherché qui présentent une signature du même type.

Ces "fausses alarmes" ont pour origine en général, des anomalies géométriques ou métallurgiques de la pièce, des perturbations physiques ou électroniques générées par le matériel de contrôle utilisé.

2. LES CND EN PRODUCTION DES PIECES MOTEURS

2.1. Généralités

L'intégration des contrôles non destructifs dans les gammes de fabrication des composants tient compte :

- de la nature des défauts recherchés ainsi que du seuil de détection escompté,
- de la géométrie de la pièce et de son état de surface,
- de la nature du matériau,
- des risques de contamination générés par le procédé d'inspection.

Parmi les techniques CND disponibles, est sélectionnée la technique la plus adaptée aux critères définis ci-dessus.

Ensuite sont réalisées successivement la validation expérimentale de la méthode ainsi retenue, la conception et la réalisation d'étalon de référence.

Enfin, la mise en place coordonnée et la surveillance des équipements et procédures d'inspection garantit en production le niveau de qualité nécessaire.

La sélection des techniques CND dans la phase initiale est fonction de la configuration des pièces et des défauts type recherchés est illustrée par le tableau ci-après :

TABLEAU 1

APPLICATION INDUSTRIELLE DES CONTROLES NON DESTRUCTIFS EN AERONAUTIQUE

Stades d'application des C.N.D.	Défauts types recherchés	Dimension type	C.N.D. envisageables
Réception des produits demi-produits	Mélange de matières Défauts d'élaboration et de première transformation (inclusions, ségrégations, criques, etc.)	0,2 à 1 mm	US
Pièces brutes			
. forgées	- aspect, tapures, criques, replis, inclusions laminées, etc.	0,5 mm	US, RX, RS
. coulées	- aspect, criques, porosités, inclusions, ségrégations, retassures, microretassures, etc. - épaisseurs parois	0,3 mm	US, RX, RS
En cours de fabrication			
. usinage	- aspect, criques de rectification corrosion, mesures d'épaisseurs, etc.	0,2 mm	US, CDF, RS, MG
. soudage	- aspect, manque de pénétration, criques, soufflures, inclusions etc.	2 à 10 mm	RX, MG, RS
Traitements thermiques :	Tapures de trempes, criques de détentionnement, caractérisation de l'état de traitement thermique (pour certains alliages) mesure d'épaisseur des couches cémentées, etc.	0,5 mm	CdF, RS
Traitement de surfaces :	Aspect, épaisseur du dépôt, fissuration, adhérence du revêtement, etc.		CdF, RS

Trois exemples concrets choisis dans la pratique courante permettent d'illustrer cette méthodologie :

2.2. Contrôle par ultrasons des disques de compresseurs et turbines

Le premier exemple est le contrôle ultrasonore réalisé sur les pièces tournantes de turboréacteur : c'est le cas de disques, tambours ou rotors de compresseur et de turbine.

L'automatisation du contrôle ultrasonore par immersion des pièces axisymétriques de turboréacteur permet :

- d'accroître le degré de confiance, la reproductibilité et les performances le cas échéant,
- de réduire le coût de l'assurance qualité,

et ce, dans le cadre d'une application en atelier de production.

Cette application se réalise dans les conditions suivantes :

- contrôle sur état pré-usiné de forme géométrique simple,
- utilisation de palpeurs focalisés de fréquence nominale 5 ou 10 MHz (en fonction de la surépaisseur d'usinage par rapport au profil de la pièce finie),
- étalonnage sur trou à fond plat ou sur génératrice de trou.

La première méthode présente l'avantage important que la dimension du réflecteur (fond plat de trou) ne varie pas en fonction de la profondeur. Par contre, deux cales étalon sont alors nécessaires pour réaliser l'étalonnage en ondes longitudinales puis transversales (figure 2).

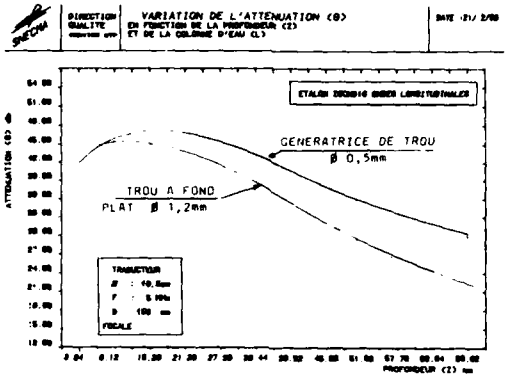

- Fig 2 -

L'introduction de l'étalonnage et du contrôle automatique a permis en moyenne une augmentation de productivité de 40 %, soit une réduction d'environ 200 KF/an/installation.

Le tableau suivant donne une illustration des gains obtenus.

TABLEAU 2

CONTROLE ULTRASONORE DE PIECES TOURNANTES CRITIQUES

REDUCTION DE LA DUREE DES CONTROLES ENTRE INSTALLATIONS SEMI-AUTOMATIQUES ET AUTOMATIQUES

INTRODUCTION DE L'ETALONNAGE AUTOMATIQUE

Type de pièce	Durées relatives (contrôle plus préparation)		
	1 - Contrôle semi-automatique	2 - Contrôle auto étalonnage manuel	3 - Contrôle auto étalonnage auto
Disque 1 turbine	(Base) 100	32	24
Disque 2 turbine	100	33	26
Disque 3 turbine	100	35	28
Arbre de compresseur	335	120	111
Disque de soufflante	144	84	79

Dans tous les cas, vitesse linéaire 450 mm/s, pas d'avance=75 % tache focale.

La figure 3 montre shématiquement les critères d'inspection correspondants.

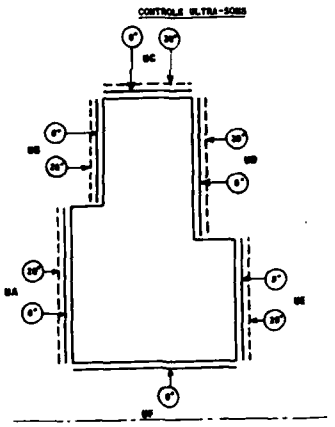

CONTROLE ULTRA-SONS				
Zones	UA,UB,UD,UE	UC,UF	UA,UB,UD,UE	UC
Rugosité Ra (m)	0,8			
Mode	LR	LG	T20NR	T20NG
Critères (% amplitude d'étalonnage)	25	25	50	50

Légende :

LR : mode longitudinal radial.
LG : mode longitudinal sur génératrice
T20NR : mode transversal radial à 20° d'incidence.
T20NG : mode transversal sur génératrice à 20° d'incidence

- Fig 3 -

Les seuils de rejet varient entre des diamètres de trou à fond plat de 0,6 à 5 mm selon les cas, un taux de rebut de l'ordre de 5 10 $^{-2}$/pièce est typiquement observé, correspondant à des criques de forge amorcées par des inclusions d'oxydes, des ségrégations du type white spots.

L'installation est programmée pour stopper automatiquement dès que le signal dépasse le niveau maximum du bruit de structure habituel, soit un diamètre de trou à fond plat de l'ordre de 0,4 mm en moyenne. L'opérateur procède alors à une évaluation manuelle (par angulation, etc), du maximum d'écho dans la zone considérée. Pour les pièces avancées en métallurgie de poudres, le nombre d'indications dépassant le niveau maximal de bruit de structure est élevé. L'installation acquiert les amplitudes point par point et identifie en final les zones où l'amplitude dépasse le seuil à des fins d 'expertise.

2.3. Contrôle des épaisseurs de parois d'aubes à cavité

Le deuxième exemple concerne la mesure dimensionnelle d'épaisseur de paroi d'aube de turbine (cas d'aubes comportant une cavité).

Dans la gamme d'épaisseur considérée, voisine du millimètre, avec des configurations géométriques complexes, notamment surfaces courbes et accidents de forme importants avec présence de "pontets", l'objectif à atteindre est de mesurer ces épaisseurs avec une précision de l'ordre de 0,05 mm. Les écarts observés industriellement proviennent des tolérances sur les carapaces céramiques et des déports des noyaux à la coulée.

Le contrôle par ultrasons ne convient pas toujours pour les raisons suivantes :

- la géométrie complexe à l'endroit de la mesure donne des oscillogrammes ininterprétables et donc des mesures peu fiables,
- dans le cas d'aubes monocristallines ou réalisées en solidification dirigée, il y a variation du module d'Young dans le matériau et donc variation de la vitesse des ondes ultrasonores suivant l'orientation de la mesure. Les écarts constatés (± 10 % sur les épaisseurs relevées par ultrasons) nous ont conduit à abandonner cette technique.
- le temps de contrôle doit être amélioré.

La mise en oeuvre du contrôle par Courants de Foucault appliqué aux aubes mobiles et aux distributeurs de turbine permet d'atteindre les objectifs techniques et économiques.

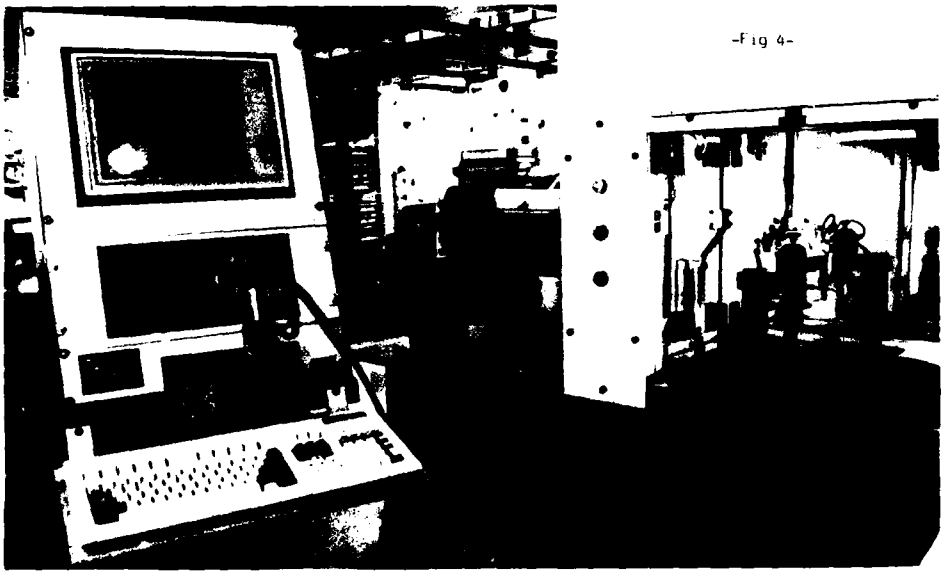

-Fig 4-

L'installation considérée, illustrée sur le cliché de la figure 4, présente les caractéristiques suivantes :

- la précision de la mesure est inférieure à 0,05 mm,
- l'intégration du système de contrôle sur un robot a permis l'augmentation des cadences comme le montre le tableau ci-dessous pour 2 applications :

	CONTROLE US	CONTROLE CdF *
Aube mobile HP 18 pts de mesure	5 à 10 min	1 min 50 s
Distributeur 3 pales 54 points de mesure	15 à 20 min	5 min 30 s

* 1 pt de mesure toutes les 6 secondes

2.4. Contrôle des soudures sur rotors de compresseur

L'évolution du contrôle radiographique de zones soudées par faisceau d'électrons sur rotor de turbomachine en alliage de titane constitue le troisième exemple.

Initialement, le contrôle par Radiographie X réalisé en mode directionnel sur la pièce permettait la détection de :

- manque de liaison sur le plan de joint (30 % de l'épaisseur de la pièce longueur mini = 1 à 10 mm),
- criques longitudinales parallèles au cordon de soudure (10 à 30 % de l'épaisseur longueur mini = 1 à 10 mm),
- soufflures (Ø 2 mm).

La nécessité d'améliorer les cadences de contrôle et l'apparition après soudage de criques transversales de très petites dimensions (longueur environ 3 mm au moins) de part et d'autre du plan de joint dans le cordon de soudure a nécessité la mise au point d'une nouvelle technique de Radiographie appelée "dynamique", c'est-à-dire avec rotation de la pièce devant le tube RX pendant le tir.

Indépendamment de l'amélioration du niveau de détection de cette technique : meilleure résolution que celle obtenue avec un tube microfocus-panoramique, un gain important de productivité a été réalisé. Les temps de contrôle ont été divisés par plus de 6.

Le tableau 3 en est l'illustration.

TABLEAU 3

CONTROLE RADIOGRAPHIQUE DE ROTOR SOUDE FE

TECHNIQUES UTILISEES	TEMPS "PREPARATION ET TIR"	RESOLUTION, PERFORMANCE DE DETECTION
RADIOGRAPHIE CONVENTIONNELLE - TUBE RX DIRECTIONNEL - PIECE ET TUBE RX FIXES - 16 TIRS PAR CORDON, SOIT 128 TIRS/PIECE	Base : 100	MANQUE DE LIAISON : 30 % DE L'EPAISSEUR CONTROLEE CRIQUES LONGITUDINALES : 10 % à 30 % DE L'EPAISSEUR CONTROLEE CRIQUES RADIALES DETECTION ALEATOIRE SOUFFLURES : ∅ 0,2 mm
RADIOGRAPHIE DYNAMIQUE (1ère ETAPE) - TUBE RX DIRECTIONNEL - TUBE RX FIXE, PIECE EN ROTATION - REGLAGE EN POSITION DU TUBE - RX MANUEL (LONG ET PEU PRECIS) - 1 TIR PAR CORDON, SOIT 8 TIRS/PIECE	38	MANQUE : 20 % à 30 % DE L'EPAISSEUR CONTROLEE CRIQUES LONGITUDINALES : 10 % à 30 % DE L'EPAISSEUR CONTROLEE CRIQUES RADIALES BIEN DETECTEES SOUFFLURES : 0,1 à 0,2 mm
RADIOGRAPHIE DYNAMIQUE (2ème ETAPE) - TUBE RX DIRECTIONNEL - TUBE RX FIXE, PIECE EN ROTATION - AUTOMATISATION DU PILOTAGE : . DES COMMANDES DE TIR . DU POSITIONNEMENT DU TUBE RX - 1 TIR PAR CORDON, SOIT 8 TIRS/PIECE DANS 2 SEQUENCES	15	IDEM (1ère ETAPE) AVEC FIABILITE ACCRUE

3. CND APPLIQUEES SUR MOTEURS EN EXPLOITATION

3.1. Généralités

La nécessité de confirmer ou d'étendre une durée de vie sûre, ainsi que la constatation de la présence de défauts de fonctionnement en réparation, ou d'incidents en utilisation, imposent quelquefois la programmation d'une inspection sur le matériel en service.

Dans le dernier cas, sur la base des résultats de l'expertise des éléments défectueux, deux types d'action peuvent être engagées :

- l'élimination des risques d'une défaillance identique : remplacement systématique des pièces incriminées (actions correctives),
- la prévention des risques d'une défaillance identique : CND des pièces incriminées (action préventive).

Dans le cas de prévention des risques, la méthodologie adoptée est la suivante :

- une analyse précise des principaux paramètres techniques dont :
  . la nature du matériau,
  . la nature de l'anomalie,
  . l'accessibilité à la zone d'initiation de l'anomalie,
  . les risques de contamination du moteur

  conditionnant le choix de la méthode CND à retenir pour cette application (voir tableau 4).

- Le déclenchement de la mise au point d'un procédé d'inspection selon la chronologie définie (tableaux 5 et 5 bis).

TABLEAU 4

INFLUENCE DES PRINCIPAUX PARAMETRES TECHNIQUES SUR LE CHOIX DES PROCEDES A EXPERIMENTER

Principaux paramètres influents / Techniques de CND utilisées	NATURE DU MATERIAU		NATURE DE L'ANOMALIE				ACCESSIBILITE		RISQUES DE POLLUTION OU DE CONTAMINATION
	Métallique	Non Métallique	Criques diverses, déchirures, replis, tapures	Usures Déformations	Nouvelle positionnement ou absence de pièces	Matière non conforme	à la pièce incriminée	à la zone d'initiation de l'anomalie	
EXAMEN VISUEL	X	X	X	X	X	-	●	●	Δ
RESSUAGE	X	X	X	-	-	-	●	●	Δ
THERMOELECTRICITE	X	-	-	-	-	X	●	●	Δ
ANALYSE VIBRATOIRE (essentiellement à titre expérimental)	X	X	X	X	X	-	O	O	Δ
ULTRASONS	X	X	X	-	-	-	●	O	Δ
COURANTS DE FOUCAULT	X	-	X	-	-	X	●	●	Δ
GAMMAGRAPHIE	X	-	X	X	X	-	O	O	Δ

Légende :

X application possible
- application impossible ou peu probable

● indispensable
O facultatif

à oui
Δ non

TABLEAU 5

CHRONOLOGIE D'UNE MISE AU POINT D'UNE METHODE CND

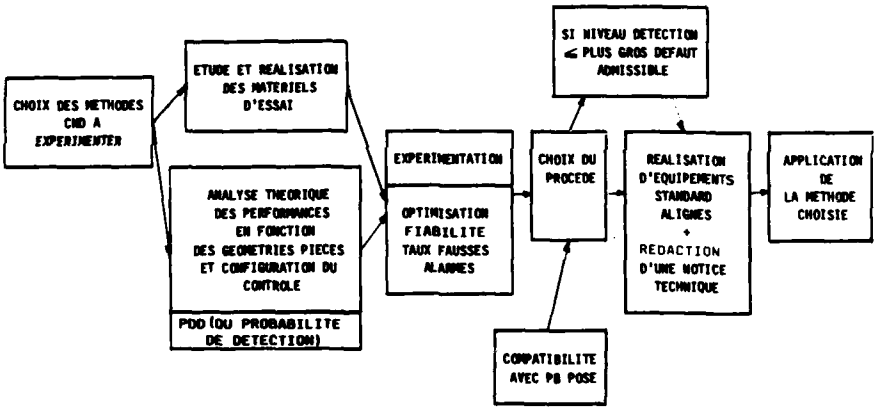

TABLEAU 5 BIS

CHRONOLOGIE D'UNE MISE AU POINT D'UNE METHODE DE CONTROLE NON DESTRUCTIF

EN VUE DE SON APPLICATION A LA SURVEILLANCE EN UTILISATION DES MOTEURS D'AVIONS

CHOIX DES METHODES DE CND A EXPERIMENTER	DEFINITION ET REALISATION SI BESOIN, DU MATERIEL NECESSAIRE AUX ESSAIS	EXPERIMENTATION	CHOIX DU OU DES PROCEDES A APPLIQUER	REALISATION D'EQUIPEMENTS STANDARD ALIGNES	APPLICATION DE LA METHODE CHOISIE
tenant compte des possibilités techniques des différents procédés (cf. tableau 4) Performances . POD . Taux de fausses alarmes	Matériel comprenant - appareillage de contrôle standard ou spécifique - pièces avec défauts significatifs (artificiels ou réels) caractérisés	1) En laboratoire sur pièces d'essais, recherche de l'établissement d'une corrélation entre indications données par procédés de CND et l'importance des défauts significatifs tenant compte si possible des éléments de dispersion (position et orientation des défauts - forme et géométrie des pièces...) 2) sur moteurs, en vraie grandeur, vérification notamment des conditions d'accessibilité du matériel de contrôle 3) Synthèse des essais et des vérifications : - Définition des performances de la méthode expérimentée (sensibilité, temps de contrôle et d'indisponibilité du moteur) - Fixation des critères d'acceptation	Seulement si performance suffisante	Si nécessité d'effectuer simultanément un même contrôle en des lieux différents	- par spécialiste de CND - par opérateurs après formation préalable

Citons 4 exemples concrets issus de notre expérience :

3.2. Fissures de fatigue sur bord d'attaque d'aubes

A la suite d'une rupture d'aube de 1er étage du compresseur sur un moteur, il a été décidé d'appliquer en maintenance un contrôle préventif sur tout le parc des turboréacteurs en service sans démontage de la pièce incriminée. Il fallait définir une méthode CND applicable directement sur moteur avionné.
Le choix de la technique se porta sur les Courants de Foucault. Un équipement de contrôle avec balayage semi-automatique de la zone à contrôler par la sonde CdF fut réalisé (voir Fig. 5 et 6).

DETECTION DE CRIQUES DE FATIGUE SUR BORD D'ATTAQUE D'AUBES

PAR COURANTS DE FOUCAULT

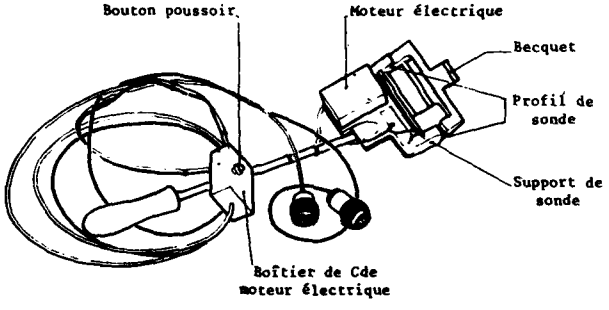

Fig. 5 - Sonde Courants de Foucault, moteur avionné.

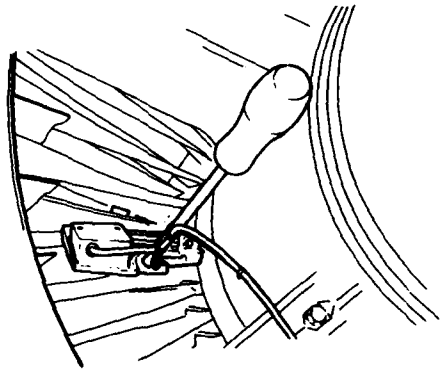

Fig. 6 - Réalisation du contrôle, moteur avionné.

La validation de la méthode a été effectuée sur pièce avec fissure de longueur développée égale à 1 mm. Cette valeur constitue le seuil de détection de la méthode.

Très peu de fausses alarmes ont été constatées, conséquence du système semi-automatique éliminant l'influence de l'opérateur. Le temps de contrôle relativement bref : une heure pour l'ensemble de la roue, est très inférieur au temps nécessaire à la dépose et repose du moteur, avec démontage et remontage de toutes les aubes de 1er étage du compresseur, soit 5 heures avec passage de l'avion en point fixe.

L'intervalle d'inspection évalué à partir de la criticité du défaut était de 50 heures.

En maintenance, 138 moteurs ont été contrôlés par les utilisateurs sur base. Sur 12 aubes, ont été détectées des indications C. de Foucault. Après dépose, 11 aubes présentaient effectivement des criques de fatigue de dimension supérieure à 1 mm (seuil) et sur une aube l'indication correspondait à un impact assez important.

3.3. *Fissures par facteur de forme dans un disque*

En utilisation, des criques de fatigue-fluage s'amorçant dans un rayon très faible au droit d'un centrage sont apparues sur des disques de compresseur en alliage léger.

La crique prenait naissance dans une zone quasi-inaccessible sans démontage de la pièce incriminée (voir Fig. 7 et 8).

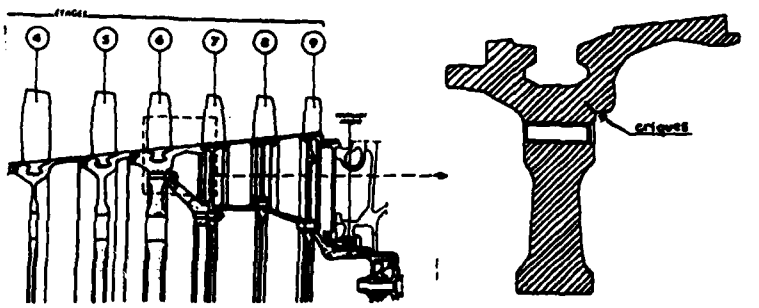

Fig. 7

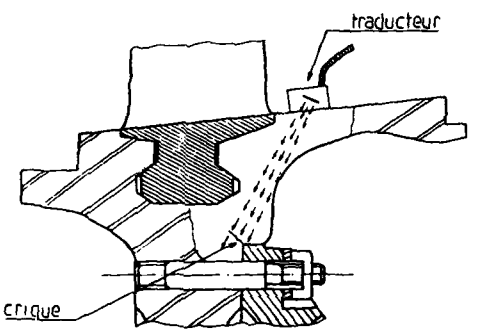

Trajet du faisceau ultrasonore

Fig. 8

Compte tenu de cette difficulté, seul le contrôle ultrasonore par contact sur rotor complet était envisageable.

Une première méthode (Fig. 8) fut mise au point et fut appliquée immédiatement à une partie du parc moteur (44 disques). Le seuil de détection établi sur défaut réel et validé par dissection d'un disque criqué était de l'ordre de 1,5 mm. Aucune fausse alarme particulière n'a été constatée dans l'application de cette méthode.

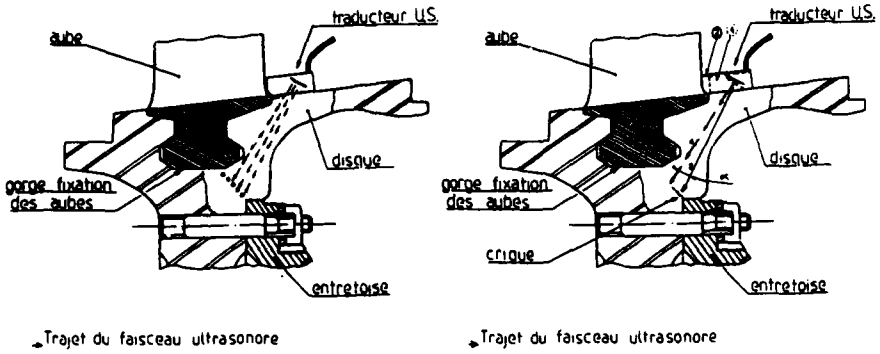

Fig. 9

Une deuxième méthode fondée sur le même principe a été définie. Les conditions de contrôle avaient été optimisées afin de réduire le seuil de détection à 0,5 mm et pour augmenter les intervalles d'inspection. Le sondage ultrason était réalisé sous un angle plus faible et dans une région proche de l'épaulement dans lequel s'initiait la crique recherchée (Fig. 9).

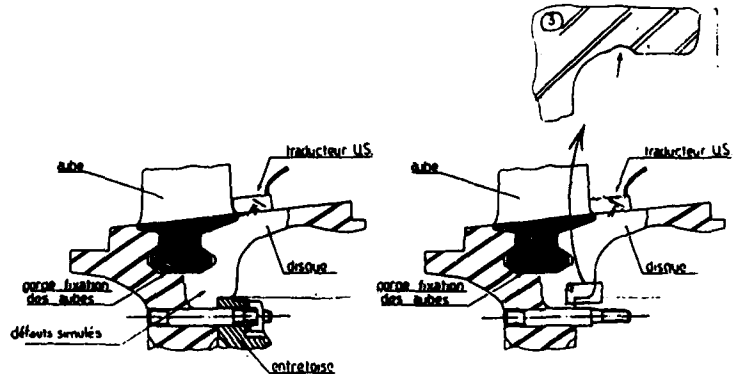

Fig. 10

Ainsi définie, la méthode fut appliquée à 38 moteurs. Les 38 disques furent trouvés criqués. Parmi ceux-là, sur un disque, la dissection au droit des indications détectées, aucune fissure n'a été constatée. C'est un "ressaut" dans l'angle de l'épaulement qui, en "fausse alarme" a généré une indication de défaut (Fig. 10).

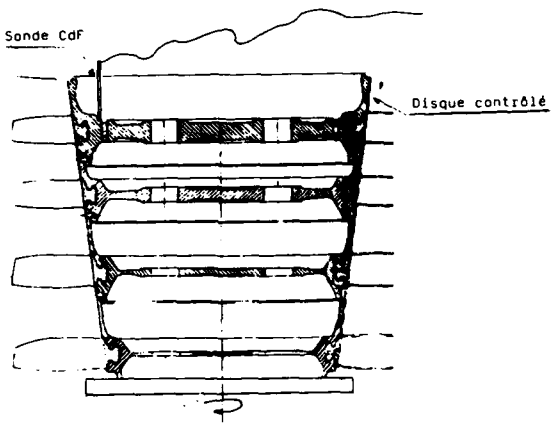

Fig. 11

Une troisième méthode par Courants de Foucault et applicable seulement sur disque déposé, a permis de concilier une faible valeur du seuil de détection (0,7 mm) et un taux de fausses alarmes acceptable (nul en l'occurrence). (fig. 11)

3.4. Fissures de fatigue sur des viroles inter-étage de compresseur

Le troisième cas d'anomalie constaté en application concerne l'amorçage de crique de fatigue sur des viroles intermédiaires positionnées entre disques de compresseur. Les criques apparaissaient préférentiellement dans des encoches destinées à équilibrer le rotor, dont certaines avaient été réalisées d'une manière non conforme en maintenance.

La configuration dans laquelle le contrôle devait être réalisé imposait un démontage minimum : dépose du rotor, et ne permettait pas d'avoir accès directement à la zone où s'initialent les criques. Une méthode de contrôle par ultrasons utilisant des réflexions multiples du faisceau acoustique a été utilisée (Fig. 12 et 13).

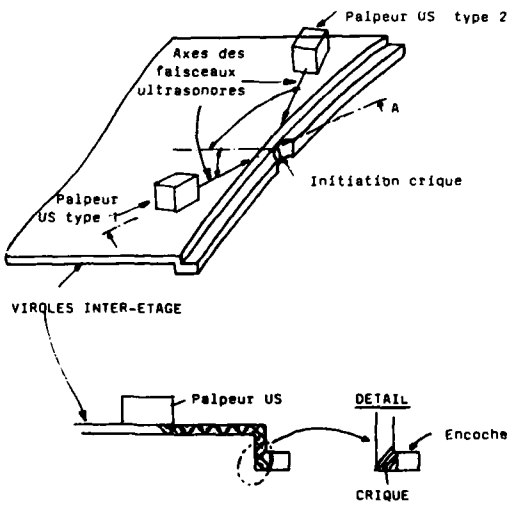

Fig. 12

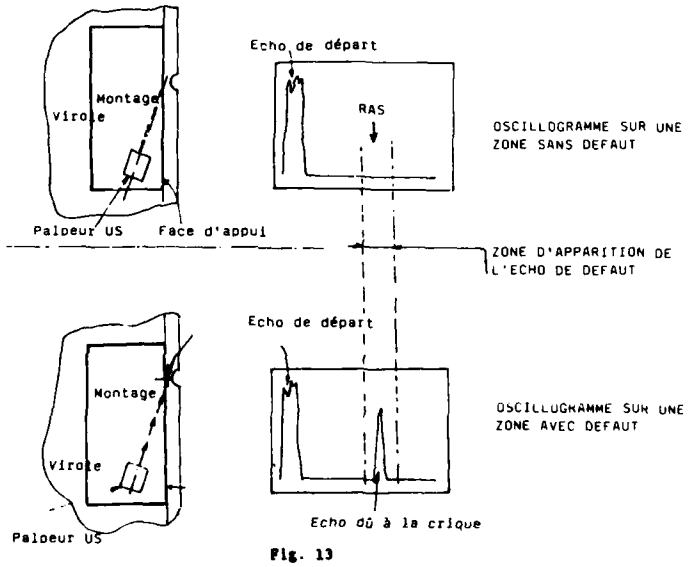

Fig. 13

Sur plus de 100 moteurs contrôlés, 5 viroles furent trouvées criquées. Bien que le seuil de détection fut initialement fixé à 3 mm, le plus petit défaut détecté présentait une longueur de 1,7 mm, cette valeur a constitué le nouveau seuil de détection.

Compte tenu du caractère mixte de l'endommagement (amorçage en fatigue oligocyclique, propagation en fatigues oligocycliques et vibrations combinées), les intervalles d'inspections sont faibles (200 h à 50 h selon les cas).

3.5. <u>Ruptures en fatigue de freins d'aubes de compresseurs</u>

Enfin, dans le dernier cas, il s'agissait de détecter des ruptures de freins d'aubes qui sont destinées à bloquer les aubes en position sur disque de compresseur. Ces ruptures se développent radialement en fatigue sur les rayons de pliage des tôles utilisées pour réaliser la fonction de frein. La méthode retenue consiste à radiographier le secteur concerné par gammagraphie. Le radio isotope (source de rayonnement γ) est introduit dans l'axe moteur de conception tubulaire, les films radiographiques étant placés sur la périphérie du réacteur.

A noter que l'une des origines de cette conception tubulaire des arbres de compresseur ou de turbine est de faciliter le contrôle en maintenance par gammagraphie.

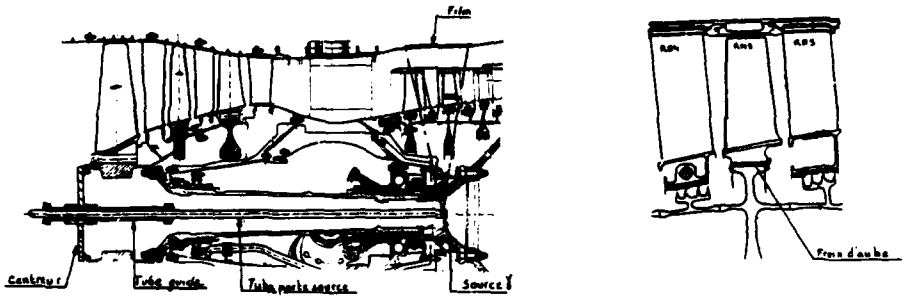

Fig. 14

4. APPROCHE STATISTIQUE DES CND

Comme les différents exemples l'ont montré, les performances des contrôles non destructifs sont conditionnées par 3 paramètres :

- le taux de non détection,
- le taux de fausses alarmes,
- le taux effectif de pièces défectueuses.

La non-détection de défaut liée ou non à des fausses alarmes peut avoir pour origine :

- une dimension de défaut inférieure au seuil garanti de détection,
- des anomalies intempestives masquant le défaut à rechercher.

Dans ce cas, le type d'anomalies appelé fausses alarmes qui peuvent être classées en 2 catégories :

- anomalies liées au système de mesure,
- anomalies liées à la pièce.

par exemple :

TECHNIQUE	ANOMALIE LIEE AU SYSTEME	ANOMALIE LIEE A LA PIECE
Courants de Foucault	"Lift off" ou éloignement sonde/pièce	- Magnétisme rémanent - Contrainte d'écrouissage - Effet de structure
Ultrasons	- Mauvais couplage capteur pièce - Bulles d'air - Bruits de fond électronique	- Herbe - Bruit de structure - Rayures - chocs sur pièce
Radiographie X	- Rayures film - Ecran plomb - Pb de développement	- Phénomène de diffraction ou rétrodiffusion - "Ligne noire" dans soudure
Ressuage	- Mauvaise application du procédé en particulier lavage	- Zone de rétention dans la pièce - Etat de surface non homogène

La prise en compte de ces différents aspects permet d'établir les performances réelles des procédés à partir :

- de la détermination de la probabilité de détection en relation avec le taux de fausses alarmes de la technique considérée,
- des études techniques d'applicabilité de la méthode CND en fonction de la configuration géométrique pièce et de l'accessibilité des zones à contrôler,
- du stade d'intervention :
  . fabrication,
  . réparation,
  . exploitation.

Un tableau de synthèse de l'évolution des CND (tableau N° 6) dresse le bilan sur les dernières années et des tendances actuelles sur les choix techniques d'application des CND tant en fabrication qu'en exploitation.

TABLEAU 6

EVOLUTION DES CONTROLES NON DESTRUCTIFS

A LA SNECMA AU COURS DES DERNIERES ANNEES

APPLICATIONS		PIECES OU ASSEMBLAGES								MOTEURS COMPLETS							
										à l'arrêt		en fonctionnement					
PRINCIPAUX STADES D'INTERVENTION	METHODES SENS DE L'EVOLUTION	VISUEL	ULTRASONS	MAGNETOSC.	C. FOUCAULT	TH. ELEC.	RADIO X	RESSUAGE	THERMOGR.	NEUTROGR.	HOLOGRAPHIE	GAMMAGR.	VISUEL TV	MICROSCOPIE	SPECTROGR.	VIBRATIONS	SUPER X
PROTOTYPES																	
en fabrication		↗	↗	→	↗	→	→	→	X	---	X						
en fonctionnement		---	---	---	---	---	---	---	---	---	---	---	---	---	---	X	X
après fonctionnement																	
sans démontage		---	---	---	---	---	---	---	---	---	---	↗	X	X	X		
après démontage		→	↗	→	↗		→	↗	X	X							
PRODUCTION																	
en fabrication		↗	↗	→	↗	↗	→	↗	X	---	X						
avant livraison des ensembles		---	---	---	---	---	---	---	---	---	---	---	X	X	---	X	
UTILISATION																	
prévention générale		---	---	---	---	---	---	---	---	---	---	↗	X	X	---	X	
prévention particulière		↗	→		↗	---	---	→	---	---	---	↗	X				
REPARATION																	
après démontage		→	↗	→	↗	---	→	↗	---								
après réparation		↗	↗	→	---	---	→	↗									
après essai des moteurs réparés		---	---	---	---	---	---	---	---	---	---	---	X	X	---	X	

↗ Accroissement → Stab. ou diminution X En cours d'études ou applic. spécifique

5. CONCLUSIONS

La qualité dans la production et l'exploitation de turbomachines impose aujourd'hui de disposer de méthodes et de moyens performants d'inspection non destructrive, adaptés aux configurations des pièces, mais en parallèle l'"inspectabilité" des composants doit être prise en compte au niveau même de leur conception.

L'intervention de la conception, la fabrication et la qualité dans la définition de nouveaux moteurs favorise l'adoption de solutions techniques issues d'un compromis entre :

- la fonction du composant,
- la faisabilité quant à sa fonction,
- la "contrôlabilité" en fabrication, maintenance et réparation.

RECORDINGS FROM AGARD SMP MEETING ON DAMAGE TOLERANCE CONCEPTS FOR ENGINE CONSTITUENTS - NON-DESTRUCTIVE EVALUATION, Luxembourg, May 1988

Dr. A.F. Blom
Structures Department
The Aeronautical Research
Institute of Sweden (FFA)
P.O. Box 11021
S-161 11 Bromma, Sweden

Major R.F. Drummond
Aerospace Maintenance
Development Unit
CFB Trenton
Astra, Ontario
Canada K0K 1B0

Through discussions occuring between each of the formal presentations, the meeting arrived at a concensus that follow-up action was needed in the following areas :

a. modelling (both of defect initiation/growth and of the non-destructive testing (NDT) process/flaw interaction);

b. statistics and data collection to define NDT reliability; and

c. the initiation of round-robin testing of standard samples with actual flaws to enlarge the probability of detection (POD) data base and to facilitate the sharing of experience between concerned agencies.

MODELLING

1. Failure occurs when design exceeds process control; certifying authorities must decide what standards/measures of process control are satisfactory and what data must be collected to verify that the specified process control is attained.

2. The destructive testing to prove component durability, and the manufacture and post-test examination of POD specimens to determine NDT reliability are expensive. At this point, such tests are conducted until a cost-benefit decision is made.

3. Newer engine structures are under complex loads and made of materials whose fatigue behaviour is not as well understood as those in older generation components. This makes a comprehensive inspection of fracture critical components to assure a "defect free case" impossible. Finding defects at the required probability is only possible at predictable locations for failure sites. However, the stress levels in critical components and the fatigue intolerance for some of the most advanced materials is heading toward a situation where cracks could initiate anywhere from extremely small initial flaws. Therefore, the introduction of retirement for cause (RFC) has slowed the trend toward increasing performance of gas turbine engines while the industry develops materials with greater crack nucleation and growth resistance. It was estimated that a further five years might be required before efforts are renewed to push at present thrust/weight barriers.

4. Eventually, the trend toward engine materials and designs improving performance will bring with it critical crack sizes which push against the physics which dictate crack detectability by NDT methods. Also, accurate prediction of crack location and orientation is mandatory for a safety-by-inspection philosophy to be successful. So far, such definite defect prediction and detection has been elusive.

5. It was mentioned that the RFC philosophy addresses these concerns by obligating the use of materials with known favourable crack growth rates. Also, analysis must provide for conservatism in design to provide surviveability for at least two inspection lives with defects at the 90 % POD 95 % confidence level. RFC will only be applied for components with critical defect sizes which NDT technology (which is continuing to develop) has been proved capable to detect.

6. Designers of gas turbine engines are not universally obligated to include "inspectability" by NDT in component designs, although most are at least educated to do so.

7. The design of engine components which meet RFC criteria is a team effort between the design and NDT engineers. The design engineer must define what defects will be produced by manufacturing processes and service conditions as well as their propagation rates, orientations and critical sizes. Then the NDT engineer attempts to characterize the inspection system's response to these features, optimize flaw detection and set pass/fail criteria.

8. While a thorough understanding of the underlying physics of all NDT methods has not been essential to their effective application to this point, such fundamental knowledge is necessary for techniques to detect defects at the sizes and reliabilities required to support engine design of the future. It was estimated that development of a model for eddy current/defect interaction to the same degree as that available for the ultrasonic method is at least five years away.

9. It was mentioned that NDT method reliability can be studied, in some instances (such as for ultrasonics), by computer modelling of the process/flaw interaction. It was pointed out that this approach was limited in that it did not add to practical knowledge or experience.

STATISTICS/DATA COLLECTION

1. While data was displayed showing generally recognized minimum detection limits for various NDT methods, practical reliability data is still not readily available. No single figure should be used to state POD as a general truth for any method.

2. Due to the expense and effort associated with NDT reliability studies, POD data is very sparse (small sample sizes in each test). Statistical methods presently used for analysis of such data was questioned; perhaps the statistical methods used in civil engineering might be tried and the results compared with present NDT reliability practices for conservatism.

3. The understanding of total POD must be broader - probability of the defect occuring, probability/rate of crack growth, probability of detection (NDT), etc.

4. Some error in POD is created by the difficulty of accurately sizing defects such as cracks, even by metallurgical examination.

5. The USAF is attempting to establish a standard for the quantitative evaluation of liquid penetration inspection and eddy current methods. A workshop on that topic is scheduled for the Quantitative NDE conference at La Jolla, California in early August 1988.

ROUND-ROBIN TESTING

1. As stated in "modelling" the manufacture and post-test examination of POD specimens to determine NDT reliability are expensive.

2. It was proposed that some round-robin testing of a standard specimen set containing "real" defects could be useful to gather sufficient data to make NDT reliability determination possible. However, a suggestion was made that the standardization of NDT systems between participants can be difficult. For instance, many parameters must be considered for highly sensitive ultrasonic testing. Nevertheless, it was concluded that such a test would be useful to establish and share an NDT reliability data base as well as to examine statistical approaches to the treatment of this data. This topic will be discussed further at the next AGARD SMP business meeting scheduled for this autumn.

REPORT DOCUMENTATION PAGE

1. Recipient's Reference	2. Originator's Reference	3. Further Reference	4. Security Classification of Document
	AGARD-R-768	ISBN 92-835-0484-4	UNCLASSIFIED

5. Originator Advisory Group for Aerospace Research and Development
North Atlantic Treaty Organization
7 rue Ancelle, 92200 Neuilly sur Seine, France

6. Title AGARD/SMP REVIEW – DAMAGE TOLERANCE FOR ENGINE STRUCTURES: 1. NON-DESTRUCTIVE EVALUATION

7. Presented at the 66th Meeting of the Structures and Materials Panel of AGARD in Luxembourg, 1–6 May 1988.

8. Author(s)/Editor(s)	9. Date
Various	November 1988
10. Author's/Editor's Address	**11. Pages**
Various	126

12. Distribution Statement This document is distributed in accordance with AGARD policies and regulations, which are outlined on the Outside Back Covers of all AGARD publications.

13. Keywords/Descriptors

Nondestructive tests
Engines
Components
Damage
Evaluation

14. Abstract

The AGARD Structures and Materials Panel is co-ordinating a series of four Workshops planned within the framework of a Review on Damage Tolerance for Engine Structures. The Review aims to address the areas critical to the acceptance of an approach based on damage tolerance concepts as an alternative lifing philosophy to that of "safe-life" for the design of engine components.

This publication includes the presentations made in the course of the first Workshop, together with the Recorders' Report.

The Workshop was devoted to Non-Destructive Evaluation of Components.

AGARD Report No.768 Advisory Group for Aerospace Research and Development, NATO AGARD/SMP REVIEW – DAMAGE TOLERANCE FOR ENGINE STRUCTURES: 1. NON-DESTRUCTIVE EVALUATION Published November 1988 126 pages The AGARD Structures and Materials Panel is co-ordinating a series of four Workshops planned within the framework of a Review on Damage Tolerance for Engine Structures. The Review aims to address the areas critical to the acceptance of an approach based on damage tolerance concepts as an alternative lifing philosophy to that of "safe-life" for the design of engine components. P.T.O.	AGARD-R-768 Nondestructive tests Engines Components Damage Evaluation	AGARD Report No.768 Advisory Group for Aerospace Research and Development, NATO AGARD/SMP REVIEW – DAMAGE TOLERANCE FOR ENGINE STRUCTURES: 1. NON-DESTRUCTIVE EVALUATION Published November 1988 126 pages The AGARD Structures and Materials Panel is co-ordinating a series of four Workshops planned within the framework of a Review on Damage Tolerance for Engine Structures. The Review aims to address the areas critical to the acceptance of an approach based on damage tolerance concepts as an alternative lifing philosophy to that of "safe-life" for the design of engine components. P.T.O.	AGARD-R-768 Nondestructive tests Engines Components Damage Evaluation
AGARD Report No.768 Advisory Group for Aerospace Research and Development, NATO AGARD/SMP REVIEW – DAMAGE TOLERANCE FOR ENGINE STRUCTURES: 1. NON-DESTRUCTIVE EVALUATION Published November 1988 126 pages The AGARD Structures and Materials Panel is co-ordinating a series of four Workshops planned within the framework of a Review on Damage Tolerance for Engine Structures. The Review aims to address the areas critical to the acceptance of an approach based on damage tolerance concepts as an alternative lifing philosophy to that of "safe-life" for the design of engine components. P.T.O.	AGARD-R-768 Nondestructive tests Engines Components Damage Evaluation	AGARD Report No.768 Advisory Group for Aerospace Research and Development, NATO AGARD/SMP REVIEW – DAMAGE TOLERANCE FOR ENGINE STRUCTURES: 1. NON-DESTRUCTIVE EVALUATION Published November 1988 126 pages The AGARD Structures and Materials Panel is co-ordinating a series of four Workshops planned within the framework of a Review on Damage Tolerance for Engine Structures. The Review aims to address the areas critical to the acceptance of an approach based on damage tolerance concepts as an alternative lifing philosophy to that of "safe-life" for the design of engine components. P.T.O.	AGARD-R-768 Nondestructive tests Engines Components Damage Evaluation

This publication includes the presentations made in the course of the first Workshop, together with the Recorders' Report.

The workshop was devoted to Non-Destructive Evaluation of Components.

Papers presented at the 66th Meeting of the Structures and Materials Panel of AGARD in Luxembourg, 1—6 May 1988.

ISBN 92-835-0484-4

This publication includes the presentations made in the course of the first Workshop, together with the Recorders' Report.

The workshop was devoted to Non-Destructive Evaluation of Components.

Papers presented at the 66th Meeting of the Structures and Materials Panel of AGARD in Luxembourg, 1—6 May 1988.

ISBN 92-835-0484-4

This publication includes the presentations made in the course of the first Workshop, together with the Recorders' Report.

The workshop was devoted to Non-Destructive Evaluation of Components.

Papers presented at the 66th Meeting of the Structures and Materials Panel of AGARD in Luxembourg, 1—6 May 1988.

ISBN 92-835-0484-4

This publication includes the presentations made in the course of the first Workshop, together with the Recorders' Report.

The workshop was devoted to Non-Destructive Evaluation of Components.

Papers presented at the 66th Meeting of the Structures and Materials Panel of AGARD in Luxembourg, 1—6 May 1988.

ISBN 92-835-0484-4